Photo-assisted Adsorptive Desulfurization of Hydrocarbon Fuels over TiO_2 and Ag/TiO_2

by

Xueni Sun

A dissertation submitted to the Graduate Faculty of
Auburn University
in partial fulfillment of the
requirements for the Degree of
Doctor of Philosophy

Auburn, Alabama
May 7, 2016

Keywords: Desulfurization, Adsorption, Hydrocarbon Fuels, Titanium Oxide, Silver, Ultra-violet (UV), Hydroxyl Group

Approved by

Bruce J Tatarchuk, Chair, Professor Director of Chemical Engineering
Allan E David, Assistant Professor of Chemical Engineering
James Radich, Assistant Professor of Chemical Engineering
Dong-Joo (Daniel) Kim, Associate Professor of Material Engineering

Abstract

Organic sulfur compounds are one of the most common impurities in crude oil which is widely used as transportation fuels such as gasoline, diesel and jet fuels. Sulfur in liquid hydrocarbon fuels is also considered as one of the major causes of environmental pollution. The sulfur level in transportation fuels is now restricted by severe regulations in many countries for environmental protection. Moreover, ultra-low sulfur fuels are also required by fuel cells because sulfur species can easily poison the catalysts in fuel cell processors. Electrodes can also be damaged by sulfur in hydrocarbon fuels. Thus, desulfurization is essential for the production of transportation fuels as well as fuel cell application area. Catalytic hydrodesulfurization (HDS) is a commercial sulfur removal technology which has been widely used in refining.

However, several desulfurization technologies now considered to replace current conventional HDS to produce ultra clean fuels at milder operation conditions and lower cost. Among these alternative processes, adsorptive desulfurization (ADS) process has shown to remove organosulfur compounds efficiently under mild conditions. Recently, Ag/TiO_2 and Ag/TiO_2-Al_2O_3 adsorbents with high sulfur removal capacities have been developed by our adsorption group. Sulfur removal pathway using Ag dispersed on TiO_2 was then studied in details. Acidic hydroxyl groups on TiO_2 surface were considered as the main active sites. As a result, the desulfurization capacity of TiO_2 is related to surface acidity.

The presented research work focused on TiO_2/UV application in adsorptive desulfurization (ADS) to improve TiO_2 adsorbents' sulfur removal performances and mechanistic investigation of adsorptive sulfur removal under UV irradiation using TiO_2 adsorbents. In this work, the development of unique UV-irradiated adsorptive desulfurization using TiO_2, TiO_2-Al_2O_3, Ag/TiO_2 and Ag/TiO_2-Al_2O_3 adsorbents has been presented here along with sulfur removal pathways and possible photo-oxidative reactions on TiO_2 surface. Ultra-violet (UV) sources at a long wavelength (λ=365 nm) have been directly applied to dynamic breakthrough process without adding any corrosive oxidative agents. It was observed that UV irradiation before and during breakthrough processes both enhanced TiO_2 adsorbents' sulfur removal capacities. For experiments without UV, breakthrough and saturation capacities of calcined TiO_2 were 2.45 mg S/g and 3.90 mg S/g using a model fuel containing 3500 ppmw sulfur as benzothiophene in n-octane. And the capacities increased to 4.05 mg S/g and 5.63 mg S/g for experiments under UV. Moreover, UV-treated TiO_2 samples can also achieve high sulfur removal capacities. The performance was persistent after thermal regeneration at 450 ℃. The negative effect of H_2O on acid based adsorbents has been reported by many studies. The same trend was observed here. However, TiO_2/UV system can solve the problem caused by H_2O additive. Highest capacities for calcined TiO_2 were obtained during photo-assisted ADS using a model fuel containing H_2O additive. The desulfurization performance under different conditions, effects of H_2O and UV on surface hydroxyl groups, and the thermal stability of photo-activated species on TiO_2 surface are all presented in Chapter III.

Silver loaded on TiO_2 proved beneficial to desulfurization performance when compared to calcined TiO_2 support. The performance of Ag/TiO_2 (4 wt%) obtained from adsorptive desulfurization under UV, the effect of H_2O, as well as chemical state change of silver ions, were studied and discussed in Chapter IV. Ag/TiO_2 showed a different behavior from calcined TiO_2 during UV-irradiated breakthrough experiments when using a model fuel containing no H_2O. The sulfur removal capacities of Ag/TiO_2 were observed to decrease dramatically due to the formation of silver metal under UV which can be demonstrated by XPS results. Adding H_2O into the model fuel could prevent silver oxides turn into Ag metals under UV which further improved desulfurization performance of Ag/TiO_2. Highest capacities for Ag/TiO_2 were obtained during UV-assisted ADS using a model fuel containing H_2O additive.

Having confirmed that UV irradiation can improve desulfurization performance of TiO_2 adsorbents, several studies were carried out to determine the effect of UV and H_2O on active surface sites (Chapter V). A relationship between surface acidity and sulfur removal capacities for TiO_2 and Ag/TiO_2 was observed by our group. And acidic -OH groups have been postulated to be the main active sites on TiO_2 surface. Thus, the sulfur removal capacities were related to the total number of surface hydroxyl groups based on previous studies. Effects of UV and H_2O on surface hydroxyl groups were carried out via *in situ* IR and XPS. The number of isolated hydroxyl groups Ti(IV)-OH increased while bridged and H-bonded hydroxyl groups were removed after the exposure to UV based on infrared and XPS spectra. The effect of H_2O on Ti(IV)-OH groups on TiO_2 treated with or without UV was also studied in details. Possible pathways of forming terminal hydroxyl groups from bridged -OH and bridged O sites were discussed in Chapter V.

Surface hydroxyl radicals were observed using fluorescence spectroscopy (Chapter V). These radicals were considered as main active species on TiO_2 surface under UV which can act as strong oxidants during desulfurization process. Organosulfur removal mechanisms under dark and UV were both investigated in Chapter VI after characterizing active sites on TiO_2 surface. Isolated -OH groups contributed in the removal of sulfur aromatic molecules, as observed by *in situ* IR. Thiophenic compounds were considered to be removed via π-interactions between surface hydroxyl groups and thiophene ring as well as aromatic ring under both dark and UV conditions. However, photo-oxidation and ring opening reactions were also observed on the TiO_2 surface under UV irradiation. The resulting oxidative products were also adsorbed via π-interactions onto the TiO_2 surface. Sulfur removal mechanisms under different conditions were illustrated in details in Chapter VI. No photo-oxidative products were detected in the liquid phase as confirmed by GC-PFPD and GC-FID results.

Acknowledgements

I would like to express my sincerest gratitude to my advisor Dr. Bruce Tatarchuk for providing me this great opportunity for my graduate research studies. I acknowledge the guidance, suggestions, advice and encouragement from Dr. Bruce Tatarchuk during my studies. And I would also like to thank my committee members: Dr. Allan David, Dr. James Radich, and Dr. Dong-Joo Kim for their time and their advice regarding my research. I had received helpful ideas and support from Dr. Hongyun Yang (Intramicron Inc.), Dr. Sachin Nair and Dr. A.H.M. Shahadat Hussain. This research work also got support from my colleagues at the Center for Microfibrous Materials Manufacturing (CM3), especially Dwight Caheal, Dr. Wenhua Zhu, Dr. Zenda Davis, Mingyang Chi, Peng Cheng, and Xinquan Cheng among many others. I would like to thank Dr. Christopher Roberts, Dr. Rui Xu and Dr. Shaima Nahreen from Chemical Engineering department for their help with Infrared spectroscopy. Also, my appreciation goes to Dr. Xinyu Zhang from Chemical Engineering department for helping me a lot in fluorescence spectroscopy. I am thankful to Karen Cochran and Elaine Manning for their administrative support through my time at Auburn. Acknowledge financial support came from the US Army (TARDEC).

Most importantly, this dissertation would not have been possible without the love and support of my parents. I am also grateful to all my friends at Auburn for their help, support and advice.

Table of Contents

List of Tables

List of Figures

I. Introduction and Literature Review

I.1. Introduction

Organic sulfur compounds are present in nearly all fossil fuels and petroleum. Sulfur represents one of the most impurities in crude oil which is a large source of energy, and is widely used as transportation fuels such as gasoline, diesel and jet fuels. So far, the sulfur content in liquid fuels is still very high, and it can vary from hundreds ppmw to thousands ppmw. The current sulfur level in global supplies of crude oil is listed in Table I.1 [1]. Sulfur and its derivatives in liquid fuels can be easily converted into sulfur oxides SO_2 and fine particles of metal sulfated during engine combustion. All those sulfur compounds are considered as major pollutants in the air. The toxic sulfur oxides especially SO_2 gas will be released into the air which can cause severe pollution such as acid rain and smog. Those fine particles of metal-sulfur can also do great damages to human health. As a result, the major challenge of refiners is the requirement for fuels containing an ultra-low level of sulfur compounds. Reduction of sulfur contents in gasoline, diesel and other transportation fuels is also the primary focus of the new environmental regulations worldwide. With the increasing sulfur concentrations in fuels theses years, sulfur removal from hydrocarbon fuels has gained great importance and research interests. Average properties of crude oils refined in the US are shown in Table I.2 [2]. As we can see from Table I.2, properties of crude oil decreased and refining crude oils tend to have higher sulfur contents for the past two decades.

Table I.1. Sulfur level (weight percentage) in crude oil worldwide in the year 2010

Region	USA	Canada	Europe	Middle East	World Average
Sulfur Weight (%)	0.88	1.62	1.10	1.71	1.27

Stringent regulations have been applied to limit the maximum sulfur emissions in many countries around the world as shown in Table I.3 [3, 4]. For example, the Environmental Protection Agency (EPA) regulations require the reductions of sulfur contents in diesel and gasoline. The allowable sulfur content for ultra-low sulfur diesel (ULSD) was forced to decrease from 500 ppmw to 15 ppmw in 2006. Also for gasoline, the allowable level of sulfur was changing from 350 ppmw to 30 ppmw in 2005 [2, 5].

Table I.2. Average properties of crude oils refined in the US during 1981-2001

Property	Year 1981	Year 1991	Year 2001
Total amounts of crude oil refined in the US (million barrel/day)	12.47	13.30	15.13
Average sulfur content of crude oil refined in the US (wt% S)	0.89	1.13	1.42

Although there are different sulfur standards for complicated cases, most of the military fuels are currently not bounded by those regulations. As a result, the total sulfur contents in those fuels can be as high as thousands ppmw as listed in Table I.4 [5]. So it is important and urgent to solve the air pollution problem due to sulfur species from these jet fuels.

Table I.3. Sulfur standards for gasoline worldwide

Country	Fuel	Year	Sulfur Limit (ppmw)
USA	Gasoline	2006	30
EU	Gasoline	2009	10
China	Gasoline	2005	50
India	Gasoline	2010	50
Australia	Gasoline	2005	150

Ultra-deep desulfurization technology is also necessary for the fuel cell application area. Fuel cell (FC) technologies have rapidly developed during recent 10 years to achieve clean electric power for the "hydrogen economy". And fuel cells are considered as energy-efficient conversion devices to provide sustainable energy. Generally, there are five types of fuel cells based on the electrolytes, which are alkaline fuel cell (AFC), phosphoric acid fuel cell (PAFC), proton-exchange membrane fuel cell (PEMFC), molten carbonate fuel cell (MCFC), and solid oxide fuel cell (SOFC). Liquid, gaseous and solid fuels can be used for the combustion systems in the fuel cells. Sulfur species from hydrocarbon fuels can easily poison the catalysts in fuel cell processors, and electrodes can also be damaged in some degrees by sulfur compounds. Therefore, different types of fuel cells have different limitations in total sulfur concentrations as listed in Table I.5 [6]. Ultra clean fuels are always required to avoid those damages in order to protect the fuel

cell systems. Normally, sulfur compounds in liquid hydrocarbon fuels need to be reduced to less than 0.1 ppmw before entering the fuel cells.

Table I.4. Total sulfur concentration in jet fuels

Fuel	Air Force JP-4	Navy Aircraft JP-5	Air Force JP-7	Air Force JP-8
Total Sulfur (ppm)	4000	<4000	1000	<3000

As a result, ultra-deep desulfurization of liquid fuels is important and has attracted great research interests recent years. Great efforts have been made to develop advanced sulfur removal technologies as well as novel materials for highly efficient desulfurization of hydrocarbon fuels in order to meet the zero sulfur emission requirements in the future.

Table I.5. Sulfur limitations of different fuel cells

	PEMFC	SOFC	PAFC	MCFC	AFC
Sulfur (as H_2S and COS)	<0.1 ppm	<1 ppm	<50 ppm	<0.5 ppm	Unknown

I.2. Literature review

I.2.1. Organic sulfur species in transportation fuels

The effectiveness of sulfur removal technologies highly depends on the structure and local sulfur atom environment of those sulfur species. Therefore, a wide range of sulfur compounds should be considered when developing an effective desulfurization process.

Organic sulfur compounds are present in almost all crude oil distillation. Aliphatic organic sulfur compounds such as thiols, mercaptans, sulfides and disulfides usually exist in low-boiling crude oil. On the opposite, most organic sulfur compounds with large molecular weights are found in high-boiling crude oil such as heavy straight run naphtha, straight run diesel and light FCC naphtha [7, 8]. The most common organic sulfur compounds presented in gasoline and diesel are thiophenes, benzothiophenes, dibenzothiophenes and their derivatives. For example, around half of the organic sulfur species in FCC gasoline come from thiophenes and their alkylated derivatives [9]. Those sulfur compounds containing thiophenic structure or aromatic rings are more difficult to remove completely from liquid fuels compared to aliphatic sulfur compounds [10]. The structure of typical organic sulfur species in hydrocarbon fuels are shown in Table I.6.

Table I.6. Typical organic sulfur compounds in liquid transportation fuels

Thiophene (T)	Benzothiophene (BT)	Dibenzothiophene (DBT)	4,6-DMDBT
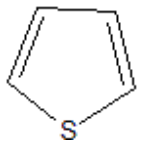	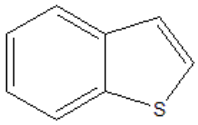	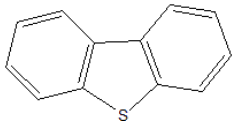	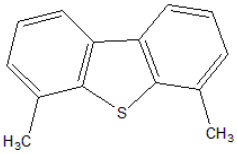

I.2.2. Current desulfurization technologies

The desulfurization technologies can be generally divided into two groups by the role of hydrogen during the sulfur removal process. In hydro-desulfurization (HDS) based processes, hydrogen (H_2) is involved to remove organosulfur from refinery streams while

non-HDS based processes do not require the involvement of H_2 during desulfurization procedure. There have been many popular technologies developed to efficiently remove organic sulfur compounds from fuels, including catalytic hydrodesulfurization (HDS), oxidative desulfurization (ODS), photocatalytic oxidative desulfurization (PODS), biodesulfurization (BDS) and adsorptive desulfurization (ADS). Among those techniques, catalytic hydrodesulfurization (HDS) is a commercial sulfur removal technology which has been widely used in refineries nowadays. And now HDS has become a major refining process. Most of the low sulfur hydrocarbon fuels can be derived directly from this conventional HDS technology. During HDS process, light oil is mixed with H_2 after being heated, then the mixture is fed into a trickle bed or packed bed reactor loaded with highly active catalysts containing Co, Mo, and Ni metals [11]. The hydrodesulfurization reactions are carried out at high temperature (300-450 ℃) and high H_2 pressure (3-5 MPa) [12, 13]. The HDS of organic sulfur compounds is highly exothermic and essentially irreversible under the reaction conditions. The hydrotreating sulfur removal process can effectively remove aliphatic organic sulfur species such as sulfides and thiols at a relatively low cost. The reactivity of HDS highly depends on the activity of the catalysts, structure of sulfur compounds, and the reaction conditions.

Catalysts play an important role in HDS to produce clean fuels. The sulfide catalysts in hydro-desulfurization process mainly consist of Mo, promoted by Co or Ni metals, and loaded on high surface area supporting materials, such as Al_2O_3, zeolite or other mixed oxides [14, 15]. The Co-Mo and Mo-Ni sites are considered as the active sites by forming the Co-Mo-S and Mo-Ni-S structures [16, 17]. Great efforts have been put to develop new catalysts and to improve the performance of modern catalysts [18-21]. To increase

catalyst's activity, many effects including active species, supporting materials and preparation procedure should be considered [22]. In 1998, highly active Co-Mo and Ni-Mo catalysts referred as STARS (Super Type II Active Reaction Sites) were introduced by Akzo Nobel. It was claimed that sulfur content was brought down to 2-5 ppm with the application of those HDS catalysts. Also, another Akzo Nobel catalyst called NEBULA catalysts have been applied in commercial units. AXENS also introduced new catalysts, which have high HDS activities. Also, the catalysts developed by Kuwait Catalyst Company can achieve low sulfur levels for diesel hydrotreating facilities. CENTINEL Ascent, CENTINEL Gold catalysts by Criterion and ART (SMART) catalysts from ART all showed remarkably high activities as hydrotreating catalysts [7].

However, current hydrodesulfurization catalysts are found to be less reactive to thiophene, benzothiophene, dibenzothiophene and their alkyl derivatives. Thus, intensive efforts have been put into further improving catalyst's activity and developing highly efficient catalysts to remove DBT related sulfur compounds [23]. New catalysts are required to be developed in order to desulfurize BT, DBT, and their derivatives because these sulfur compounds are the keys to achieve deep hydrodesulfurization of hydrocarbon fuels. An extensive number of studies have been reported in the literature on catalysts for HDS. Almost all the transition metals in their sulfides form have been tested for their desulfurization activities toward HDS. Molybdenum catalysts supported on Al_2O_3, TiO_2, SiO_2 and mixed oxide supports have been investigated in details for deep HDS. Also, many different supports have been investigated in an attempt to enhance the HDS activity of the catalysts. Effects of supports were studied in order to understand the role played by supports in dispersing the active components and promoters. It has been reported that

support effects formed an important aspect of hydrodesulfurization. Many materials have been tried as supports to Mo and W active components.

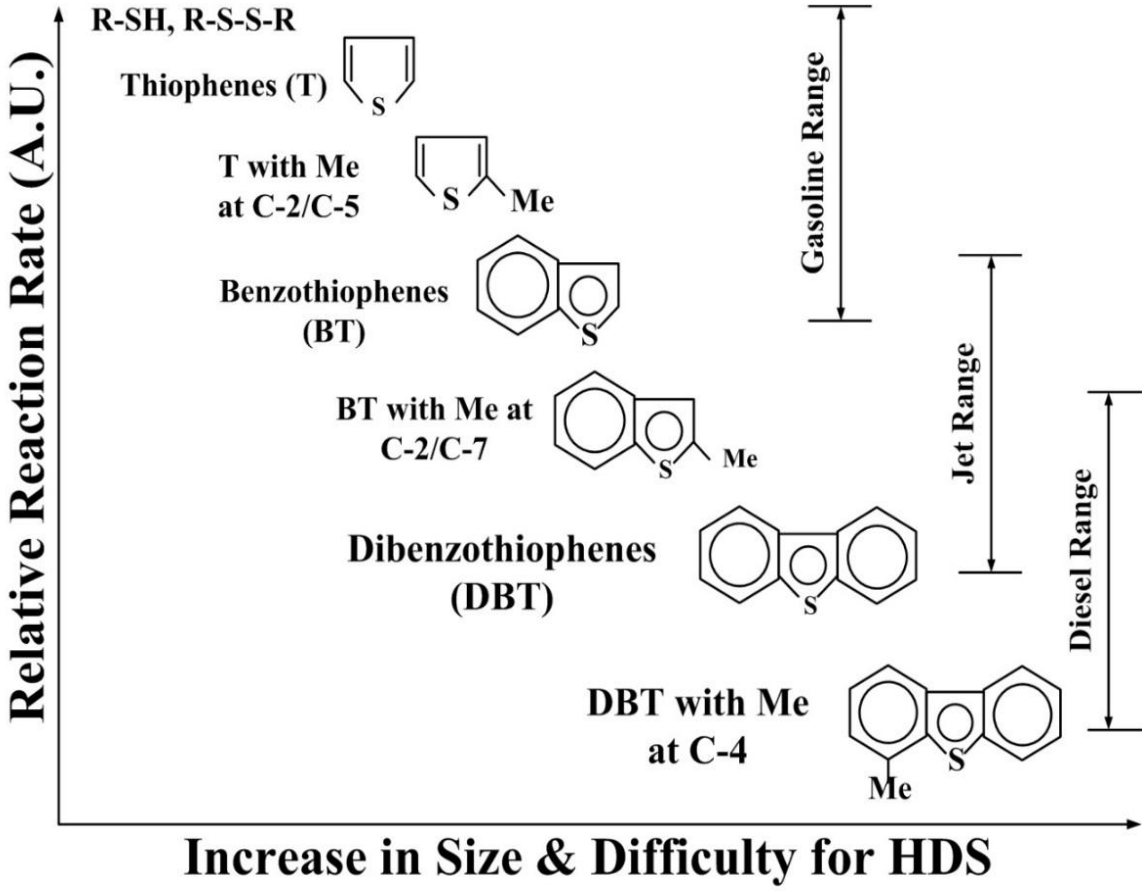

Figure I.1. Reactivity of various organic sulfur compounds in hydro-desulfurization (reproduced from C. Song, Catalysis Today, 2003 [2])

Some of the supports are SiO_2, MgO, ZrO_2, TiO_2, activated carbon, zeolites, MCM-41, SBA-15 and mixed oxides. And mixed oxide supports received maximum attention in the last two decades because these mixed oxides showed outstanding activities for deep HDS. Among those mixed oxide supports, Al_2O_3 containing mixed oxides, TiO_2 containing mixed oxides and ZrO_2 mixed oxides have attracted lots of attentions. In the past few decades, TiO_2-Al_2O_3 mixed oxides have been extensively studied because of

their commercial prospects and high desulfurization activities. TiO_2-Al_2O_3 supports can be prepared by various ways like chemical vapor deposition, impregnation, and co-precipitation techniques. All these methods finally lead to TiO_2-Al_2O_3 of high surface area. Effects of catalyst supports are not well researched.

Table I.7. Reactivities of organic sulfur in HDS

Sulfur Species	Pseudo-first-order Rate Constant (L/g catalyst/s)
Thiophene	1.38×10^{-3}
Benzothiophene	8.11×10^{-4}
Dibenzothiophene	6.11×10^{-5}
4, 6-DMDBT	4.92×10^{-6}

Various organic sulfur compounds exist in liquid fuels, and the effectiveness of sulfur removal process is also related to the structure of sulfur compounds. Figure I.1 shows the relative reactivity of various organic sulfur compounds in HDS based on experimental results. The selectivity and reactivity of organosulfur species in HDS follows the order (from highest to lowest) as shown in Figure I.1: aliphatic organic sulfur > thiophene > alkylated thiophene > benzothiophene (BT) > alkylated benzothiophene > dibenzothiophene (DBT) > alkylated dibenzothiophene > 4, 6-dimethyldibenzothiophene (DMDBT) [24, 25]. The methyl substitutions cause the steric hindrance making sulfur atom inaccessible to active sites on catalysts which can inhibit the activity towards HDS

[26, 27]. The HDS of several organic sulfur compounds is listed in Table I.7 which is described by pseudo-first-order kinetics [28].

A lot of research studies have been carried out on the reaction pathways for those organic sulfur compounds in HDS [29]. It has been suggested that thiophene compounds can be removed by HDS process via two parallel pathways which are hydrogenation and hydrogenolysis. The thiophene reaction pathways in HDS are shown in Figure I.2 [24].

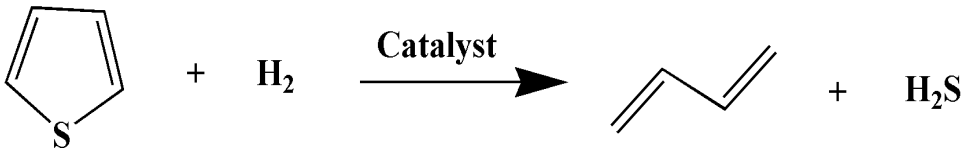

Figure I.2. Thiophene reaction pathways in hydrodesulfurization process

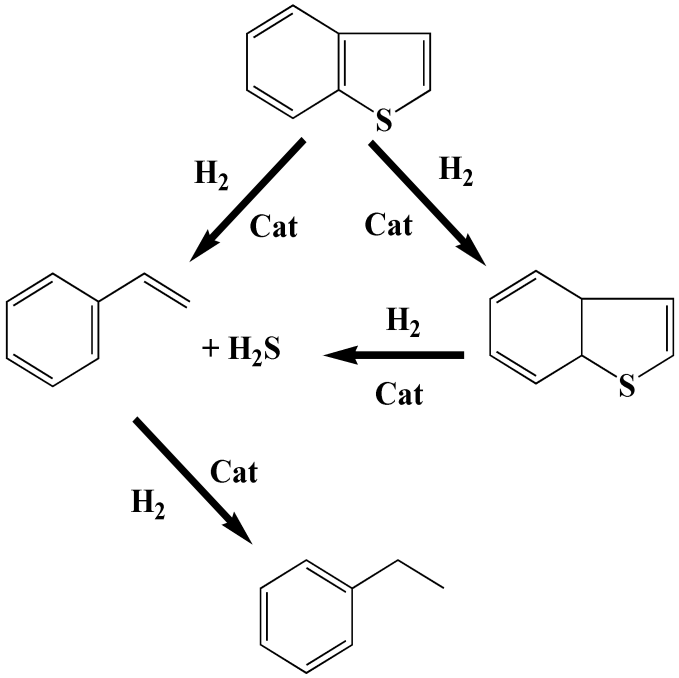

Figure I.3. Parallel reaction pathways for benzothiophene in HDS (reproduced from I.A. Vanparijs et al. Industrial & Engineering Chemistry Product Research and Development, 1986 [30])

The pathway that thiophene ring is hydrogenated prior to desulfurization is known as the hydrogenation mechanism. In hydrogenolysis pathway, thiophene ring is split and sulfur is removed in the form of H_2S. For benzothiophene, the pathways in HDS are shown in Figure I.3 [30]. For dibenzothiophene, reaction mechanisms were proposed in details as shown in Figure I.4 [31]. Studies show that H_2S can inhibit hydrogenolysis process, and methyl substitution will reduce the reaction rate of hydrogenation process [32-34]. Thus, BT, DBT and their derivatives, especially 4, 6-DMDBT will remain stable in the stream after HDS process. As a result, current hydrodesulfurization cannot meet the requirement for zero sulfur emission in the future.

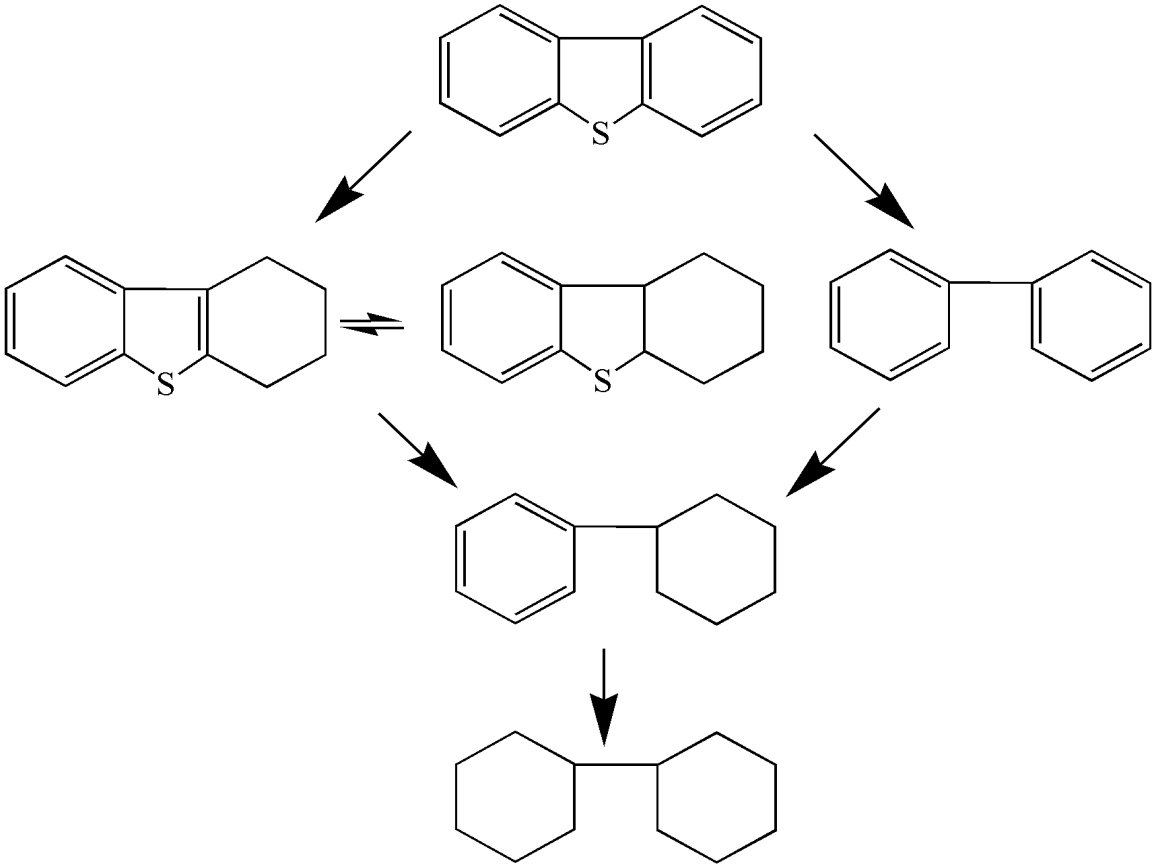

Figure I.4. Proposed reaction pathways for dibenzothiophene in HDS (reproduced from R. Shafi et al. Catalysis Today, 2000 [24])

The requirement in severe sulfur reduction will also have a large impact on HDS's operation conditions in order to increase catalyst activities, such as reaction temperature, H_2 pressure, reactor size, and catalyst volume [35, 36]. Table I.8 shows the estimated increase in catalyst activity and bed temperature in order to meet required sulfur level [36]. Kinetics studies have shown that sulfur content can be decreased to lower levels with the increase of temperature and H_2 partial pressure [12, 37].

Table I.8. Estimated increase in catalyst activities and temperature to achieve required sulfur content in diesel.

Required Sulfur Content (ppmw)	Catalyst Activity (%)	Increase in Temperature (℃)
500	100	0
350	130	7
200	190	17
100	300	29
50	420	38

Temperature is raised to maintain the performance of HDS catalysts in order to meet the stringent standard. Moreover, benefits will be gained by increasing H_2 partial pressure or temperature. Higher H_2 pressure can significantly reduce the inhibiting effects by alkyl groups. And higher temperature can remove thermodynamic equilibrium limits associated with aromatic compounds. However, higher temperature and hydrogen partial pressure

will definitely raise the H_2 demand level as well as total operating costs. Moreover, increasing operation temperature and pressure can cause a significant loss in octane number, which will affect the final quality of fuel products. As a result, extra octane recovery step have to be added in order to modify current HDS process. Current hydro-desulfurization is a high temperature, high-pressure catalytic process. This makes HDS a very costly option for deep desulfurization.

Commercial HDS is a refining process that passes a mixture of heated feedstock and hydrogen over catalysts to remove sulfur compounds. Most commercial HDS operations also remove nitrogen compounds and some metal impurities. Thus, there are several constraints in commercial HDS process. The low sulfur requirement for liquid fuels is the greatest challenge for the refining industries. This is due to the large concentration of aromatic compounds and high olefin contents in the feedstock. Another problem is the increased volume of H_2S emission due to the additional steps of the HDS process. It has also been reported that HDS process can be modified for ultra-low sulfur production by application of highly active catalysts, an increase of operating severity, using additional reactors and improving feed distribution. Modification on deep HDS to remove sulfur aromatic compounds can put lots of pressure on investment. Many new concepts and technologies have been developed during the last 20 years to reach zero sulfur requirement. Some new catalytic hydrotreating technologies and removal processes have been developed and commercialized for ultra-deep HDS. Several academic and industrial studies are still working to modify and to improve current HDS technology in refineries.

Although HDS process has dominated sulfur removal area in the past, new desulfurization technologies have been explored in order to enhance the performance of

hydrodesulfurization process, or to replace current HDS technology. Several alternative technologies which have high selectivity under mild operation conditions have been developed recently and attracted many research interests to produce ultra-clean fuels with zero sulfur content.

I.2.3. Alternative sulfur removal processes

I.2.3.1. Oxidative desulfurization (ODS)

Technologies that do not use hydrogen for catalytic decomposition of organosulfur compounds are referred as non-HDS based desulfurization technologies. Those approaches are considered to remove organosulfur compounds without the involvement of H_2. Oxidative desulfurization (ODS) is considered as one of the alternative approaches to replace HDS for deep desulfurization from light oil. ODS is considered as a new method to produce low sulfur fuels to meet future legislation on sulfur content, and ODS has drawn wide attention [38-40]. High oxidation reactivity for benzothiophene, dibenzothiophene and their derivatives at ambient temperature and pressure made ODS a favorable desulfurization process, eliminating the need for severe conditions required by conventional HDS to remove organosulfur compounds. The ODS process can be simply divided into two stages including oxidation and further extraction or distillation sulfur removal steps [41, 42]. The schematic biphasic oxidative removal process for organic sulfur compounds is shown in Figure I.5. During the oxidation step, organic sulfur compounds are oxidized to corresponding compounds [43-45]. Oxidative reactions occur in the presence of strong oxidants such as H_2O_2, peroxy salts, nitrogen oxides and ozone

[46]. The oxidation of those organosulfur compounds increased their polarity and molecular weight. This facilitated their separation by extraction, distillation or adsorption. After the oxidative process, the oxidized products can be subsequently removed from the oil phase by the separation process in the second step [47-49].

A significant research effort has been conducted on oxidative desulfurization over years. The greatest advantages of oxidative sulfur removal technology are mild operation conditions with relatively low temperature and pressure. Using oxygen, air or other oxidants rather than hydrogen to remove sulfur from refinery streams is attractive due to the availability of the reacting agents and its relatively low cost. Expensive consumption of hydrogen is not required during the entire process. Although oxidative desulfurization has been proven to remove organosulfur compounds from liquid fuels efficiently, this technology still faces several challenges and needs further improvements.

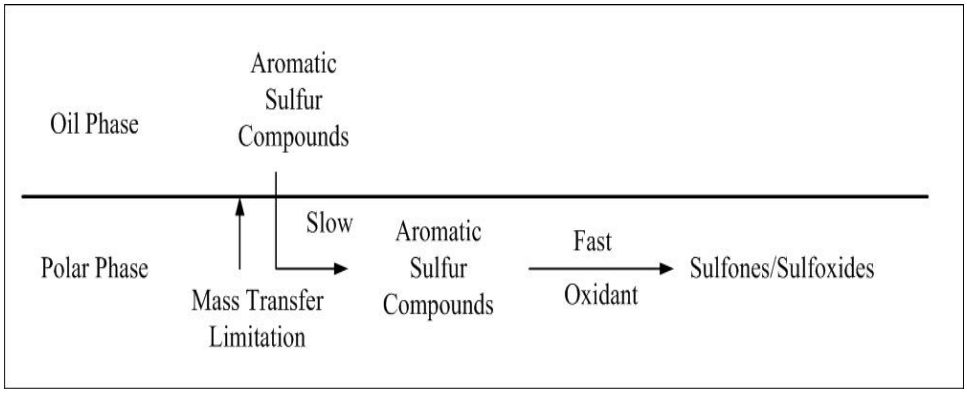

Figure I.5. Schematic biphasic ODS process

There are several drawbacks of ODS. The major problem is that the oxidants used in ODS are highly corrosive which can raise the limitation on operation conditions. Also, the oxidative reaction pathways of organosulfur species are complicated. ODS desulfurization performance depends on the oxidative reactions of the sulfur aromatic

compounds. It is hard to control unwanted side reactions. Some oxidants cause unwanted side reactions and unwanted side products will form in liquid fuels. The unwanted side reactions can reduce the quantity and quality of the hydrocarbon fuels. Also, the low catalytic activity at low H_2O_2/S ratio limits the desulfurization efficiency in oxidative sulfur removal process [50]. The oxidization reaction can occur in a short time only for few catalysts at the molar ratio close to stoichiometric (H_2O_2/S=2). Also, the low mass transfer in a biphasic system containing oil and polar phases limits the overall sulfur removal rate [51, 52]. Moreover, using the wrong solvent may result in removing desirable compounds from fuels. In addition, the adsorbed sulfones and metal leaching of molybdenum catalysts used in ODS can deactivate the catalysts as well as affect the stability of the operation system [43]. As a result, oxidative desulfurization (ODS) faces many challenges and is quite hard to achieve ODS at large scales due to those limitations on realistic application areas. In order to overcome those disadvantages of ODS, efforts have been made to develop new catalysts and to modify the process.

I.2.3.2. Photocatalytic ODS (PODS)

Photocatalytic oxidative desulfurization (PODS) is a modified ODS process. Sulfur aromatic compounds are oxidized under UV or visible light with or without photocatalysts [53-55]. Then the oxidized sulfur products are removed generally by extraction. During the last decades, photocatalysis has gained considerable research interests in different application areas such as compounds degradation, water splitting, semiconductors and catalyst supports [56-62]. TiO_2/UV system has already been introduced into desulfurization process based on its high photo-oxidative efficiency [63]. Photo-oxidation of organic sulfur compounds in liquid oil has been studied since the

1990s [64]. UV light was firstly applied for photo-oxidation process of organic sulfur species including benzothiophene and dibenzothiophene without any catalysts during the sulfur removal process [65]. The photo-oxidized products of BTs and DBTs have been determined [66, 67]. Also, the corresponding photo-oxidative reaction schemes have been illustrated in details by Shiraishi's group [65].

Recently, TiO_2 and TiO_2 based photocatalysts have been successfully introduced into oxidative desulfurization process, developing the photocatalytic oxidative desulfurization (PODS) technology. PODS has been proven to be another effective sulfur removal method [68]. Photo-assisted ODS has already been studied with TiO_2 under both laboratory and pilot-plant scales using UV light, simulated and natural solar lights [69]. And the technology on the ultra-deep removal of thiophene compounds over catalyst assisted by UV (URTCU) has been developed successfully in 2013 using TiO_2 loaded zeolite as catalysts [70]. Based on experimental results, about 99% of the thiophene compounds can be oxidized under UV irradiation, and then removed from model diesel fuels to reach ultra-deep desulfurization. Moreover, ultra-deep sulfur removal by PODS now can be able to carry out under the low molar ratio of H_2O_2/S when compared with traditional ODS [71]. The reported conversion of DBT in model fuels by TiO_2 in the ionic liquid can achieve 96% by PODS.

Desulfurization assisted by a photocatalyst is a potential method to deeply remove sulfur aromatic compounds from liquid fuels. However, PODS still has several disadvantages. Because the desulfurization mechanism of PODS is based on photocatalytic oxidative reactions, unwanted side reactions can still occur during the oxidation which can cause poor selectivity. Also, PODS is derived from ODS, and the

total efficiency of photocatalytic sulfur removal technology is still limited by mass transfer in the biphasic system. Moreover, long reaction time makes PODS inapplicable for industrial refineries.

I.2.3.3. Bio-desulfurization (BDS)

Bio-desulfurization (BDS) is a new technology which has been developed recently by applying the biological method for sulfur removal from hydrocarbon fuels [72, 73]. BDS is considered a complementary method used with HDS and highly advantageous for removal of sulfur in fossil fuels. This process allows efficient sulfur removal at moderate temperature and pressure. BDS focuses on microbiological or biochemical methods to remove organosulfur from the liquid phase. BDS is estimated to have 10-15% lower operating cost and 70-80% lower CO_2 emissions than conventional HDS. About 0.5-1% of bacterial cell dry weight is formed by sulfur atom [74]. Sulfur is required for growth and biological activities of many micro-organisms. So some organic sulfur compounds such as DBT can be consumed by specific microorganisms. As a result, the microorganisms can be applied for sulfur removal to reduce sulfur content depending on their enzymes and metabolic pathways. Bio-desulfurization technique includes bio-catalytic degradation of organic sulfur compounds followed by a distillation step [75]. This process can be carried out under mild temperature and pressure as an energy-saving technology without lowering the value of fuels. What's more, the desulfurization process should be highly selective because biocatalysts are involved. The major pathway in bio-desulfurization has been reported in many papers and the mechanisms to remove DBT with specific enzymes have been well studied [76, 77]. The metabolic pathway of DBT was called "4S" in reference to the four intermediates formed (DBT sulfoxide, DBT

sulfone, hydroxyphenyl benzene sulfonate, sulfate). The "4S" pathway for the biodesulfurization of DBT is shown in Figure I.6.

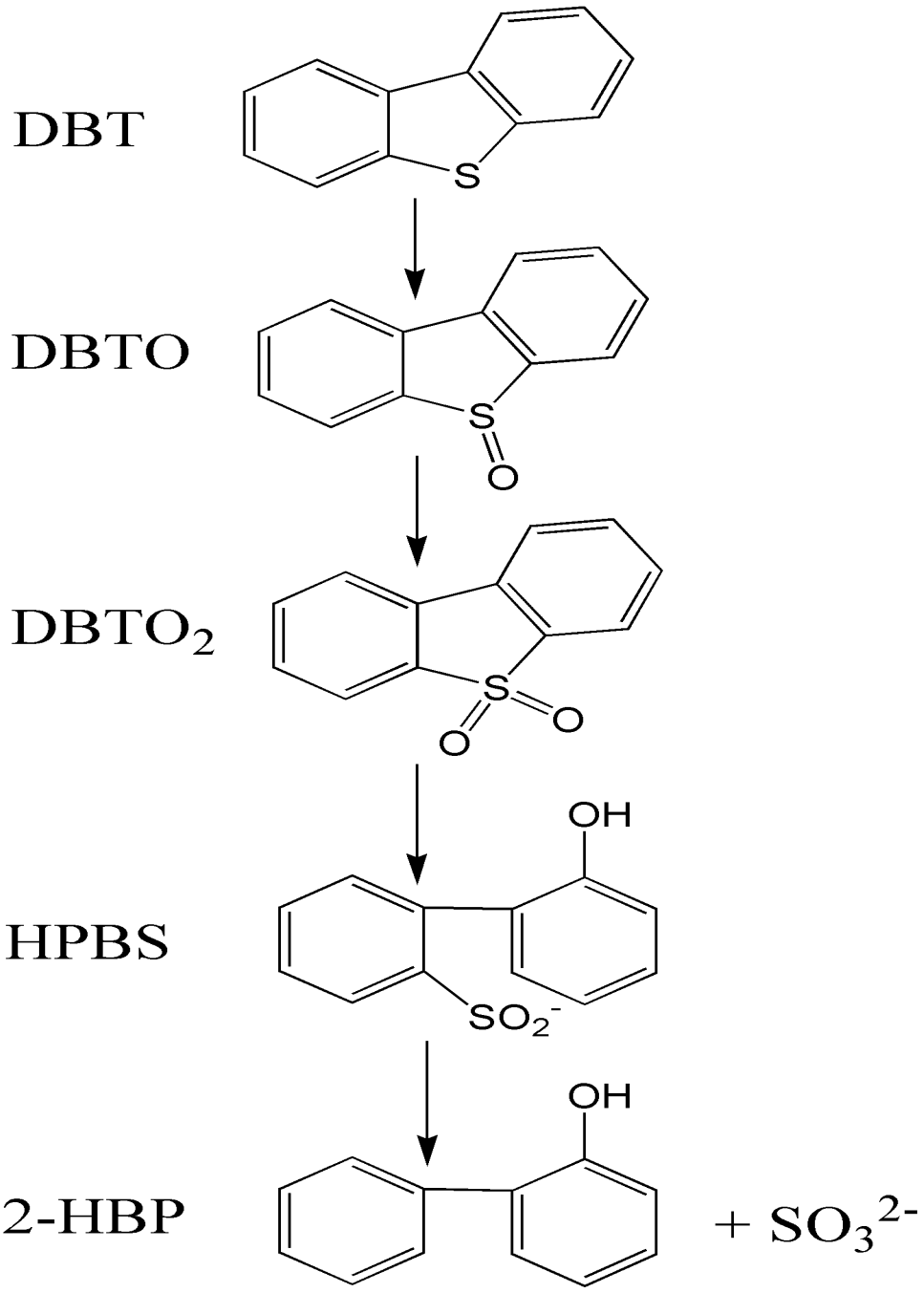

Figure I.6. The "4S" pathway for the biodesulfurization of DBT (reproduced from D. Boniek et al., Clean Technologies and Environmental Policy, 2015 [76])

However, the delicate bio-catalysts have relatively poor thermostability, which cannot stand high heat. The optimum temperature of those enzymes is usually around 50 ℃. And enzymes used in BDS have relatively short lifetime along with long reaction time, all causing a low efficiency in BDS [72, 76]. Until today, the search for stable biocatalysts has not succeeded in meeting industrial standards. Nowadays, industrial-scale BDS process has been still under investigation. Over the past 10 years, researchers on improving the efficiency of desulfurization process have increased. However, the highest activity obtained in BDS now cannot fulfill the industrial requirement. The application of large-scale bio-desulfurization technology is still only at the pilot project level study. During recent years, intensive research efforts have been increased in bio-desulfurization to better understand the mechanisms, and to improve the activity of those bio-catalysts. Bio-desulfurization technology is still at the pilot level study and has not been commercially used by petroleum industry yet.

I.2.3.4. Adsorptive desulfurization (ADS)

With the development of new technologies for ultra-deep sulfur removal, adsorptive desulfurization (ADS) is considered as a competitor for commercial hydrodesulfurization [78-81]. Adsorption has been applied variously for removal of sulfur compounds from liquid hydrocarbon fuels. This technology uses adsorbents to selectively remove organosulfur under ambient environmental conditions. Sulfur aromatic compounds can be removed from the liquid phase by adsorption in a fixed bed reactor or a batch reactor. Those adsorbents used in ADS can be regenerated for several cycles. Removal of sulfur aromatic compounds has been studied over alumina, zinc oxide, activated carbon, TiO_2 and zeolites. Moreover, adsorption sulfur removal process does not require the

involvement of hydrogen nor any other corrosive agents, making the reactor design much simpler when compared to other desulfurization techniques discussed before. In addition, these reactors used in ADS can be operated under atmospheric pressure which significantly lowers the investment compared with current HDS. Adsorptive desulfurization (ADS) shows many advantages in petroleum refining.

There are still future challenges for desulfurization by adsorption. The efficiency and sulfur removal capacity of ADS mainly depends on the performance of adsorbents. The adsorbents should have the highest affinities for thiophene or sulfur aromatic compounds, medium affinities towards aromatic compounds, and lowest affinities for those alkanes and branched alkanes. However, the selectivity and capacities of those commercial adsorbents are relatively low. And the activity lost after regeneration. Thus, increasing and maintaining the sulfur removal capacities are the major challenges in adsorptive desulfurization technology.

I.3. Adsorbents for ADS

I.3.1. Adsorbents based on π-complexation

Adsorptive desulfurization is based on the selective interaction between adsorbents and organic sulfur compounds in hydrocarbon fuel under mild conditions without H_2. A lot of adsorbents were studied and developed by many research groups [79, 82-85]. And sulfur removal has been observed through three types of mechanisms differed by the strength of interactions, including weak physisorption, strong chemisorption and a combination of both. Activated carbons are widely used as adsorbents for the treatment of

environmental pollutants. Most commercial activated carbons have good porosity and high surface areas and consequently activated carbon have high efficiency for the adsorption of various types of organic compounds. Different types of activated carbons have been studied for their sulfur removal capacities. Also, silica gel and activated alumina are most widely used for the removal of organic compounds from aqueous solutions. The adsorption capacities of SiO_2, Al_2O_3 and TiO_2 also have been reported in the literature. Sulfur removal mechanisms of a few materials for ADS were investigated in details. Recently, new adsorbents based on π-complexation attracted many attentions and were developed for adsorptive desulfurization. Transition metal ion exchanged zeolites were developed to remove organic sulfur compounds selectively from commercial fuels. The zeolite-based adsorbents loading with Cu^{+}, Ni^{2+} or Zn^{2+} developed by Yang and co-workers were studied for desulfurization of diesel, gasoline, and commercial jet fuels [86-88]. Based on the experimental results, sulfur content can be reduced to less than 1 ppmw with those π-complexed adsorbents. The π-complexation mechanism has been approved by experiments as well as theoretical calculations [89, 90]. The coordination configurations of thiophene in organometallic complexes are shown in Figure I.7. For selective adsorption, two specific configurations which are η^1S and S-μ^3 bonding are considered [79]. Cations can form σ bonds with s-orbitals and their d-orbitals can back-donate electron density to the π*-orbitals of the organic sulfur rings. The calculation results suggest that the mechanism is based on the interaction between highest occupied molecular orbital (HOMO) of sulfur and lowest unoccupied molecular orbital (LUMO) on metal species. The π-complexation bonds are stronger than the bonding formed by van der Waals interaction, and can be easily broken by engineering means.

Thus, these π-complexed adsorbents can be simply regenerated for several cycles. During adsorptive desulfurization process using adsorbents based on π-complexation, guard beds are suggested to be placed in front of these adsorbents to enhance the sulfur removal performance. Furthermore, an additional step is needed to recover those transition metal ions back to the reduced state.

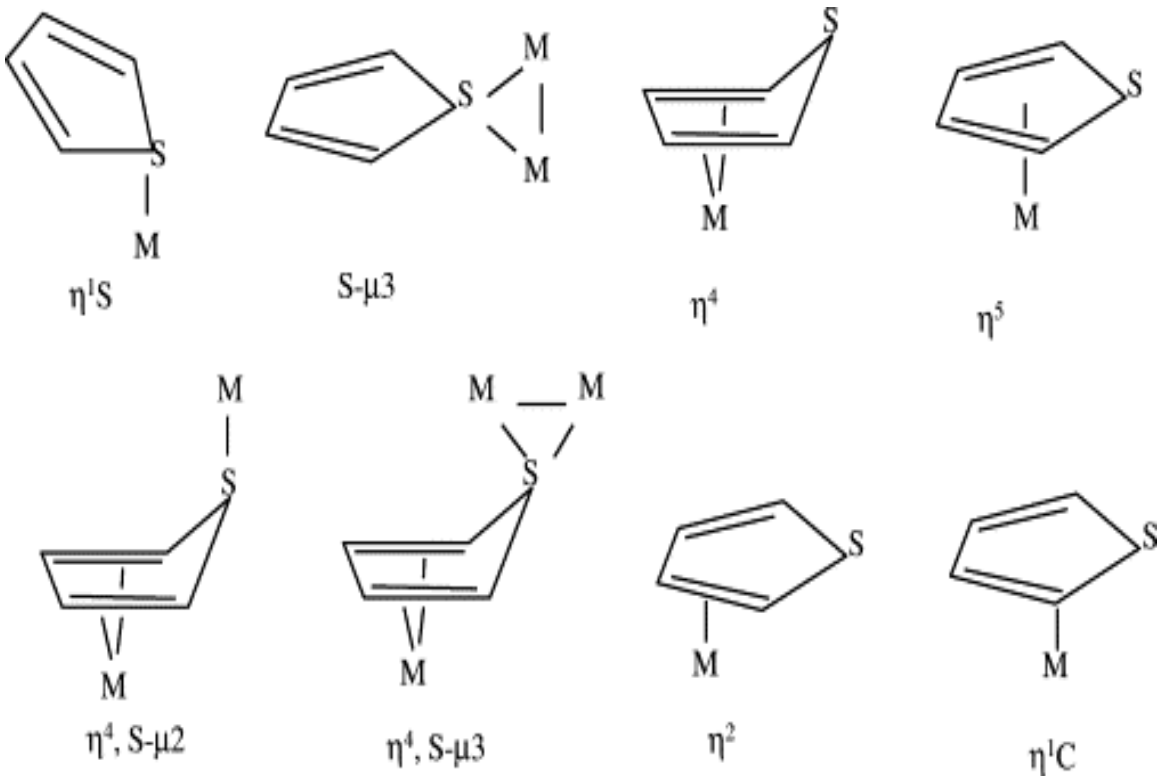

Figure I.7. Eight coordination geometries of thiophene in organometallic complexes (reproduced from X. Ma et al., Catalysis Today, 2002 [79])

I.3.2. Ag/TiO_2 and Ag/TiO_2-Al_2O_3

Several adsorbents have shown high desulfurization capacities. Recently, the adsorption group at Auburn University Center for Microfibrous Materials Manufacturing

(CM3) has developed silver loaded on TiO_2 adsorbents for adsorptive desulfurization from refined fuels with a high level of sulfur under ambient conditions [91-93]. Table I.9 shows the capacities of some popular adsorbents for ADS [78, 86, 89-91, 93].

Table I.9. Sulfur adsorption capacities for some popular adsorbents

Adsorbents	B.T Capacity (mg S/g)	S.A.T Capacity (mg S/g)	Inlet Challenge Fuel	Initial Sulfur Concentration (ppmw S)
Activated carbon	7.15	16.29	Model Diesel	687
Activated alumina	1.57	2.41	Model Diesel	687
Ni/SiO_2-Al_2O_3	2.18	3.40	Model Diesel	687
Cu(I)-Y	5.34	11.97	Diesel	297
Ni(II)-Y	4.58	8.03	Diesel	297
Zn(II)-Y	2.78	6.30	Jet fuel	364
Ag/TiO_2	4.91	6.68	Model Fuel	3500
Ag/TiO_2	0.79	5.65	JP5	1172
Ag/TiO_2-Al_2O_3	0.90	10.11	JP5	1172

Silver on TiO_2 adsorbents demonstrated good desulfurization performance towards commercial fuels containing high sulfur concentration. Active silver components in oxidized form are loaded onto TiO_2 based supports by total wetness impregnation. Ag/TiO_2 adsorbents are different from π-complexed adsorbents, where the active silver

on Ag/TiO_2 is Ag_2O instead of reduced Ag^0. This new type Ag/TiO_2 adsorbent can reduce sulfur content down to ppmw level without any sulfidation or activation. Besides, Ag/TiO_2 and Ag/TiO_2-Al_2O_3 adsorbents are demonstrated to be regenerated for over 10 cycles without apparent loss in sulfur removal capacities. As a result, Ag loaded TiO_2 adsorbents have promising sulfur adsorption capacities from liquid hydrocarbon fuels based on our research results. The active sites and possible sulfur removal pathway were investigated in details and will be discussed in the next section.

I.3.3. Surface acidic sites

As we mentioned before, Ag/TiO_2 and Ag/TiO_2-Al_2O_3 adsorbents are different from those adsorbents based on π-complexation. Ag is in the oxidized state as Ag_2O instead of its reduced state Ag^0. The surface sites of Ag on TiO_2 adsorbents were characterized by the combination of XPS, ESR, UV-vis spectroscopy, XRD, ammonia chemisorption and potentiometric titration. One of the main surface active sites on Ag/TiO_2 is considered as Ag^+ [94]. The interaction between thiophene compounds and Ag/TiO_2 was studied by *in situ* temperature-programmed XPS, ESR, Temperature-Programmed Desorption (TPD) and Temperature-Programmed Reaction spectroscopy (TPRS) [95-97]. Ag^+ ions on TiO_2 adsorbents are bonded to sulfur atoms under ambient conditions as illustrated in Figure I.8. Also, surface acidity and the role of surface hydroxyl (-OH) groups were reported for the novel Ag loaded TiO_2 based adsorbents [98]. Both Bronsted and Lewis acid centers were observed by IR spectroscopy. One of the possible sulfur removal mechanisms for Ag/TiO_2 and Ag/TiO_2-Al_2O_3 at room temperature is postulated by an interaction between π electrons on sulfur molecules and acidic -OH groups on TiO_2 surface [99, 100]. The

hydroxyl groups present in TiO_2 participates in the adsorption of sulfur compounds. Active sulfur adsorption centers on Ag/TiO_2 and Ag/TiO_2-Al_2O_3 adsorbents were acidic in nature confirmed by several techniques mentioned before. Based on research results, a relationship between surface acidity and sulfur removal capacity was discovered for Ag loaded TiO_2 adsorbents. And desulfurization performance is considered to be related to the concentration of surface isolated hydroxyl groups on TiO_2 surface. Also, the addition of silver increased the Bronsted acidity of TiO_2 as well as the sulfur affinity. Organic sulfur removal pathways onto Ag/TiO_2 through Ag^+ active site and isolated -OH groups can be illustrated in Figure I.8. However, there are also possibilities of sulfur adsorption onto Ag/TiO_2 through other minor pathways. Sulfur removal pathways onto Ag/TiO_2 and Ag/TiO_2-Al_2O_3 adsorbents still need more extensive researches.

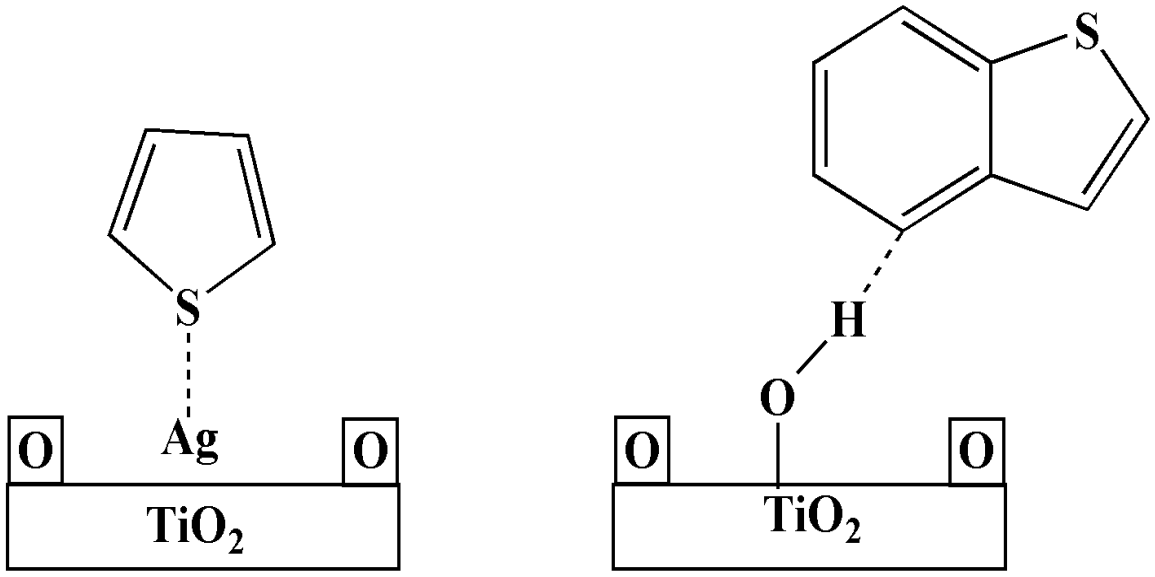

Figure I.8. Organic sulfur adsorption pathways onto Ag/TiO_2 through Ag^+ and -OH

Considering the desulfurization mechanism of Ag/TiO_2 and Ag/TiO_2-Al_2O_3 as well as the effect of UV on the surface -OH groups on TiO_2 adsorbents, further improvement on

desulfurization performance for TiO_2 based adsorbents may be achieved by UV-assisted adsorptive desulfurization process. Moreover, photo-assisted adsorptive desulfurization could be a new technology to deeply remove organic sulfur from liquid fuels.

I.4. Innovation and objectives

Although many efforts have been put on photocatalytic oxidative desulfurization (PODS) from liquid fuels, there is seldom literature showing TiO_2/UV application in adsorptive desulfurization area according to our knowledge.

One of the goals of this research is to increase the surface hydroxyl groups on TiO_2 surface by introducing UV irradiation into dynamic sulfur adsorption process. As a result, the desulfurization performance of TiO_2 will be enhanced. Different from complicated and energy-consuming technologies, low output (4 watts) ultraviolet (UV) sources have been directly applied to dynamic breakthrough process without involving any corrosive oxidative agents. No oxidative products of organic sulfur compounds are formed in the liquid phase. Highest sulfur removal capacities of TiO_2, Ag/TiO_2, and Ag/TiO_2-Al_2O_3 can be obtained during photo-assisted adsorptive desulfurization (ADS) process using the model fuel in the presence of H_2O additive. The problems caused by water additive can be simply solved by TiO_2/UV application in ADS. Effects of UV and H_2O on sulfur removal active sites on TiO_2, TiO_2-Al_2O_3, Ag/TiO_2 and Ag/TiO_2-Al_2O_3 are all studied by breakthrough experiments.

Furthermore, effects of UV irradiation and H_2O molecule on surface acidic -OH groups have been studied via *in situ* IR and XPS spectroscopy. The interaction between

organic sulfur compounds and UV-irradiated TiO_2, the possible mechanism to form more -OH on TiO_2 under UV and photo-activated hydroxyl radicals on TiO_2 surface have been also investigated and discussed in details. Possible sulfur removal pathway of benzothiophene onto TiO_2 under UV has been postulated in this research.

The innovations for this research work are as follows:

1) To improve desulfurization performance of TiO_2 based adsorbents by applying UV irradiation into dynamic sulfur adsorption system;
2) To develop a unique UV-irradiated adsorptive desulfurization process;
3) To prevent reduction in surface Bronsted acid sites caused by H_2O contaminant during adsorptive desulfurization process;
4) Investigated the mechanism to form more isolated hydroxyl groups Ti(IV)-OH by bridged -OH and bridged O under UV illumination;
5) Explored possible sulfur adsorption pathway under UV irradiation onto TiO_2 adsorbents.

II. Experimental Details

II.1. Adsorbent preparation

Anatase TiO_2 pellets (ST61120) were purchased from Saint Gobain Norpro as 3.2 mm pellets. Al_2O_3 supports were obtained from Alfa Aesar. TiO_2 and Al_2O_3 pellets were crushed and sieved to 850-1400 μm followed by drying in a convection oven for at least 6 h at 110 ℃. Calcined TiO_2 and Al_2O_3 samples were obtained by calcining dry TiO_2 and Al_2O_3 supports in a tube furnace in flowing air for 2 h at 450 ℃ prior to use. Titanium isopropoxide (97%) $C_{12}H_{28}O_4Ti$ from Alfa Aesar dissolved in isopropyl alcohol was used as titanium precursor to prepare TiO_2-Al_2O_3 mixed oxide supports. Incipient wetness impregnation method was used to disperse TiO_2 on dry Al_2O_3 supports. The concentration of impregnation solution was adjusted to obtain 10 wt% titanium metal loading on TiO_2-Al_2O_3 support. After impregnation, mixed oxide supports were dried in the oven for 6 h at 110 ℃ followed by calcination in flowing air at 550 ℃ for another 2 h. Then these TiO_2-Al_2O_3 supports were ready for following experiments.

BET surface areas and pore volumes of TiO_2, Al_2O_3, and TiO_2-Al_2O_3 adsorbents were obtained with the Quantachrome AS1 surface area and pore size analyzer. The analysis was carried out using N_2 adsorption at 77K. All samples were outgassed at 150 ℃ for 2 h for moisture removal. The sample weight was kept between 0.1-0.15 g during each analysis. The properties of these supporting materials are listed in Table II.1.

Crystalline silver nitrate was purchased from Alfa Aesar. The aqueous $AgNO_3$ solution was used as a silver precursor to disperse silver on dry TiO_2 and calcined TiO_2-Al_2O_3 supports also by means of incipient wetness impregnation. After impregnation, resulting Ag/TiO_2 particles were dried in the oven for over 6 h at 110 ℃ followed by calcination in dry air at 450 ℃ for 2 h in a tube furnace. And the calcination temperature for Ag/TiO_2-Al_2O_3 is 550 ℃. Silver weight loadings on supports were maintained at 4 wt% for Ag/TiO_2 and 10 wt% for Ag/TiO_2-Al_2O_3.

Table II.1. Properties of TiO_2, Al_2O_3 and TiO_2-Al_2O_3 supports

Supports	Vendor	BET Surface Area (m^2/g)	Pore Volume (cc/g)
TiO_2	Saint Gobain Norpro	163	0.45
Al_2O_3	Alfa Aesar	267	1.06
TiO_2-Al_2O_3	-	237	0.75

II.2. Desulfurization experiments

Breakthrough capacities and saturation capacities of TiO_2 based adsorbents were determined by breakthrough experiments. Desulfurization performance of adsorbents was evaluated by sulfur adsorption studies with and without UV. Breakthrough experiments were all carried out under ambient temperature and atmospheric pressure. 10.0 g of adsorbents was used in each breakthrough experiment. And TiO_2, TiO_2-Al_2O_3, Ag/TiO_2 and Ag/TiO_2-Al_2O_3 adsorbents were prepared by the procedures mentioned in section II.1. Vertical packed column configuration was used for sulfur adsorption. The inner diameter

and length of the quartz tube reactor were 16 mm and 62 mm respectively. Both ends of the quartz tube were supported by quartz wool. After loading the adsorbents into the packed bed reactor, the adsorbent bed was first treated with dry N_2 for 1 h in order to remove any packed moisture, O_2, and other impurities. After N_2 treatment, the model fuel or hydrocarbon fuel was pumped into the packed bed reactor by a peristaltic pump at a flow rate of 0.5 mL/min (LHSV=2 h^{-1}). Challenge fuels flowed upward from the bottom of the bed to the top. This configuration can minimize tube channeling and wall slip effects and ensure consistent experimental data.

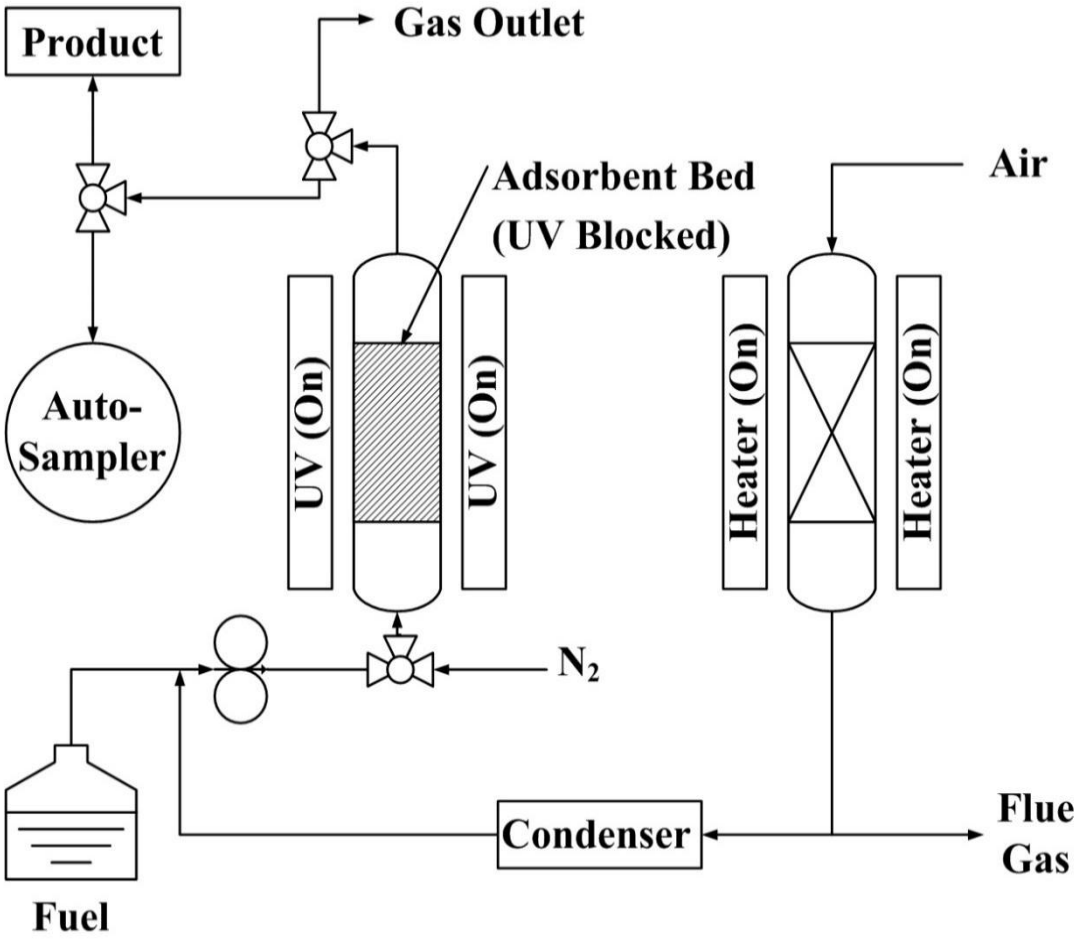

Figure II.1. Breakthrough experimental setup without UV irradiation

For breakthrough experiments carried out without UV, the whole reactor bed was wrapped with alumina foil to shield against UV light while UV lamps were turned on. The setup for breakthrough study without UV is shown in Figure II.1. This setup ruled out the effect of temperature rise on adsorbents' sulfur removal capacities when compared with UV-assisted breakthrough experiments. The temperature in the reactor's outside wall was measured by a thermal couple. For breakthrough experiments under UV irradiation, a clear quartz tube was used to let UV light penetrate into the packed bed. Figure II.2 shows the setup for UV-assisted sulfur removal process and thermal regeneration unit. Two UV lamps were placed symmetrically on both sides of the packed reactor for uniform distribution of illumination. Once the model fuel contacted the bottom of the adsorbents, UV lights were turned on immediately.

For regeneration process, used adsorbent bed was regenerated using the thermal system after the adsorption step. Sulfur saturated bed was heated in flowing air to 220 ℃ and held for 2 h in order to ensure the vaporization of fuels in adsorbent's pores. Then the bed temperature was raised to 450 ℃ and held for another 2 h for adsorbent regeneration. The reactor bed was cooled down in dry air. Packed bed reactor was then treated with N_2 for 1 h and ready for next adsorption-regeneration cycle.

For all breakthrough experiments, bed output samples were collected at regular time intervals and analyzed by Antek 9000VS Total Sulfur Analyzer. The outlet total sulfur concentration at time t (C_i) was first normalized by initial sulfur concentration (C_0) in the model fuel. Breakthrough curves were then obtained by plotting C_i/C_0 against time t. Breakthrough capacity was calculated at threshold limit at $C_b/C_0 = 0.01$ by the following equation:

$$q_b = \frac{\rho_f V_f t_b (C_0 - C_b)}{1000m}$$

Where,

$q_b =$ breakthrough capacity (mg S/g adsorbent)

$\rho_f =$ density of fuel (g/mL)

$V_f =$ volumetric flow rate (mL/min)

$t_b =$ breakthrough time (min)

$C_0 =$ initial sulfur concentration (ppmw S)

$C_b =$ threshold sulfur concentration (ppmw S)

$m =$ adsorbent weight (g)

And saturation capacity was obtained by integration of breakthrough curves using following equation:

$$q_{sat} = \frac{\rho_f V_f \sum_n \left(C_0 - \frac{C_n + C_{n-1}}{2}\right)(t_n - t_{n-1})}{1000m}$$

Where,

$q_{sat} =$ saturation capacity (mg S/g adsorbent)

$\rho_f =$ density of fuel (g/mL)

$V_f =$ volumetric flow rate (mL/min)

$t_n =$ cumulative time (min)

C_0 = initial sulfur concentration (ppmw S)

C_n = sulfur concentration at t_n (ppmw S)

m = adsorbent weight (g)

The density of model fuels varied between 0.70-0.75 g/mL, and that of commercial fuels was between 0.80-0.85 g/mL. All the values were calculated experimentally.

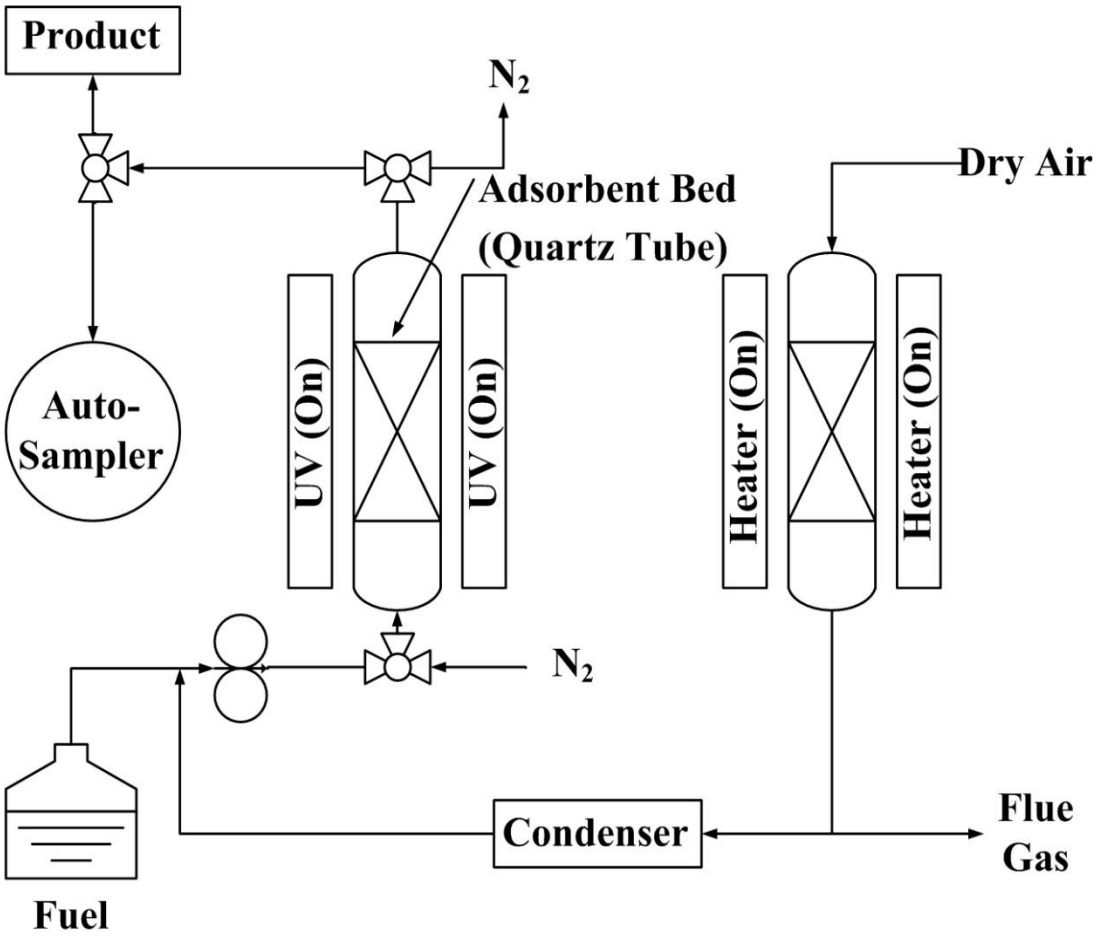

Figure II.2. UV-assisted breakthrough setup and thermal regeneration unit

For the desulfurization experiments, static saturation tests were also carried out in order to assess the sulfur adsorption capacities of the adsorbents. In each saturation test,

the fuel was mixed with the adsorbent. The fuel to adsorbent ratio was 20 mL/g sorbent. The mixture was agitated mechanically for 48 h at ambient conditions in order to reach the equilibrium state. The equilibrated fuel samples were then analyzed to measure the final total sulfur contents. The equilibrium saturation capacity was calculated from the following formula:

$$Q_{Sat} = \frac{(1 - C_{Sat}/C_0)\rho V C_0}{1000}$$

Where,

$$Q_{Sat} = \text{ equilibrium saturation capacity (mg S/g adsorbent)}$$

$$C_{Sat} = \text{ sulfur concentration of fuel after saturation (ppmw)}$$

$$C_0 = \text{ initial sulfur concentration of fuel (ppmw)}$$

$$\rho = \text{ density of fuel (g/mL)}$$

$$V = \text{ volume of fuel/adsorbent weight (mL/g adsorbent)}$$

All values were calculated experimentally. The selectivity towards different sulfur compounds by saturation tests was carried out at room temperature and ambient pressure. The adsorption equilibrium isotherms were studied by saturation experiments under atmospheric pressure but at different temperatures.

II.3. Challenge fuels

For breakthrough experiments, model fuels containing 3500 ppmw total sulfur were prepared by mixing benzothiophene with n-octane. Benzothiophene (98%) and n-octane

(97%) were purchased from Alfa Aesar and Acros Organics separately. In order to study the effect of H_2O molecules on sulfur removal performance of TiO_2 based adsorbents during ADS, distilled water was added to model fuels as the additive. JP5 and JP8 with a total sulfur concentration of 1172 ppmw and 630 ppmw were obtained from NAVSEA Philadelphia and TARDEK respectively.

II.4. UV source and lamp test unit

Compact UV lamps were purchased from UVP, LLC. The 4 watt UV source is at 365 nm. The fraction of light absorbed in the unit, light intensity, and lamp calibration can be determined by using the lamp test unit [101]. The unit setup is shown in Figure II.3.

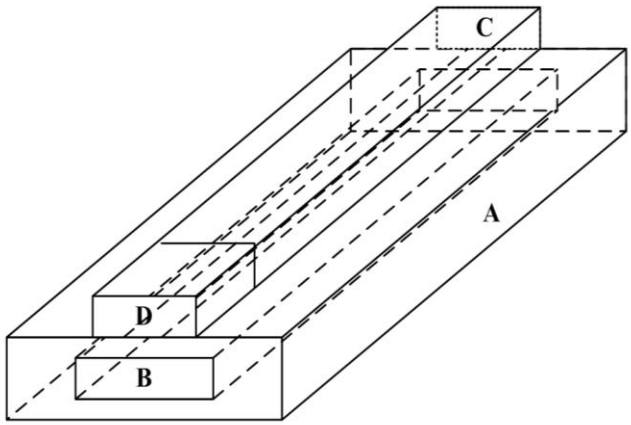

Figure II.3. Lamp test unit: (A) lamp holder with inner surface covered with alumina foil and 1-cm opening at the top through whole tunnel; (B) UV lamp; (C) tunnel allowing the radiometer to be placed; (D) UVX radiometer placed at a fixed distance from the light source (reproduced from B. Serrano et al., Industrial Engineering Chemistry Research, 1997 [101])

II.5. Sulfur analysis

The method to determine the total sulfur concentration in liquid hydrocarbon fuels is by total sulfur analyzer (TSA) instrument. The operation principle of the total sulfur analyzer (TSA) is based on combustion of organic sulfur compounds to SO_2 and the quantitative measurement of SO_2 using the intensity of UV fluorescence of the SO_2.

Total sulfur concentrations in liquid fuel samples were all analyzing by Antek 9000S Total Sulfur Analyzer (TSA). Ultra high purity (UHP) oxygen (O_2) and helium (He) from Airgas South were used as pyro and carrier gasses respectively. The lowest detection limit of this equipment was 200 ppbw. This instrument was calibrated using standard samples of subsequent dilutions of hydrocarbon fuels.

II.6. Infrared spectroscopy

Effects of UV irradiation and H_2O molecules on TiO_2 surface sites were analyzed via *in situ* Infrared (IR) Spectroscopy. For infrared analysis, 50.0 mg dry TiO_2 power in 251-354 μm was pressed into a self-supporting pellet by Carver hydraulic press at 16000 psi followed by calcination at 450 ℃ for 2 h in dry air. After loading calcined TiO_2 pellet into a customized IR cell equipped with ZnSe windows, the sample cell was heated at 200 ℃ for 1 h in flowing dry air and then treated with N_2 for another 1 h at room temperature. The IR cell was evacuated to 100 mTorr before infrared analysis. To study the effect of UV irradiation on TiO_2 surface, UV sources were applied directly on IR cell during evacuation step. In order to study the effect of H_2O molecules on TiO_2 surface active sites in the absence and in the presence of UV, the IR cell was treated with water

vapor by N_2 bubbling with or without UV irradiation for a certain time followed by evacuation. Treatment with H_2O and UV for IR analysis were all performed *in situ*. Experimental setup for in situ infrared analysis is shown in Figure II.4.

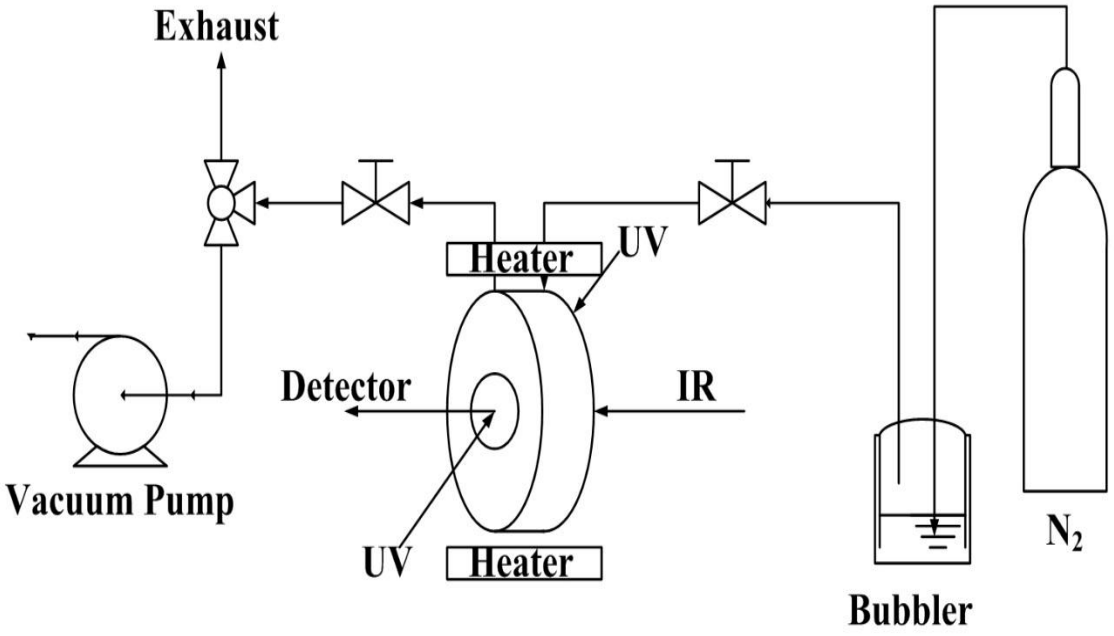

Figure II.4. Experimental setup for *in situ* infrared (IR) analysis

II.7. X-ray spectroscopy

All XPS data were collected by AXIS Ultra delay lines detector (DLD) X-ray photoelectron spectrometer (XPS) from Kratos analytical Ltd. The end station consists of a fast entry load lock, a sample treatment chamber (STC) and a sample analysis chamber (SAC) as shown in Figure II.5. Calcined TiO_2 and Ag/TiO_2 samples were analyzed in SAC under 10^{-9} Torr. To study the effect of UV irradiation on TiO_2 and Ag/TiO_2 sorbents, samples were first exposed to UVL-28 UV lamp purchased from UVP for 2 h through the

quartz window in load lock under 10^{-8} Torr before entering the analysis chamber. The typical radiation value measured inside sample treatment chamber (SAC) is 1.2 mW/cm^2. A monochromatic Al Kα X-ray source was used as the photon source. High resolution spectra were obtained for C 1s, O 1s, Ti 2p and Ag 3d using a passing energy of 20 eV. The binding energy shifts due to surface charging were corrected using the C 1s level at 284.6 eV. Core level peaks of O 1s, Ti 2p, and Ag 3d were deconvoluted by using Gaussian-Lorentzian (20%) peaks.

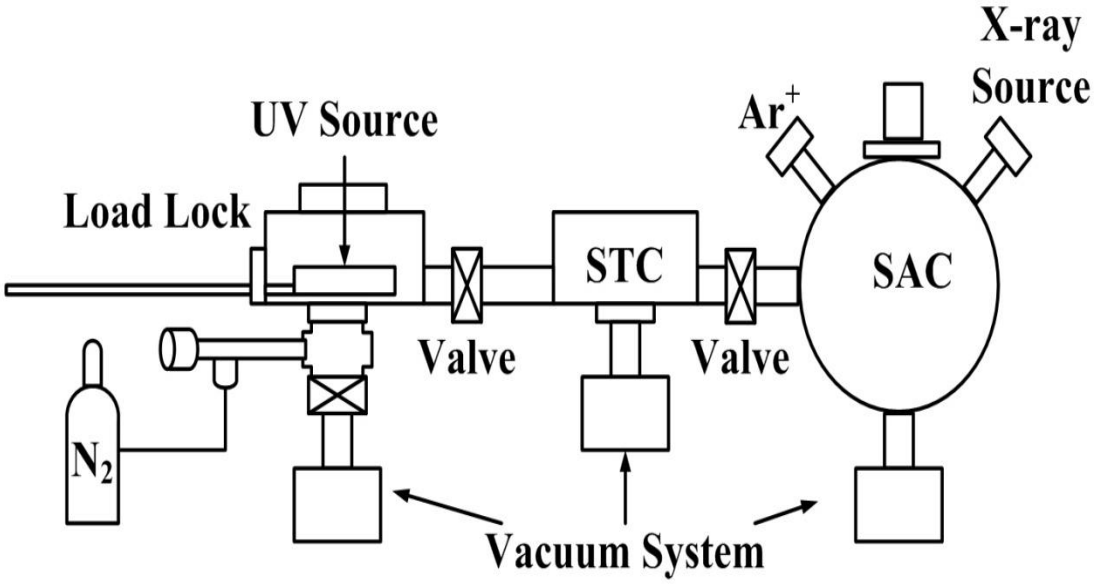

Figure II.5. Configuration of XPS apparatus equipped with a UV lamp

II.8. Measurement of hydroxyl radicals

The relative concentration of surface hydroxyl radicals was measured by fluorescence technique using terephthalic acid (TA). The reaction between hydroxyl radicals and

terephthalic acid is shown in Figure II.6. Highly fluorescent reaction product which was 2-hydroxyterephthalic acid was formed through such reaction [102].

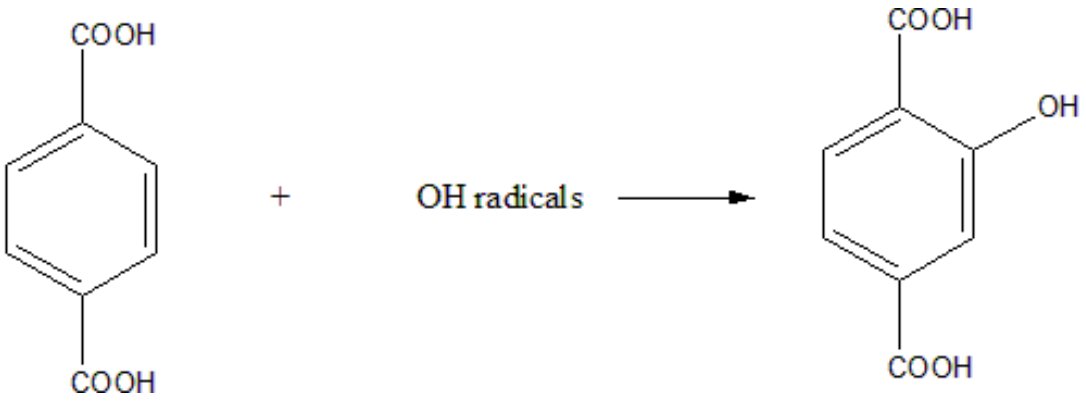

Figure II.6. Reaction between hydroxyl radicals and terephthalic acid (TA)

Terephthalic acid was purchased from Alfa Aesar and sodium hydroxide (NaOH) was purchased from Fisher Scientific. Measurement of hydroxyl radicals was carried out in a continuous flow tubular reactor as shown in Figure II.7. Terephthalic acid was dissolved in 0.2 M NaOH aqueous solution forming a well-mixed solution with a concentration of 0.05 M. 10.0 g calcined TiO_2 adsorbents were loaded into a fixed bed reactor. 100 mL terephthalic acid in NaOH mixture was pumped into the packed column from the bottom of the reactor to the top. Then the bed outlet liquid went back to the mixture container. Experiments were carried out without UV and with UV using calcined TiO_2. Also, the measurement was carried out without UV illumination using UV-treated TiO_2. The relative concentration of hydroxyl radicals can be determined by intensities of fluorescence spectra of generated 2-hydroxyterephthalic acid products under different experimental conditions. The detailed configuration of fluorescence spectroscopy setup is shown in Figure II.8.

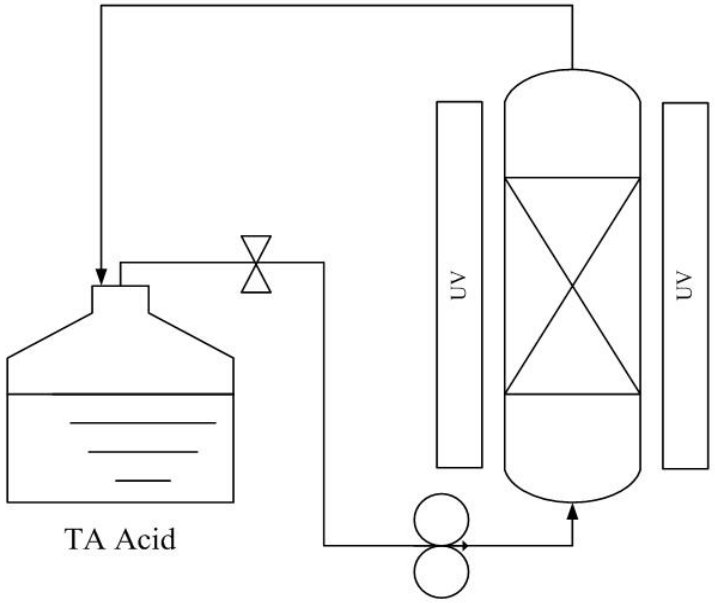

Figure II.7. Continuous flow tubular setup to determine relative concentration of surface hydroxyl radicals on TiO_2

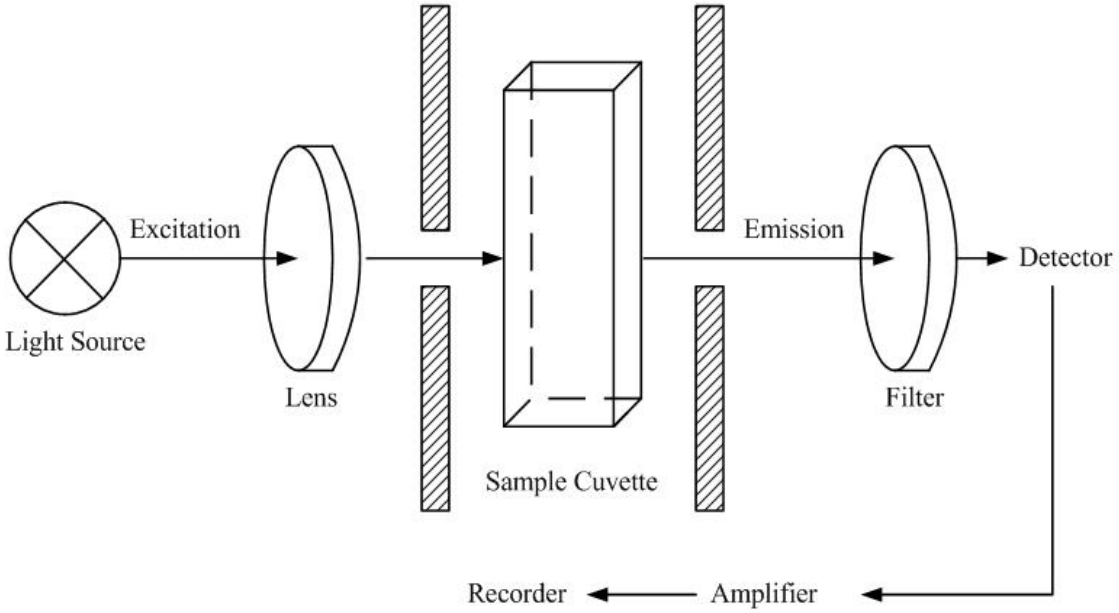

Figure II.8. Configuration for fluorescence spectroscopy

II.9. UV-vis DRS Spectroscopy

Commercial AvaSpec-2048 UV-vis spectrometer was used for UV Diffuse Reflectance Spectroscopy (UV-DRS) measurements. Diffuse reflectance UV-vis spectroscopy in the reflectance mode was carried out in the wavelength ranging 200-800 nm. The UV-vis DRS immersion probe was directly inserted into the adsorbent sample in a closed quartz vessel under a dark environment at room temperature during the analysis. The collected UV-DRS spectra were analyzed on the basis of Kubelka-Munk equation to calculate the values of band gap for TiO_2, TiO_2–Al_2O_3, Ag/TiO_2 and Ag/TiO_2–Al_2O_3 at room temperature by the following formula:

$$F(R) = \frac{k}{s} = \frac{(1-R)^2}{2R}$$

Where,

$F(R) =$ Kubelka-Munk function

$k =$ absorption coefficient

$s =$ scattering coefficient

$R =$ reflectance

III. UV-assisted Desulfurization of TiO_2 Adsorbents

III.1. Introduction

Desulfurization breakthrough studies were carried out in different conditions under atmospheric pressure using TiO_2 based supports. The effect of UV irradiation on sulfur removal capacities was observed first using calcined TiO_2 with both model fuels and jet fuels. Desulfurization performance of UV-irradiated TiO_2 was also studied to confirm that the effect of UV was on the solid phase. It was observed that UV irradiation before and during breakthrough experiments both enhanced TiO_2's sulfur removal capacities. The negative effect of H_2O molecules on acid based adsorbents has been reported by many studies. Thus, desulfurization performance of TiO_2 adsorbent without UV was evaluated by studies using model fuels containing H_2O additive. Photocatalytic reactions of H_2O molecules on TiO_2 surface have been studied for years. Both experimental data and simulation results showed that hydroxyl groups can generate on TiO_2 surface under UV in the presence of H_2O. As a result, breakthrough experiments for calcined TiO_2 were then carried out under UV condition using model fuels containing H_2O additive.

For calcined TiO_2, regeneration was carried out in dry air. Adsorption without and with UV was performed for 5 cycles using regenerated adsorbents. Moreover, the stability of photo-induced sulfur removal species was investigated by multi-cycle studies using UV-irradiated TiO_2 adsorbents.

Finally, breakthrough studies with UV illumination and water molecules have been studied for TiO_2-Al_2O_3 mixed oxides. UV-assisted desulfurization has been demonstrated to be an effective process to efficiently remove organosulfur using TiO_2 based adsorbents.

III.2. Effect of UV irradiation on TiO_2

The effect of UV on dynamic desulfurization process was evaluated using calcined TiO_2 adsorbents. First, the effect of temperature rise on desulfurization capacities caused by UV irradiation was studied.

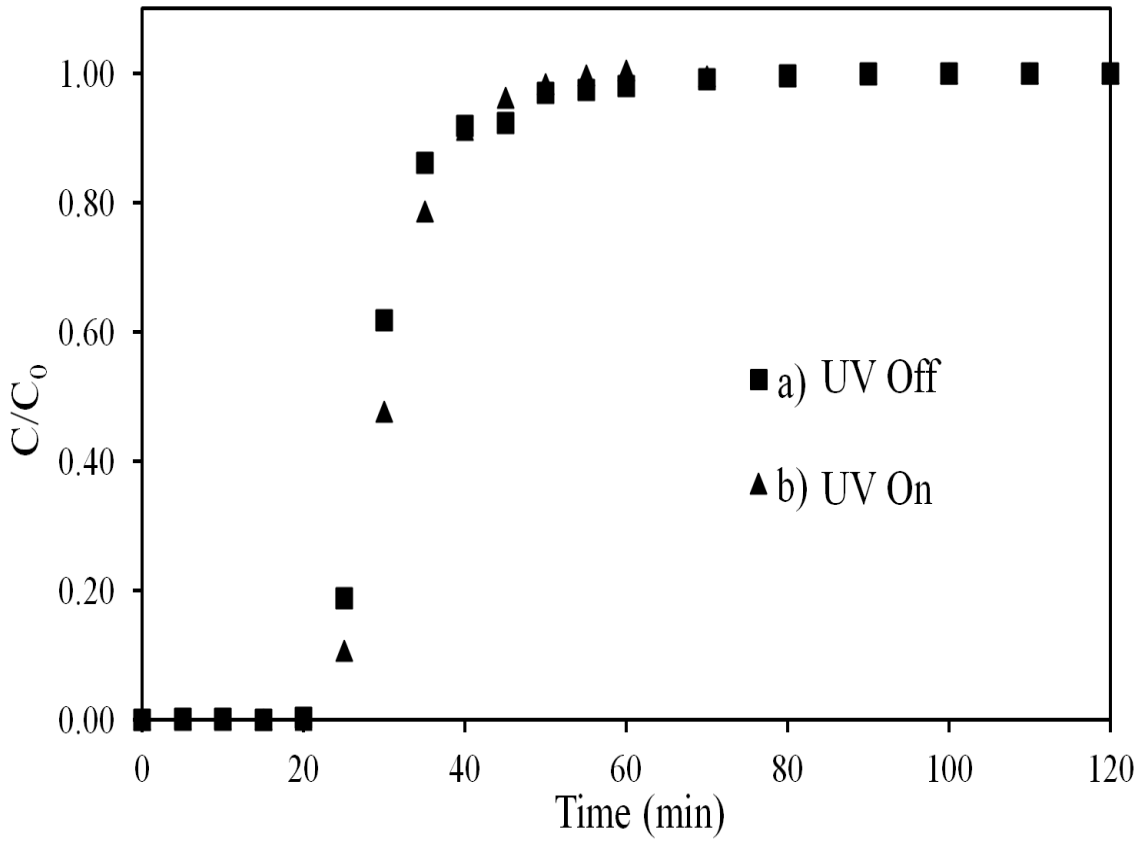

Figure III.1. The effect of temperature rise on desulfurization performance of TiO_2 caused by UV irradiation

Two breakthrough experiments of TiO_2 were carried out using the setup with the quartz tube painted black as shown in Figure II.1. One experiment was carried out with UV lamps off and the other was with UV lamps on. The results are shown in Figure III.1. Judging from the curves in Figure III.1, there was a very small difference between these two studies. Sulfur removal capacities were barely affected by the thermal effect. As a result, the effect of temperature rise on desulfurization performance caused by UV lamps can be neglected. After eliminating the thermal effect caused by UV irradiation, the effect of photo-irradiation on sulfur removal performance was studied.

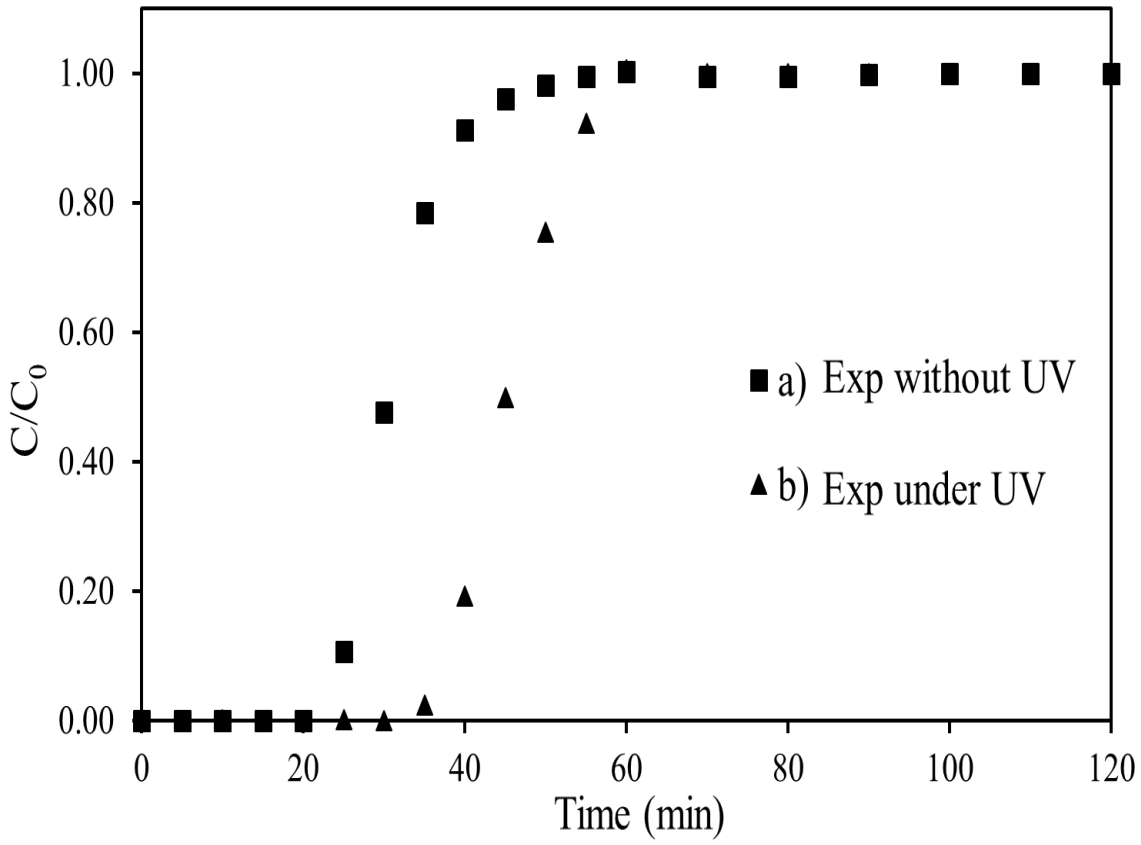

Figure III.2. Breakthrough experiments of calcined TiO_2 carried out a) without UV; b) with UV irradiation (bed weight: 10.0 g, LHSV: 2 h^{-1}, S concentration: 3500 ppmw S; UV wavelength: 365 nm)

In order to keep the same conditions, experiments without UV were all carried out using the setup with UV lights on as shown in Figure II.1. Lamp test unit was employed to measure UV intensity in a certain distance from the UV light. The typical radiation flux at 1 cm from UV light source was measured varying from 1800 to 2000 $\mu W/cm^2$. Capacities from experiments with and without UV were obtained and compared in order to study the effect of UV on desulfurization performance. Breakthrough curves obtained from experiments with and without UV of calcined TiO_2 are shown in Figure III.2.

At breakthrough threshold concentration (C/C_0=0.01), calcined TiO_2 only showed the sulfur adsorptive capacity of 2.45 mg S/g sorbent without UV irradiation calculated from breakthrough curves. However, TiO_2's breakthrough capacity increased to 4.05 mg S/g sorbent for the desulfurization process under UV environment. Also, the saturation capacity increased from 3.90 to 5.63 mg S/g sorbent for the UV-assisted sulfur removal process. The summary of breakthrough and saturation capacities of calcined TiO_2 estimated from breakthrough studies is listed in Table III.1.

Table III.1. Sulfur removal capacities of calcined TiO_2 during breakthrough experiments with and without UV

Operation Condition	ADS without UV	UV-assisted ADS
Breakthrough Capacity (mg S/g adsorbent)	2.45	4.05
Saturation Capacity (mg S/g adsorbent)	3.90	5.63

Based on the results got from experiments, UV illumination was demonstrated to have a positive effect on TiO_2's sulfur removal performance. However, oxidative reactions of aromatic sulfur compounds could also occur under photo-illumination in the liquid phase. Thus, in order to confirm that the improvement in sulfur removal performance was due to the photo-assisted effect on the solid phase, another set of experiment was carried out.

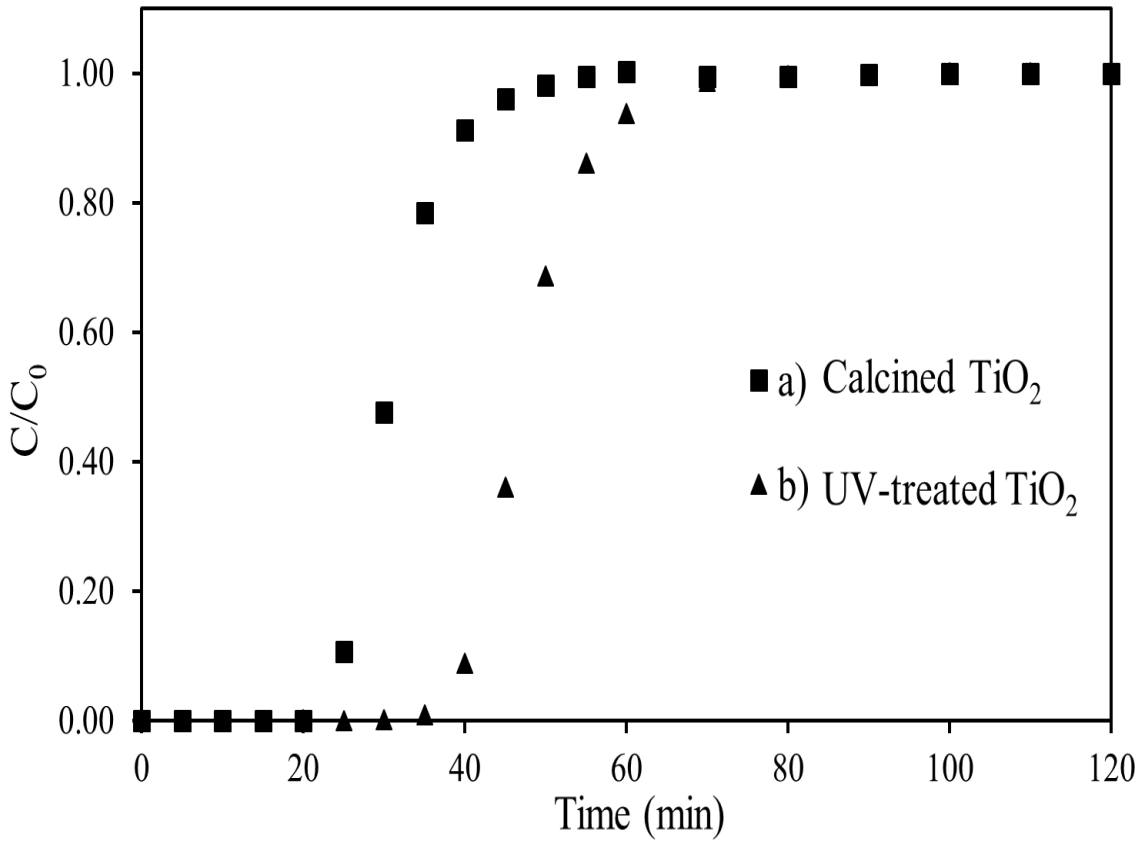

Figure III.3. Breakthrough experiments without UV irradiation using a) calcined TiO_2; b) UV-treated TiO_2 (bed weight: 10.0 g, LHSV: 2 h^{-1}, S concentration: 3500 ppmw S; UV wavelength: 365 nm)

Breakthrough experiments were then carried out using calcined TiO_2 and UV pre-treated TiO_2 adsorbents without UV irradiation. For UV-treated TiO_2, the packed bed loaded with calcined TiO_2 was first exposed to UV irradiation for 2 h after N_2 treatment. After pretreatment, breakthrough experiment using this UV-treated TiO_2 samples was carried out without any UV irradiation. Breakthrough results obtained from experiments without UV using calcined TiO_2 and UV-treated TiO_2 are both plotted in Figure III.3.

Breakthrough and saturation capacities for UV-treated TiO_2 adsorbents were 4.29 and 5.95 mg S/g individually as listed in Table III.2. Both breakthrough and saturation capacities for UV-treated TiO_2 samples were much higher than the capacities of calcined TiO_2 adsorbents. The results clearly indicated that great improvement in desulfurization performance was caused by the photo-modification on TiO_2 surface instead of the liquid phase. As we mentioned before, the sulfur removal mechanism was related with surface hydroxyl groups on TiO_2 surface. As a result, more sulfur removal active sites were considered to be formed under UV irradiation which finally increased the sulfur adsorptive capacities of TiO_2 adsorbents.

Table III.2. Sulfur removal capacities using calcined TiO_2 and UV-treated TiO_2

Operation Condition	Calcined TiO_2	UV-treated TiO_2
Breakthrough Capacity (mg S/g adsorbent)	2.45	4.29
Saturation Capacity (mg S/g adsorbent)	3.90	5.95

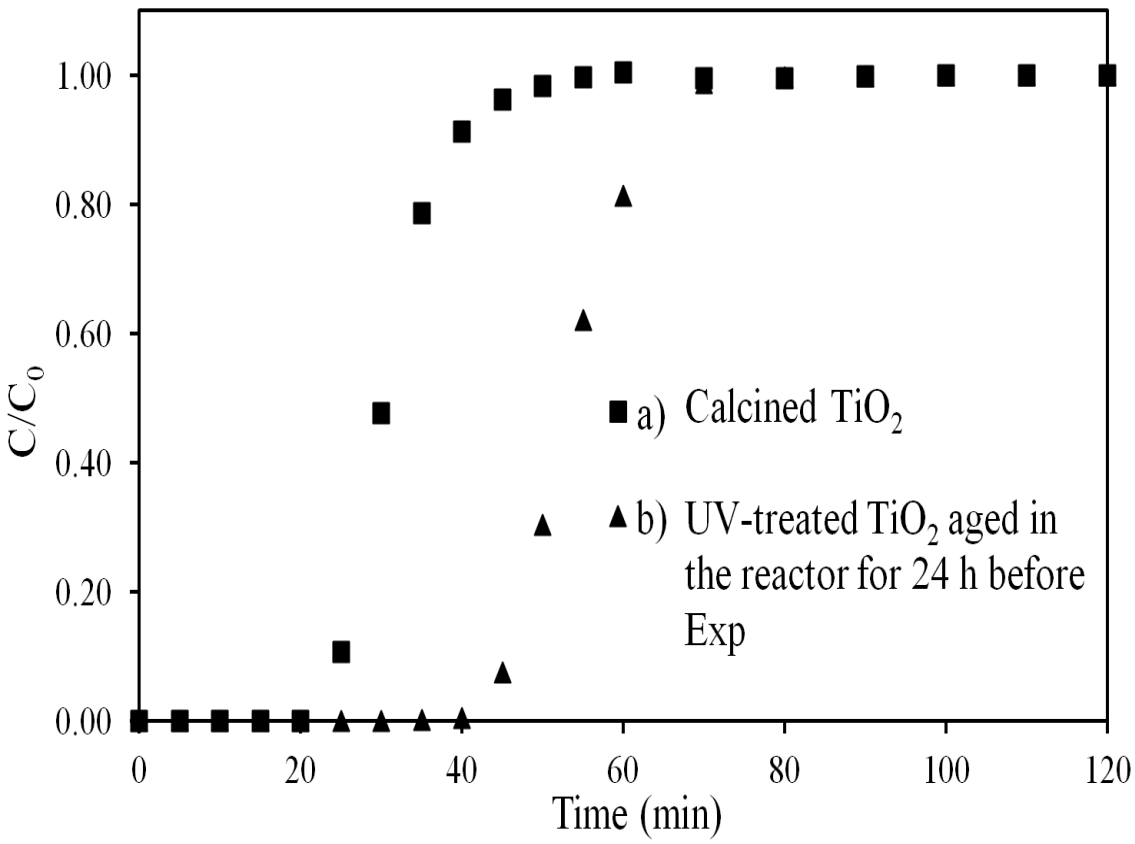

Figure III.4. Breakthrough experiments without UV using a) calcined TiO_2; b) UV pre-treated TiO_2 aged in reactor for 24 h (bed weight: 10.0 g, LHSV: 2 h^{-1}, S concentration: 3500 ppmw S; UV wavelength: 365 nm)

To further study the effect of UV treatment on TiO_2 adsorbent, another breakthrough experiment was carried out using these UV pre-treated TiO_2 adsorbents. Calcined TiO_2 adsorbents were loaded into packed bed reactor followed by N_2 treatment. Then UV lamps were turned on to treat calcined TiO_2 inside the reactor for 2 h. After the UV treatment, this UV-treated TiO_2 sample was left in the reactor and aged for 24 h without photo-irradiation followed by breakthrough experiment without UV. Breakthrough results obtained from experiments without UV irradiation using calcined TiO_2 and UV-treated TiO_2 aged for 24 h are both plotted in Figure III.4. The breakthrough and

saturation capacities for UV-treated TiO_2 adsorbents aged for 24 h were 4.29 and 6.00 mg S/g calculated from breakthrough curves. After aging for 24 h in packed bed reactor under ambient conditions, the desulfurization performance of UV pre-treated TiO_2 adsorbents maintained excellently. There was no apparent difference in sulfur removal capacities between fresh and aged UV-treated TiO_2 samples. These results indicated that the active sites formed under UV on TiO_2 surface were quite stable under room temperature and atmospheric pressure.

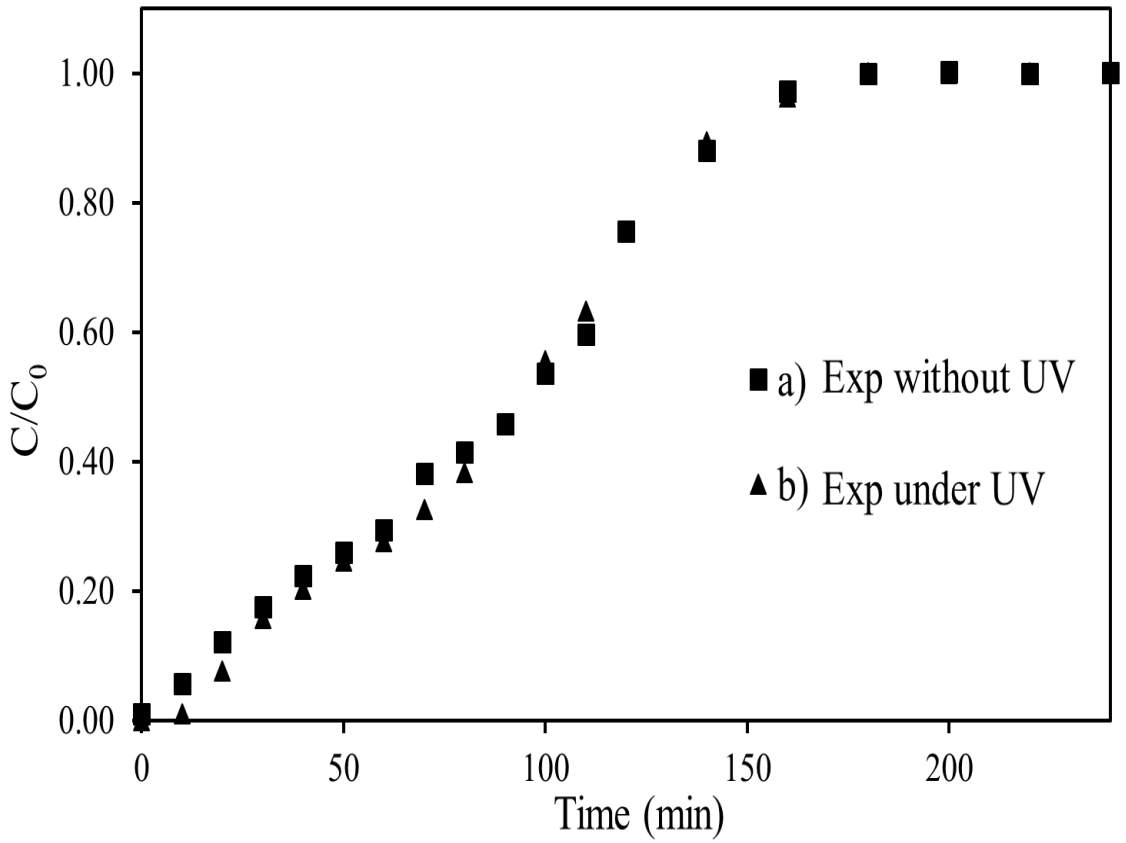

Figure III.5. Desulfurization performance of calcined TiO_2 using JP8 during breakthrough a) without UV; b) with UV (bed weight: 10.0 g, LHSV: 2 h^{-1}, S concentration: 630 ppmw S; UV wavelength: 365 nm)

Finally, the desulfurization performance of calcined TiO_2 adsorbents was tested using jet fuel JP8 by breakthrough experiments with and without UV irradiation. However, the desulfurization performance for JP8 of TiO_2 adsorbents only improved slightly under UV condition as shown in Figure III.5. The effect of UV on sulfur removal performance is not apparent when using JP8 as real challenge fuel. The additives, the complicated organosulfur components and other non-sulfur aromatic compounds in real fuels might affect the final results. Those active sites generated under UV could be killed by additives and other components in real hydrocarbon fuels. In order to gain more details, competitive adsorption during UV-assisted sulfur removal process with different organic sulfur and aromatic compounds needed to be studied in future research work.

III.3. Effect of H_2O molecules on TiO_2

III.3.1. Effect of H_2O in the absence of UV

Several components as additives in fuels can affect the sulfur removal capacities of acid based adsorbents. Water is commonly present in almost all hydrocarbon degradation products and Fischer-Tropsch synthesis. Adsorption of H_2O molecules onto TiO_2 surfaces and the reactions between H_2O and surface sites on TiO_2 have been studied by many researchers. In order to study the effect of H_2O on desulfurization performance of TiO_2 adsorbents, distilled water (1000 ppmw) was added as a fuel additive to the model fuel during sulfur removal experiments with and without UV irradiation. In other words, desulfurization studies were carried out using the model fuel containing 3500 ppmw sulfur with 1000 ppmw H_2O. The sulfur in the model fuel was benzothiophene. At first,

the effect of H_2O on TiO_2 during sulfur removal process was only studied without UV irradiation.

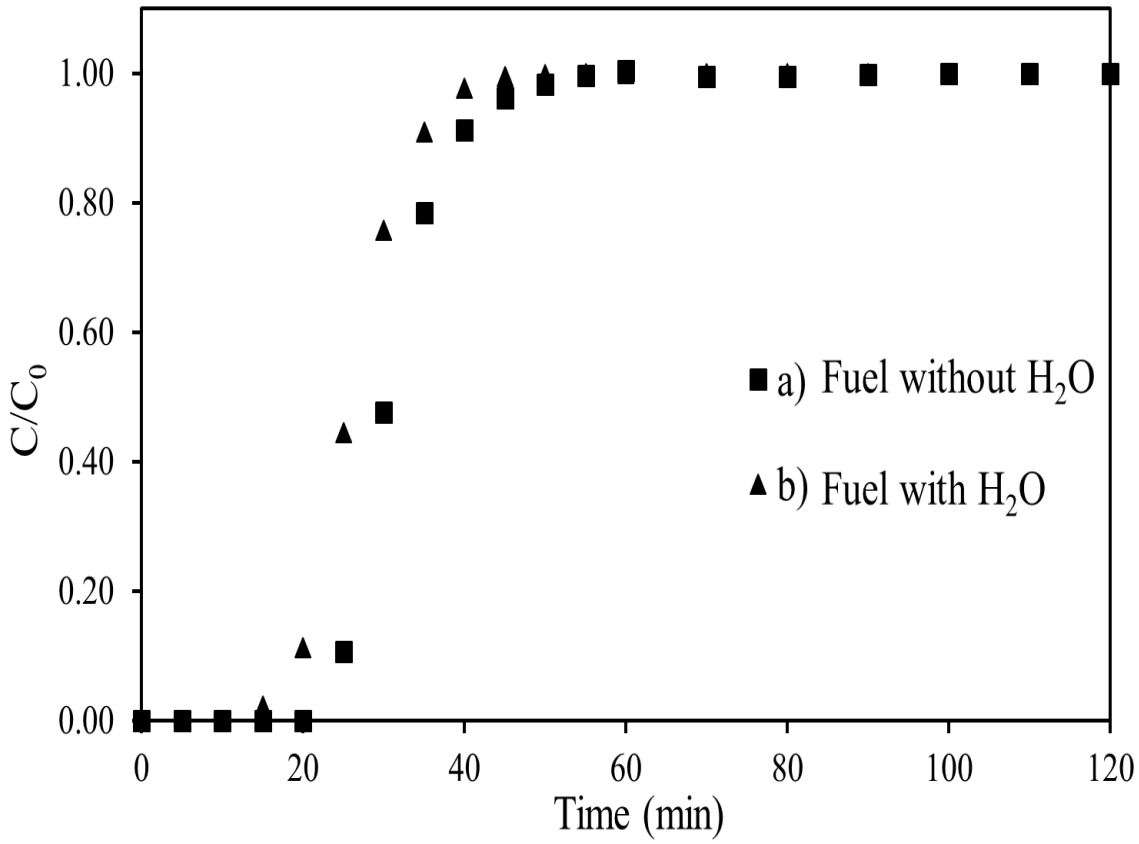

Figure III.6. Breakthrough performance for TiO_2 using model fuel containing a) no H_2O; b) 1000 ppmw H_2O (bed weight: 10.0 g, LHSV: 2 h^{-1}, S concentration: 3500 ppmw)

An apparent loss of sulfur removal capacities of TiO_2 was observed when adding water to the model fuel during desulfurization as shown in Figure III.6. Details on sulfur adsorption capacities obtained from the curves in Figure III.6 are listed on Table III.3. From the data, we can see that both breakthrough and saturation capacities decreased when H_2O was present in the liquid model fuel. Water as fuel additive reduced sulfur removal capacities of calcined TiO_2 adsorbents during the sulfur adsorptive process in the

absence of photo-irradiation. The interaction between H_2O and TiO_2's active sites were then studied in details via *in situ* IR. It was observed by many studies that water molecules had negative effects on TiO_2 adsorbents. Research is still being carried out to discover the interactions between H_2O and TiO_2's surface sites.

Table III.3. Sulfur capacities of TiO_2 adsorbents using model fuels during breakthrough studies without UV

Model Fuel Condition	No H_2O	With 1000 ppmw H_2O
Breakthrough Capacity (mg S/g adsorbent)	2.45	1.59
Saturation Capacity (mg S/g adsorbent)	3.90	3.27

The negative effect on sulfur removal performance might be attributed to the effect of water on the surface acidity of TiO_2 based materials according to some studies [103]. Some research results showed that trace amount of H_2O reduced a certain number of available Bronsted sites on TiO_2 surfaces [104]. And a large amount of water could form extra water layer on adsorbent's surface to block the further interaction between adsorbates and adsorbents [105]. Also many studies showed that H_2O molecules would compete with adsorbates for acid sites on TiO_2 surface which affected the performance of these adsorbents [106]. Based on both experimental studies and computational results, water molecules could reduce surface -OH groups on TiO_2 as well as compete with organosulfur for active acid sites during desulfurization. Thus, sulfur removal capacities of TiO_2 will be reduced with H_2O in desulfurization system.

III.3.2. Desulfurization performance in the presence of H_2O and UV

However, different trending was observed in this study when adding H_2O into the model fuel during UV-irradiated breakthrough experiments for TiO_2 adsorbents. Desulfurization performance of calcined TiO_2 was tested by sulfur adsorption studies without and with UV using model fuels containing 1000 ppmw H_2O. And the final resulting curves are shown in Figure III.7. Moreover, the breakthrough curve for desulfurization process without UV using the model fuel in the absence of H_2O is also shown in Figure III.7 for reference.

Table III.4. Effects of H_2O and UV on sulfur capacities of TiO_2 adsorbents

Operation Conditions	No UV, No H_2O	No UV, With H_2O	With UV and H_2O
Breakthrough Capacity (mg S/g adsorbent)	2.45	1.59	4.91
Saturation Capacity (mg S/g adsorbent)	3.90	3.27	6.20

For UV-assisted adsorptive desulfurization process, highest sulfur removal capacities were obtained for TiO_2 adding H_2O into the model fuel as indicated in Figure III.7. The capacities estimated from breakthrough curves in this section are listed in Table III.4. Judging from the curves and capacities, UV irradiation along with H_2O improved TiO_2's desulfurization performance dramatically. Both breakthrough and saturation capacities were increased by about 50% when UV was applied during the sulfur removal process. Furthermore, the combination of UV and H_2O worked even better than TiO_2/UV system.

Summary of breakthrough and saturation capacities for TiO_2 adsorbents under different conditions are listed in Table III.5.

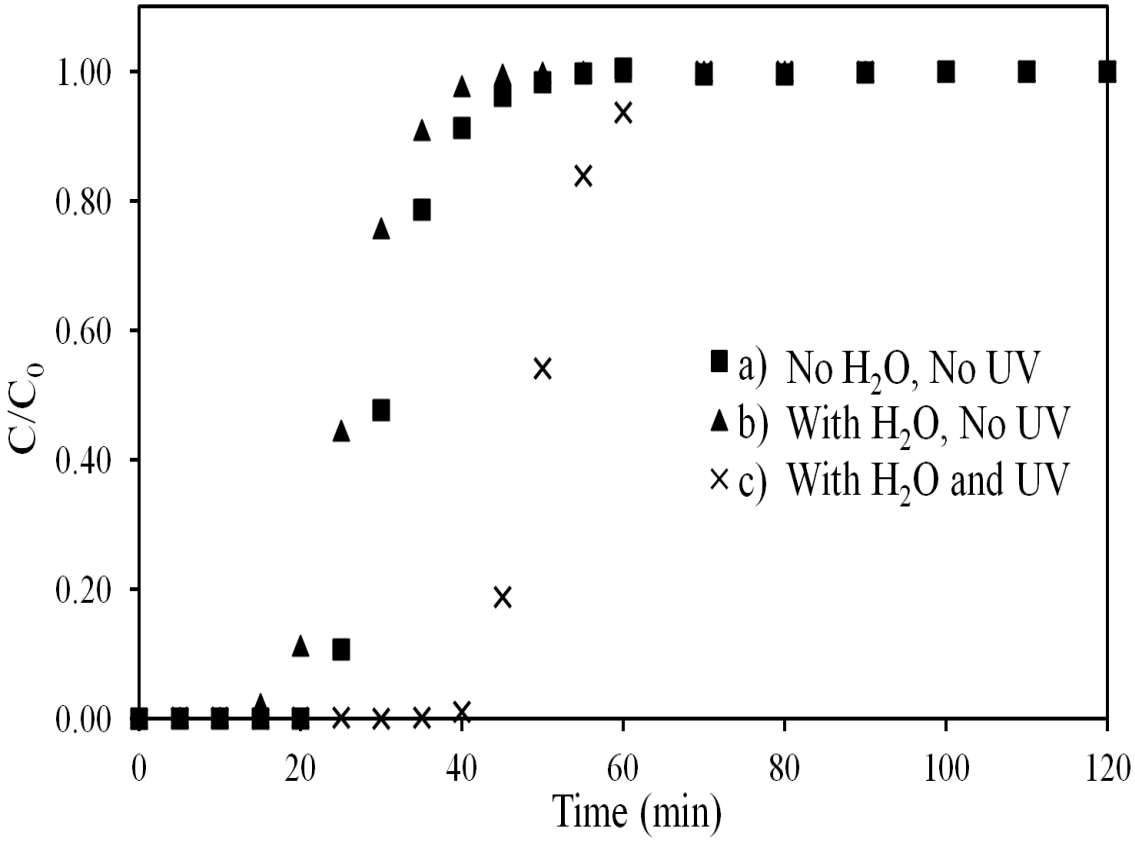

Figure III.7. Sulfur removal capacities of TiO_2 from a) the experiment without UV using a model fuel without H_2O; b) the experiment without UV using a model fuel containing H_2O; c) study under UV using a model fuel with H_2O (adsorbent weight: 10.0 g, LHSV: 2 h^{-1}, S concentration: 3500 ppmw S, H_2O concentration: 1000 ppmw)

For TiO_2, experimental and theoretical results indicated that H_2O molecules could react with oxygen vacancies and bridged -OH groups, or even interact with Ti^{4+} sites under certain circumstance, giving rise to chemisorbed isolated -OH groups [107-109]. Thus, the improvement in desulfurization performance was possibly caused by the

formation of more Ti(IV)-OH groups on TiO_2's surface in the presence of H_2O under UV irradiation. Details on surface hydroxyl groups on TiO_2 under different conditions will be studied by *in situ* IR and XPS. And possible mechanism will be discussed later.

Table III.5. Effects of UV and H_2O on sulfur removal capacities for TiO_2 using model fuel containing 3500 ppmw sulfur as benzothiophene in n-octane

Conditions	No H_2O		With 1000 ppmw H_2O	
	No UV	With UV	No UV	With UV
Breakthrough Capacity (mg S/g adsorbent)	2.45	4.05	1.59	4.91
Saturation Capacity (mg S/g adsorbent)	3.90	5.63	3.27	6.20

III.4. Multi-cycle performance

TiO_2 adsorbents were tested for their sulfur removal desulfurization performance under different operation conditions for several cycles. The multi-cycle study could also test the stability of sulfur removal sites on TiO_2 surface. After adsorption, the saturated bed was heated in flowing dry air at 220 ℃ for 2 h. Then the bed temperature was further raised to 450 ℃ and kept for 2 h. After cooling down in air, the bed reactor was treated in N_2 for 1 h to remove moisture and impurities. After N_2 treatment, the regenerated bed was finally ready for the next adsorption cycle.

The breakthrough performance of calcined TiO_2 was proven to be consistent during multi-cycle desulfurization-regeneration processes without UV irradiation as shown in Figure III.8. The regenerated TiO_2 adsorbents had a similar desulfurization performance

as freshly calcined TiO_2. No apparent loss in sulfur removal capacities was observed for regenerated TiO_2 after multiple adsorption-desorption cycles. The obtained result also indicated that sulfur removal active sites on TiO_2 surface were quite stable after the high-temperature regeneration step.

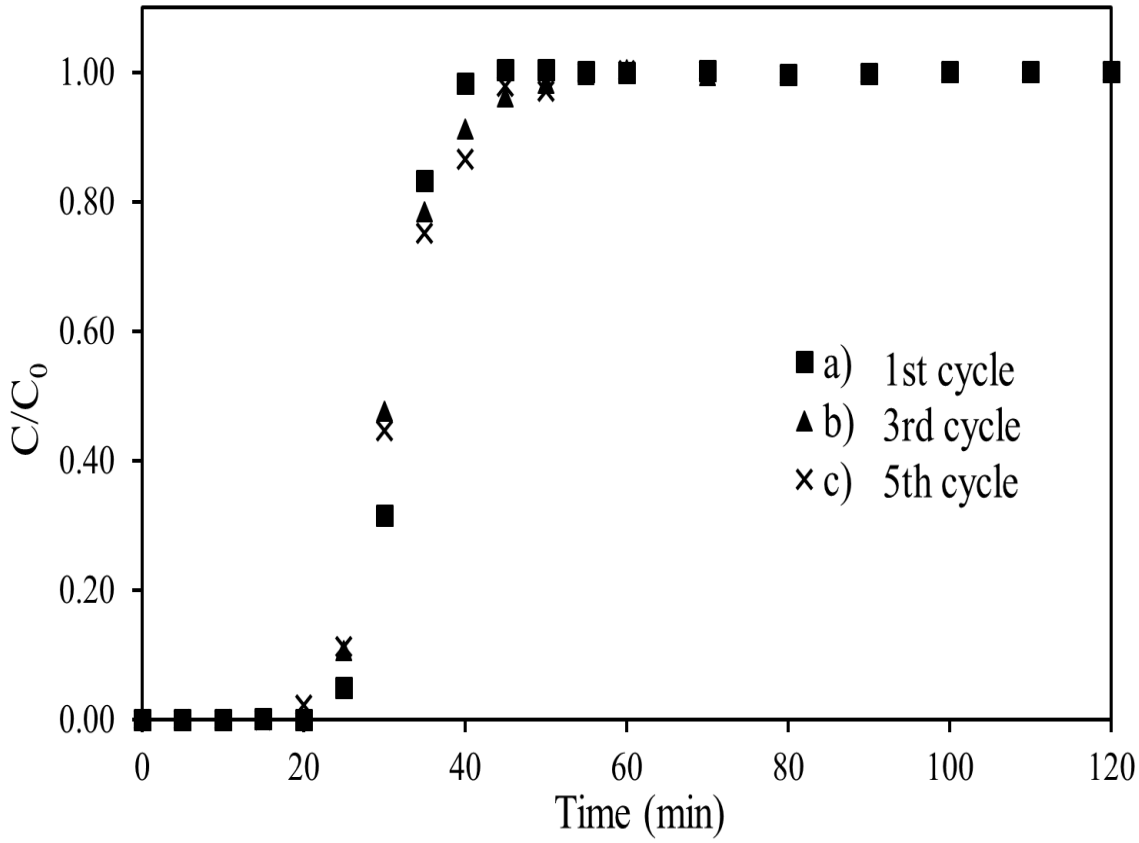

Figure III.8. Desulfurization performance of fresh and regenerated TiO_2 adsorbents during breakthrough experiments without UV (bed weight: 10.0 g, LHSV: 2 h^{-1}, S concentration: 3500 ppmw S)

TiO_2 adsorbents were also tested through multi-cycle studies where the adsorption process was carried out under UV irradiation using model fuels in the absence of H_2O. After the thermal regeneration step, the adsorption step was carried out under UV

environment. Figure III.9 illustrates the breakthrough curves for calcined and regenerated TiO_2 adsorbents from adsorption experiments under photo-irradiation. Apparently, sulfur removal capacities could maintain high for TiO_2 adsorbents during UV-assisted adsorptive desulfurization based on research results. There was no significant loss in sulfur removal capacities for regenerated TiO_2 during UV-assisted ADS.

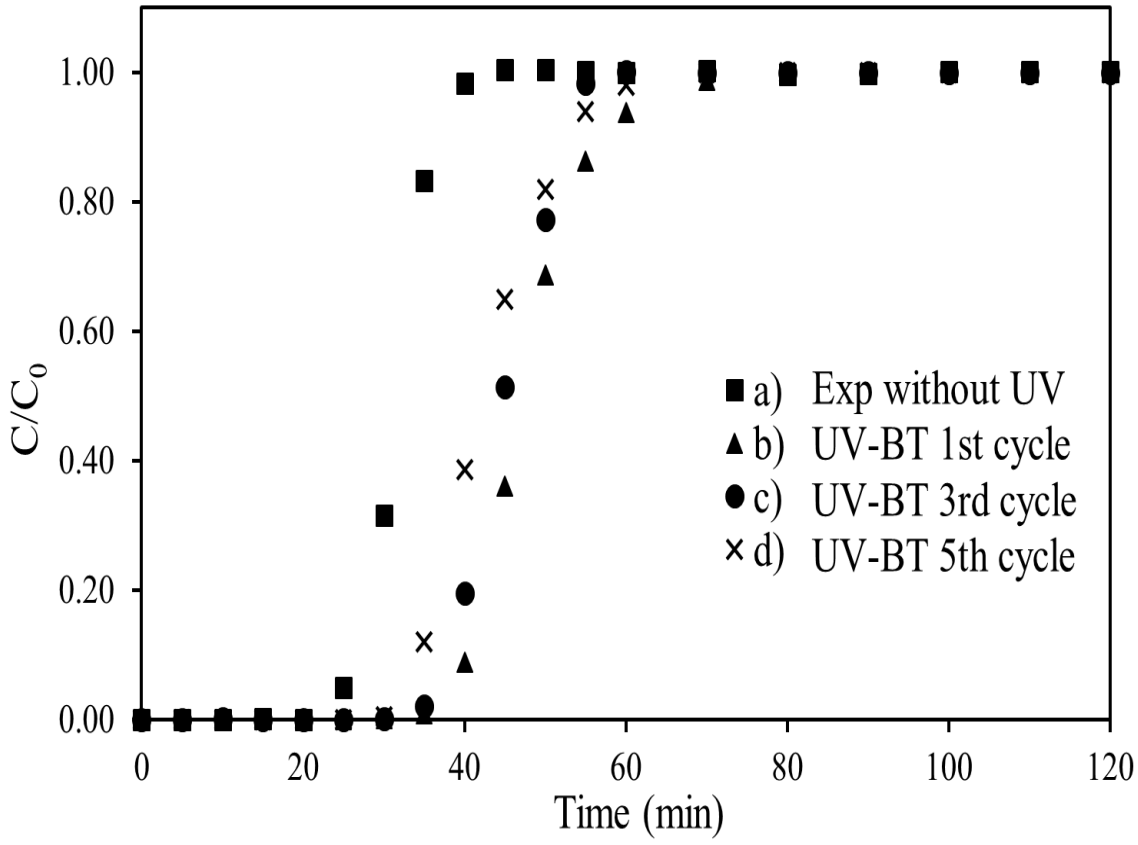

Figure III.9. Desulfurization performance of fresh and regenerated TiO_2 adsorbents during breakthrough experiments under UV irradiation (bed weight: 10.0 g, LHSV: 2 h^{-1}, S concentration: 3500 ppmw S, UV wavelength: 365 nm)

Finally, the regenerability of UV-irradiated TiO_2 adsorbent was tested. TiO_2 samples were only pre-treated once under UV for 2 h before the first adsorption step. Then the

adsorption was carried out without any UV irradiation followed by thermal regeneration step. Figure III.10 shows the resulting curves for UV initially treated TiO_2 samples using the model fuel with no H_2O. No significant loss could be observed, indicating persistent desulfurization performance of UV-treated TiO_2 samples. Breakthrough capacities of UV pre-treated TiO_2 can maintain its high desulfurization performance. In addition, the obtained results also indicated that those active sites generated on TiO_2 surface under UV were quite stable and will not be destroyed under a high-temperature condition.

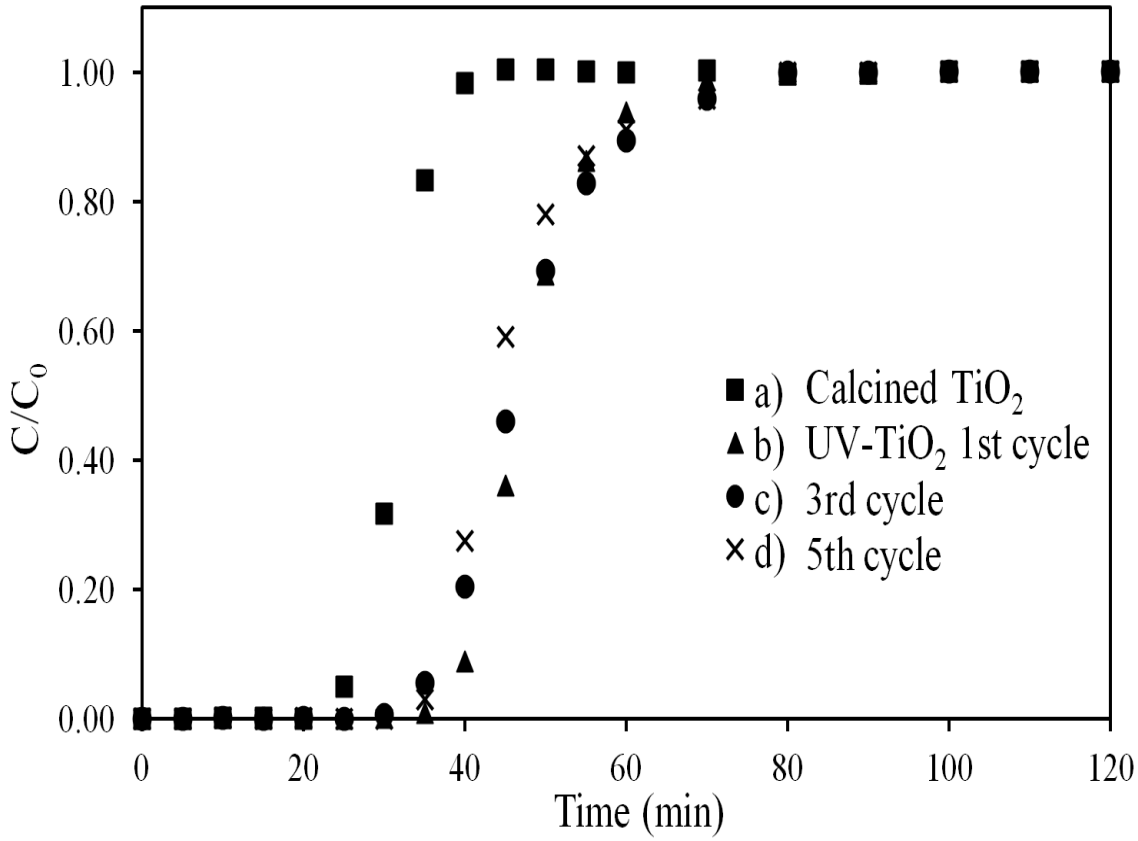

Figure III.10. Breakthrough performance comparison of fresh and regenerated UV initially treated TiO_2 adsorbents during breakthrough experiments under UV (bed weight: 10.0 g, LHSV: 2 h^{-1}, S concentration: 3500 ppmw S, UV wavelength: 365 nm)

In order to confirm the advantage of UV irradiation on sulfur removal performance, another set of experiments was designed using calcined TiO_2. Desulfurization adsorption and thermal regeneration procedures without the involvement of UV were performed for four times. Then the regenerated TiO_2 bed was treated with UV irradiation for 2 h before the fifth adsorption step. After UV treatment, the fifth adsorption step was carried out without UV irradiation. It seems that sulfur removal capacities could be increased when TiO_2 was treated with UV anytime during adsorptive desulfurization process. Resulting breakthrough curves are shown in Figure III.11. Results indicated that active sites generated under UV were unique and were only formed under UV irradiation.

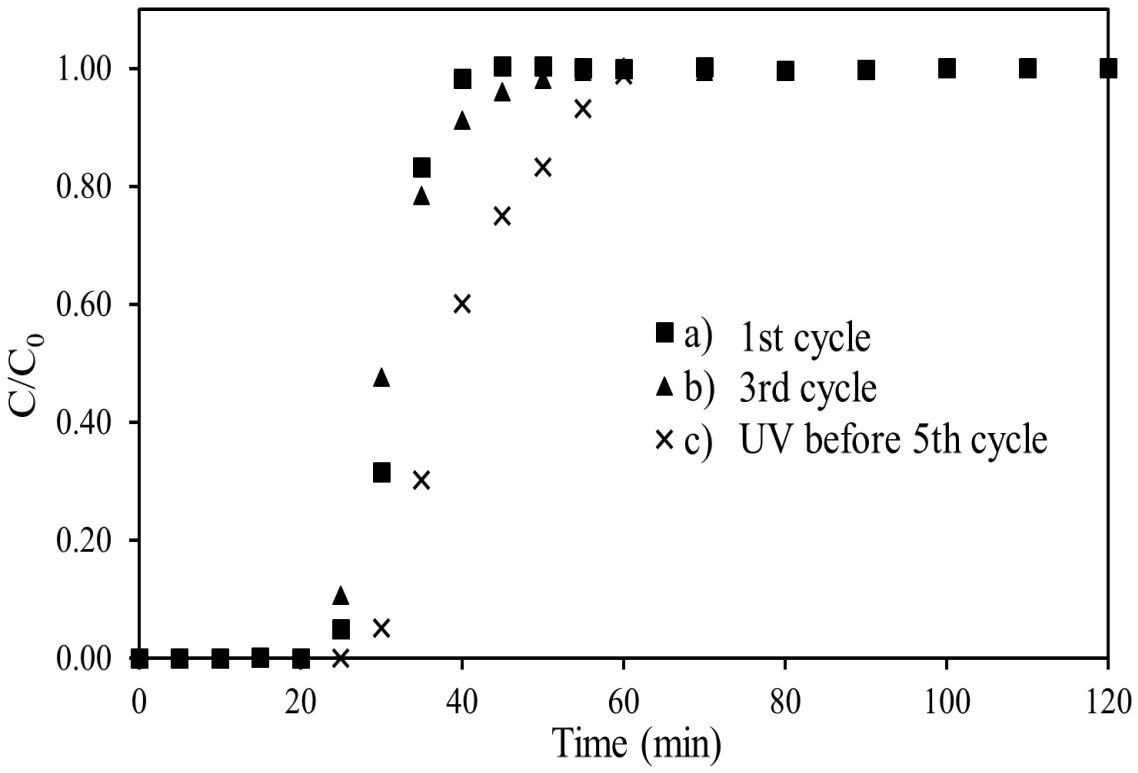

Figure III.11. Breakthrough performance of a) fresh TiO_2; b) regenerated TiO_2; c) UV-treated TiO_2 before 5th cycle for ADS experiment without UV (bed weight: 10.0 g, LHSV: 2 h^{-1}, S concentration: 3500 ppmw S, UV wavelength: 365 nm)

III.5. Effects of UV and H_2O on TiO_2-Al_2O_3

TiO_2 showed promising sulfur removal capacities under UV environment. The introduction of UV into desulfurization using TiO_2 improved its sulfur removal performance. TiO_2-Al_2O_3 adsorbents with high sulfur removal capacities were developed based on the mechanisms of TiO_2 which were the surface acidity and hydroxyl groups.

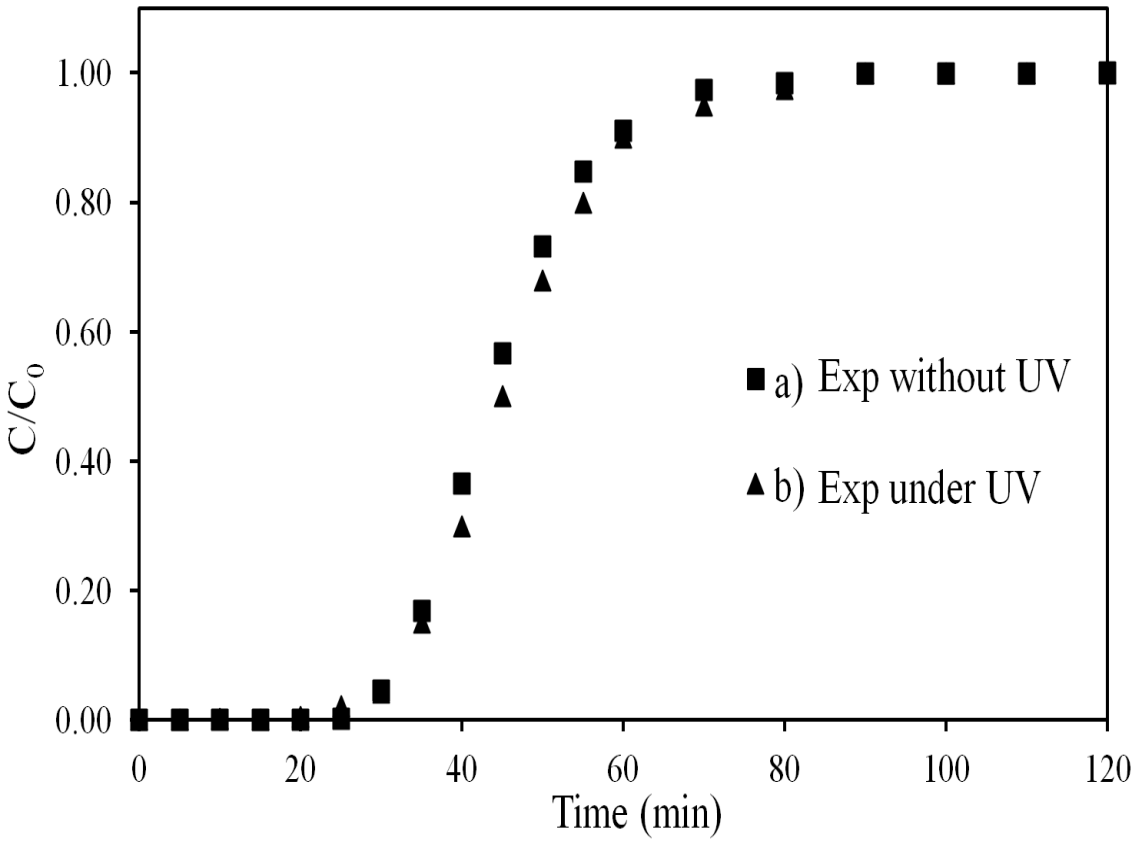

Figure III.12. Breakthrough performances of Al_2O_3 during experiments a) without UV; b) with UV (bed weight: 10.0 g, LHSV: 2 h^{-1}, S concentration: 3500 ppmw S, UV wavelength: 365 nm)

As a result, we should get the same trends as we got for TiO_2. H_2O molecules will have a negative effect on TiO_2-Al_2O_3 during desulfurization. And UV treatment should improve

the desulfurization performance of TiO_2-Al_2O_3. Breakthrough experiments were first carried out with and without UV using calcined Al_2O_3. As shown in Figure III.12, the sulfur removal capacities of Al_2O_3 supports were not affected by UV irradiation. It could due to the wide band gap of Al_2O_3 compared with TiO_2. Then, the effects of UV and H_2O molecules on sulfur removal capacities using 10 wt% TiO_2-Al_2O_3 adsorbents were evaluated and the resulting curves are shown in Figure III.13.

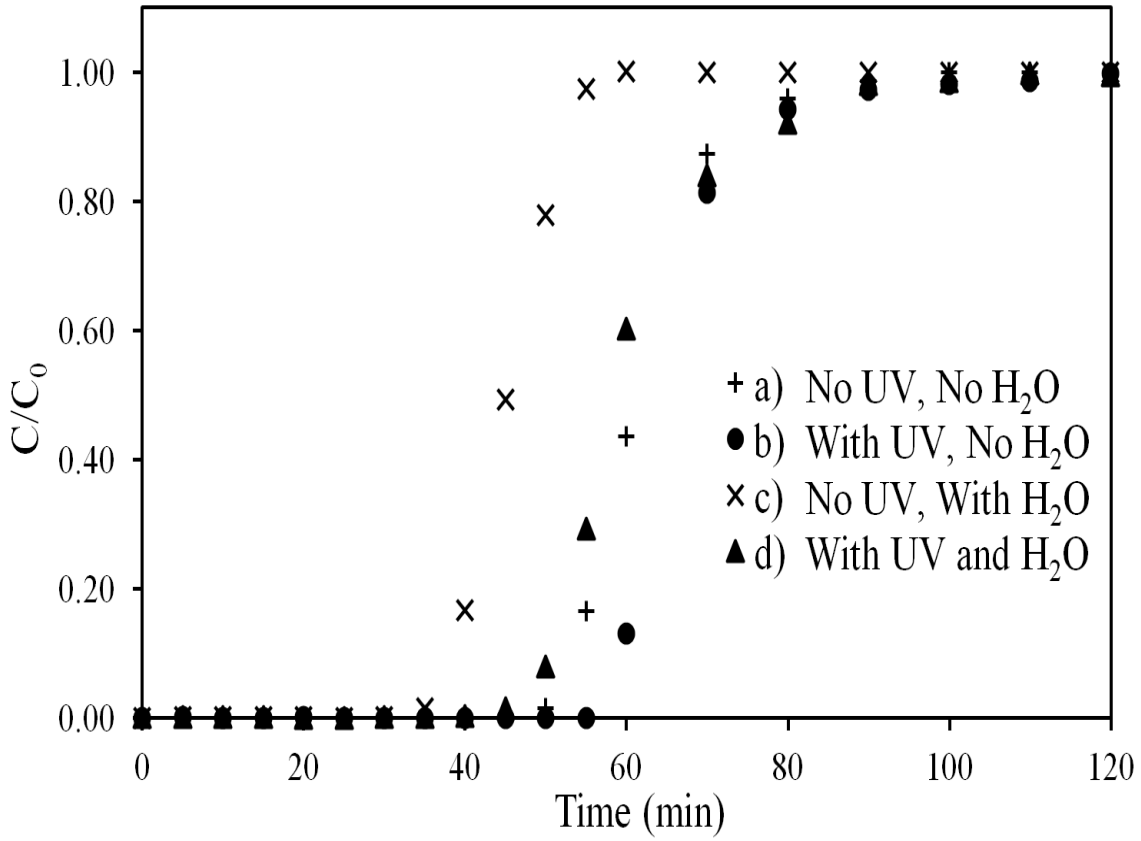

Figure III.13. Breakthrough performances of 10 wt% TiO_2-Al_2O_3 from a) experiment without UV in the absence of H_2O; b) experiment under UV without H_2O; c) study without UV with H_2O; d) study under UV with H_2O molecules (adsorbent weight: 10.0 g, LHSV: 2 h^{-1}, S concentration: 3500 ppmw S, H_2O concentration: 1000 ppmw, UV wavelength: 365 nm).

Higher capacities were obtained for TiO_2-Al_2O_3 during breakthrough experiments under UV in the absence and in the presence of H_2O. However, the improvement in the sulfur removal performance by UV treatment was not as obvious as we got for TiO_2. The weight loading of TiO_2 onto Al_2O_3 could affect the final results in this case. Although the negative effect caused by H_2O can be eliminated by UV application, UV along with H_2O did not yield the highest capacities for TiO_2-Al_2O_3. H_2O molecules could interact with active sites on both TiO_2 and Al_2O_3's surfaces. The photoreaction of H_2O only occurred on TiO_2's surface under UV irradiation at 365 nm, but no photo-effect on Al_2O_3's surface. Further analysis should be carried out to characterize TiO_2-Al_2O_3's surface sites. Effects of UV and H_2O on TiO_2-Al_2O_3 also need to be studied in details.

III.6. Conclusions

Photo-irradiation was introduced into adsorptive desulfurization (ADS) system using calcined TiO_2 adsorbents. UV irradiation during breakthrough experiment and UV treatment on TiO_2 adsorbents were both observed to improve the desulfurization performance efficiently. Breakthrough experiments with and without UV were also carried out using TiO_2-Al_2O_3. UV irradiation enhanced adsorption capacities of both TiO_2 and TiO_2-Al_2O_3 adsorbents. During UV-assisted breakthrough experiments, calcined TiO_2 demonstrated breakthrough and saturation capacities of 4.05 and 5.63 mg S/g adsorbent using the model fuel containing no H_2O. Also, UV pre-treated TiO_2 adsorbents were able to maintain high capacities at 4.29 and 5.95 mg S/g adsorbent respectively. Moreover, UV irradiation on mixed oxide TiO_2-Al_2O_3 can also increase the number of sulfur adsorptive sites as demonstrated by the improvement in desulfurization capacities.

However, desulfurization performance of TiO_2 samples from experiments using real fuel JP8 improved slightly under UV condition due to the additives in jet fuels. One of the common additives H_2O in liquid fuels was studied for TiO_2 and TiO_2-Al_2O_3. H_2O molecules were demonstrated to decrease sulfur removal capacities of TiO_2 based adsorbents by reducing surface acid sites. However, UV-assisted desulfurization process became more effective in sulfur adsorption in the presence of H_2O because of the formation of more surface hydroxyl groups on TiO_2 and TiO_2-Al_2O_3. No obvious differences in sulfur removal performance were observed during multi-cycle adsorption-regeneration studies with and without UV using calcined TiO_2. What's more, UV initially treated TiO_2 adsorbent can also maintain its capacity and stability after multiple cycles of adsorption-regeneration using model fuel in the absence of H_2O. The active sites generated under UV on TiO_2 surface were considered to be unique and consistent under both ambient and high-temperature conditions. Future work will focus on the effects of UV and H_2O on Ag/TiO_2 adsorbents as well as the surface characterization of TiO_2 under UV irradiation.

IV. UV-assisted Desulfurization of Ag/TiO_2 Adsorbents

IV.1. Introduction

Desulfurization capacities of calcined TiO_2 are still relatively low which cannot meet the ultra-low sulfur requirement. Silver impregnated on TiO_2 and TiO_2-Al_2O_3 adsorbents were then developed by our adsorption group in order to enhance sulfur adsorption capacities of TiO_2 adsorbents. And this silver impregnated adsorbent is one of the few adsorbents that can reduce sulfur down to ppmw level without requiring any activation. Silver loaded on TiO_2 and TiO_2-Al_2O_3 surfaces proved beneficial to desulfurization performance when compared to calcined supports. The UV/TiO_2 system has been demonstrated to be effective for adsorptive desulfurization process from liquid hydrocarbon fuels using calcined TiO_2 adsorbents. And UV irradiation can also eliminate the negative effect caused by H_2O in fuels on TiO_2 materials during breakthrough experiments. In order to further increase the sulfur removal capacities of Ag/TiO_2, UV irradiation was applied on these silver loaded adsorbents to test the effect of UV.

The objective of this work in this section is to examine the performance of Ag/TiO_2 adsorbents for adsorptive desulfurization with and without UV irradiation. Then the effect of H_2O on Ag/TiO_2 during breakthrough experiments with and without UV was also studied here. Breakthrough experiments were carried out with and without UV using model fuels in the absence and in the presence of H_2O for Ag/TiO_2 adsorbents. The effect of UV on Ag phase was also studied using XPS.

IV.2. Effect of UV on Ag/TiO_2

IV.2.1. Effect of UV on desulfurization performance of Ag/TiO_2

For calcined TiO_2 and TiO_2-Al_2O_3 supports, the apparent improvement in desulfurization performance was observed in Chapter III. For Ag/TiO_2 and Ag/TiO_2-Al_2O_3 adsorbents, the effect of UV was also needed to be investigated. UV-assisted desulfurization was then carried out using Ag/TiO_2 adsorbent here. The weight loading of Ag metal on Ag/TiO_2 adsorbent was kept at 4 wt% for all breakthrough experiments in this research. And 10.0 g Ag/TiO_2 adsorbents were loaded into the fixed bed reactor. The effect of UV on sulfur adsorption was evaluated by comparing desulfurization capacities got from experiments without and with UV irradiation.

Desulfurization performance using 4 wt% Ag/TiO_2 during breakthrough studies without and with UV is shown in Figure IV.1. And sulfur removal capacities calculated from those curves are listed in Table IV.1. The effect of UV on Ag/TiO_2 during the sulfur adsorptive process was different from the effect of UV on calcined TiO_2.

Table IV.1. Effect of UV on desulfurization performance of 4 wt% Ag/TiO_2

Operation Condition	No UV	UV-assisted ADS
Breakthrough Capacity (mg S/g adsorbent)	4.29	2.45
Saturation Capacity (mg S/g adsorbent)	5.84	3.63

Breakthrough capacity reduced from 4.29 mg S/g to 2.45 mg S/g when introducing UV into ADS. Also, the saturation capacity of Ag/TiO_2 decreased to 3.63 mg S/g during

UV-assisted ADS. In addition, the color change was observed for Ag/TiO_2 adsorbents during UV-assisted ADS. The color of Ag/TiO_2 adsorbents changed from light gray to black during the breakthrough test under UV irradiation. The color change could indicate chemical state changes of silver particles.

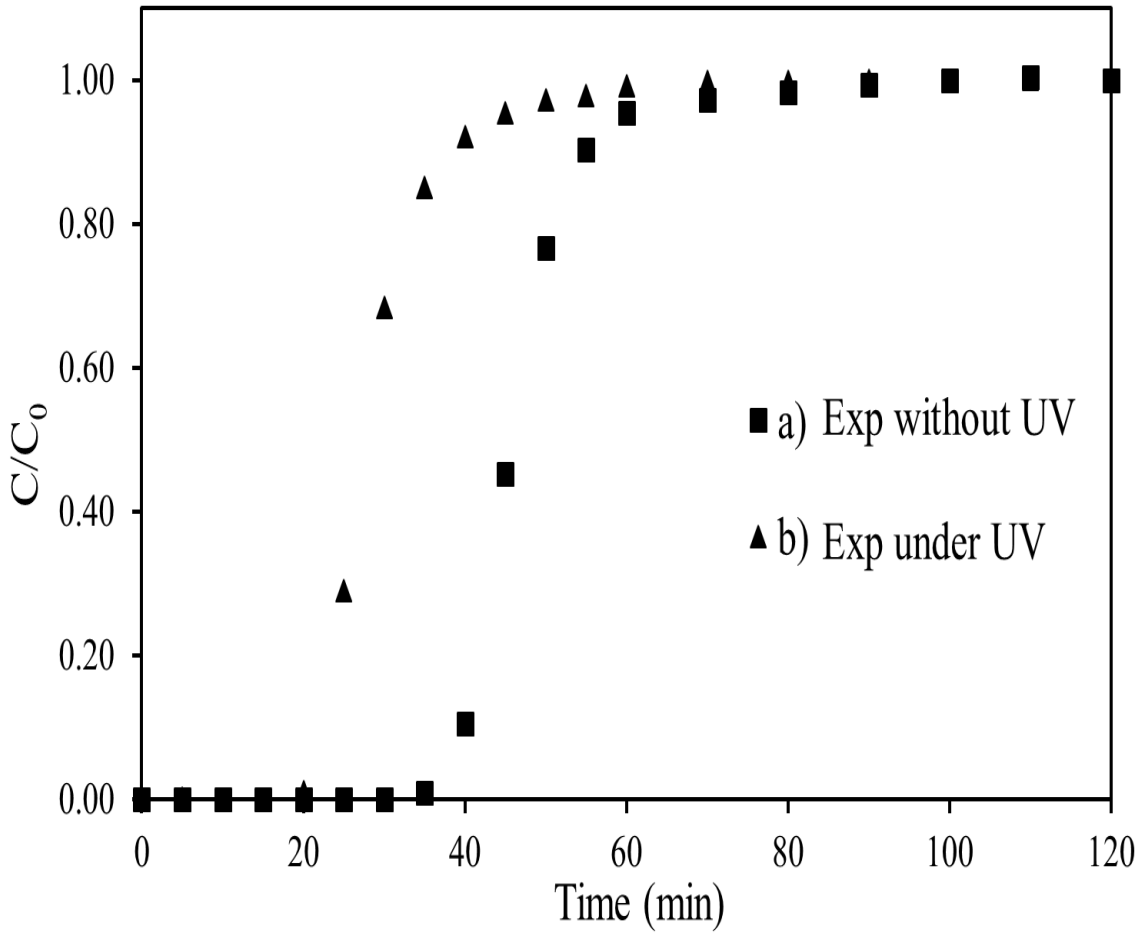

Figure IV.1. Effect of UV irradiation on breakthrough experiments for 4 wt% Ag/TiO_2 using the model fuel (bed weight: 10.0 g, LHSV: 2 h^{-1}, S concentration: 3500 ppmw S, UV wavelength: 365 nm)

IV.2.2. Effect of UV on the chemical state of Ag

Based on the desulfurization results got from experiments under UV, photoreduction reaction of Ag was considered to occur on TiO_2 surface. The Ag^+ ions were reduced to Ag^0 metals under UV irradiation. Photo-reduction of Ag particles on TiO_2 supports were studied by X-ray Photoelectron Spectrometer (XPS). Figure IV.2 shows the high-resolution XPS spectra for Ag 3d line scans for 4 wt% Ag/TiO_2 treated with and without UV separately.

For Ag/TiO_2 sample under dark without UV irradiation, Ag $3d_{5/2}$ peak has a binding energy of 367.5 eV with a 6 eV splitting of the 3d doublet corresponding to Ag^+ ion [110, 111]. XPS peaks attributed to Ag^0 were not found for this sample as shown in Figure IV.2 a). For silver on TiO_2 treated under UV irradiation, the Ag $3d_{5/2}$ peak was divided into two individual peaks at 367.4 eV and 369.3 eV as shown in Figure IV.2 b) which can be attributed to Ag^+ ions and metallic Ag^0 [110-114]. According to previous reports, the Ag $3d_{5/2}$ binding energy of metal Ag is around 368.2 eV. However, both $3d_{5/2}$ and $3d_{3/2}$ peaks for Ag^0 shifted to higher binding energy values for our sample. This binding energy shift could be attributed to final state effect or surface photovoltage effect (SPV) [115-117]. Upon illumination with UV, electrons and holes are generated on TiO_2 surface, and charge transfers from support to the surface. Thus, the XPS 3d peaks for Ag^0 are shifted toward higher binding energy.

Ag impregnated on TiO_2 will increase surface acidity which will improve desulfurization performance. However, being exposed to UV irradiation, Ag metals were formed which confirmed by XPS. Based on breakthrough experimental results and XPS spectra, UV irradiation had a negative effect on sulfur removal capacities for Ag/TiO_2.

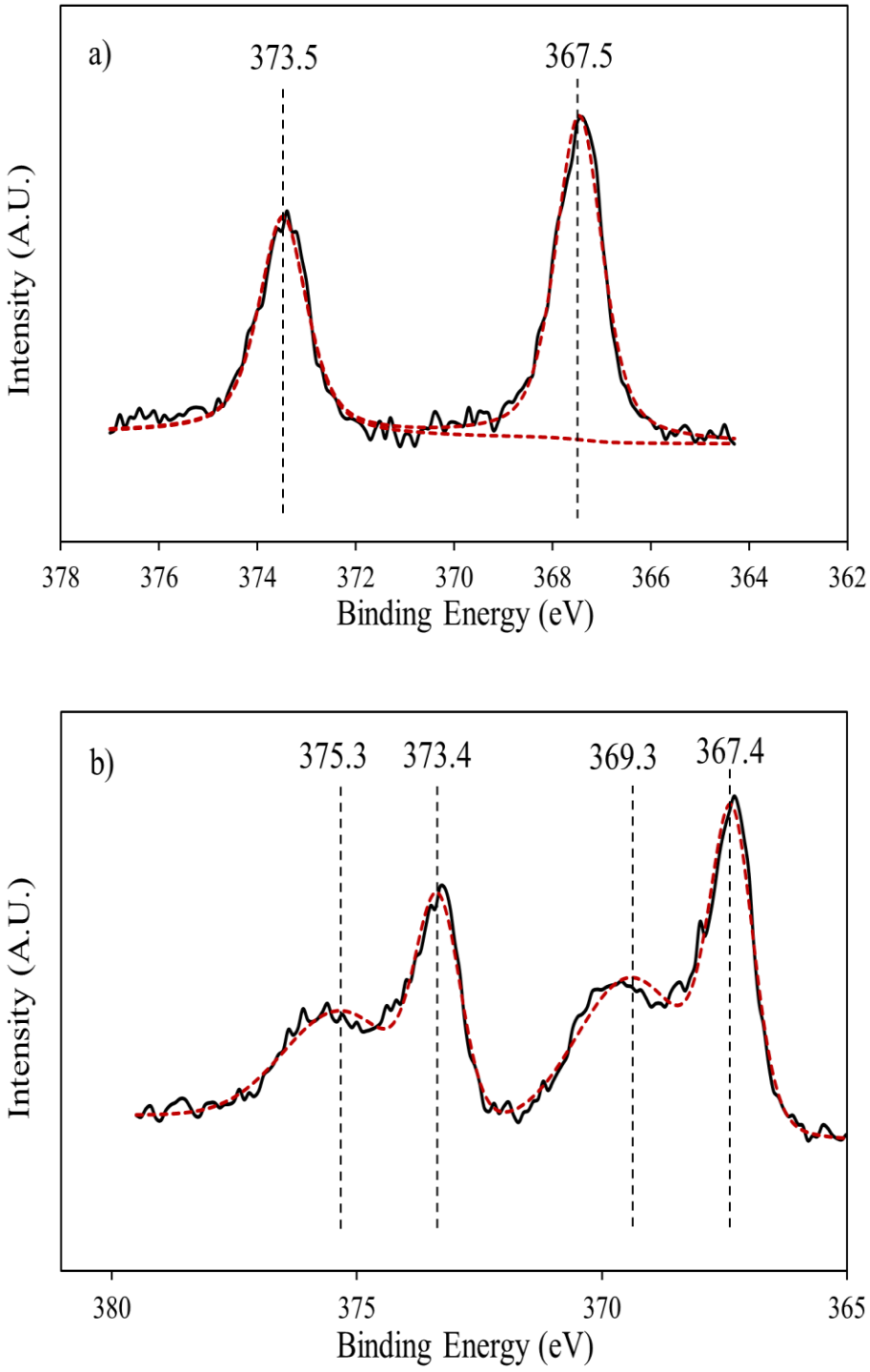

Figure IV.2. High resolution XPS spectra of Ag 3d for Ag/TiO_2 samples treated a) without UV and b) under UV environment (UV light wavelength: 365 nm)

IV.3. Effect of H_2O on Ag/TiO_2

IV.3.1. Effect of H_2O in the absence of UV

Reduction in Bronsted acidic sites caused by H_2O molecules was observed on TiO_2 surface which decreased sulfur removal capacities for TiO_2 related adsorbents. Based on previous studies, adding water caused a negative effect on TiO_2 and TiO_2-Al_2O_3 adsorbents. Water additive might reduce the surface acidity and decrease sulfur removal capacities of Ag/TiO_2 adsorbents as well.

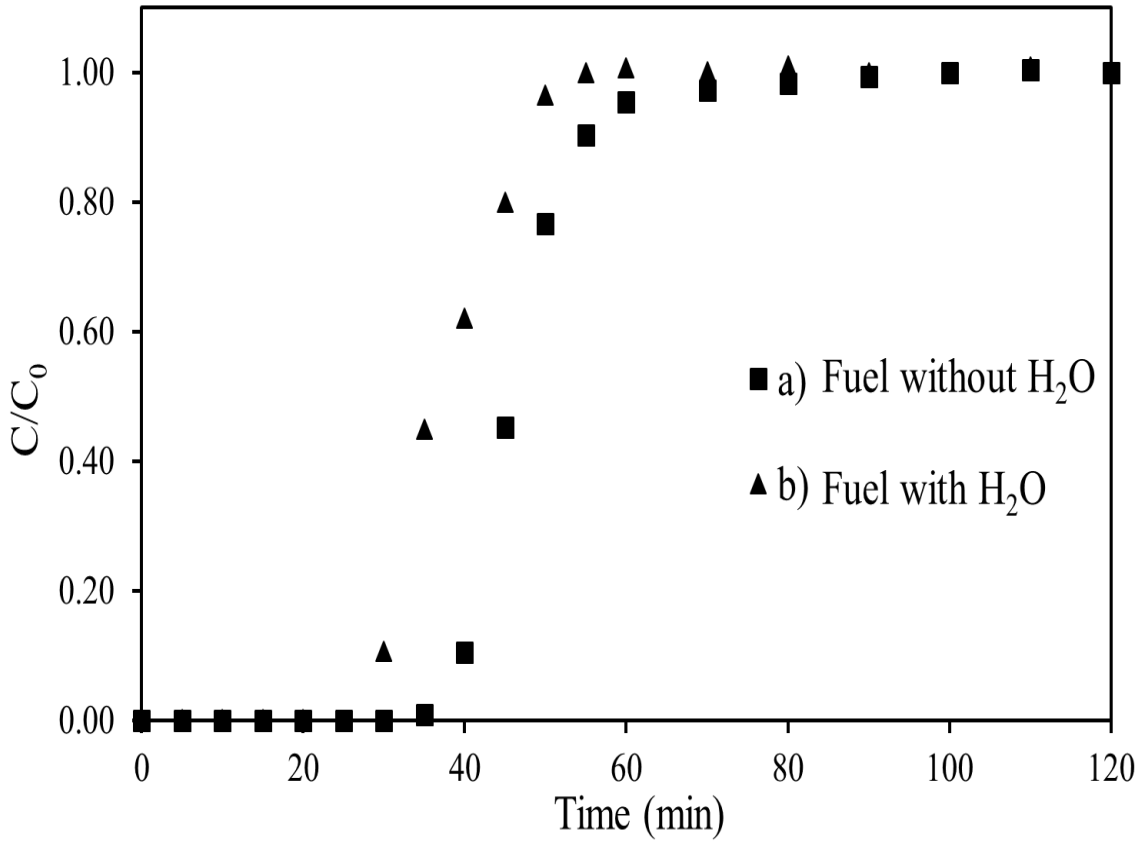

Figure IV.3. Sulfur capacities for 4 wt% Ag/TiO_2 during breakthrough experiments without UV using model fuels a) in the absence of H_2O; b) with water H_2O (bed weight: 10.0 g, LHSV: 2 h^{-1}, S concentration: 3500 ppmw S, H_2O concentration: 1000 ppmw)

The resulting breakthrough curves of 4 wt% Ag/TiO_2 using the model fuel containing H_2O for experiments without UV are shown in Figure IV.3. Sulfur removal capacities of Ag/TiO_2 were also decreased when adding H_2O into the system. This is the same trending we observed in calcined TiO_2 and TiO_2-Al_2O_3 when H_2O was added to model fuels during ADS without UV. The effect of H_2O on Bronsted sites on adsorbent's surface decreased sulfur removal capacities. As a result, H_2O in the model fuel also reduced the sulfur adsorptive capacities of Ag/TiO_2.

IV.3.2. Effect of H_2O during UV-assisted desulfurization process

Both UV and H_2O molecules reduced sulfur removal capacities of Ag/TiO_2 based on experimental results. Two problems including the photo-reduction of Ag ions caused by UV irradiation and the decrease in surface acidity on TiO_2 caused by H_2O need to be solved. In order to prevent Ag^+ ions turn into Ag^0 metal particles during photo-irradiated desulfurization process, oxidants are needed to be introduced into the system. And, H_2O can act as a mild oxidant in many photocatalytic reactions.

Table IV.2. Effects of UV and H_2O on Sulfur removal capacities of 4 wt% Ag/TiO_2

Operation Conditions	No UV, No H_2O	No UV, With H_2O	With UV and H_2O
Breakthrough Capacity (mg S/g adsorbent)	4.29	3.07	4.91
Saturation Capacity (mg S/g adsorbent)	5.84	4.63	6.35

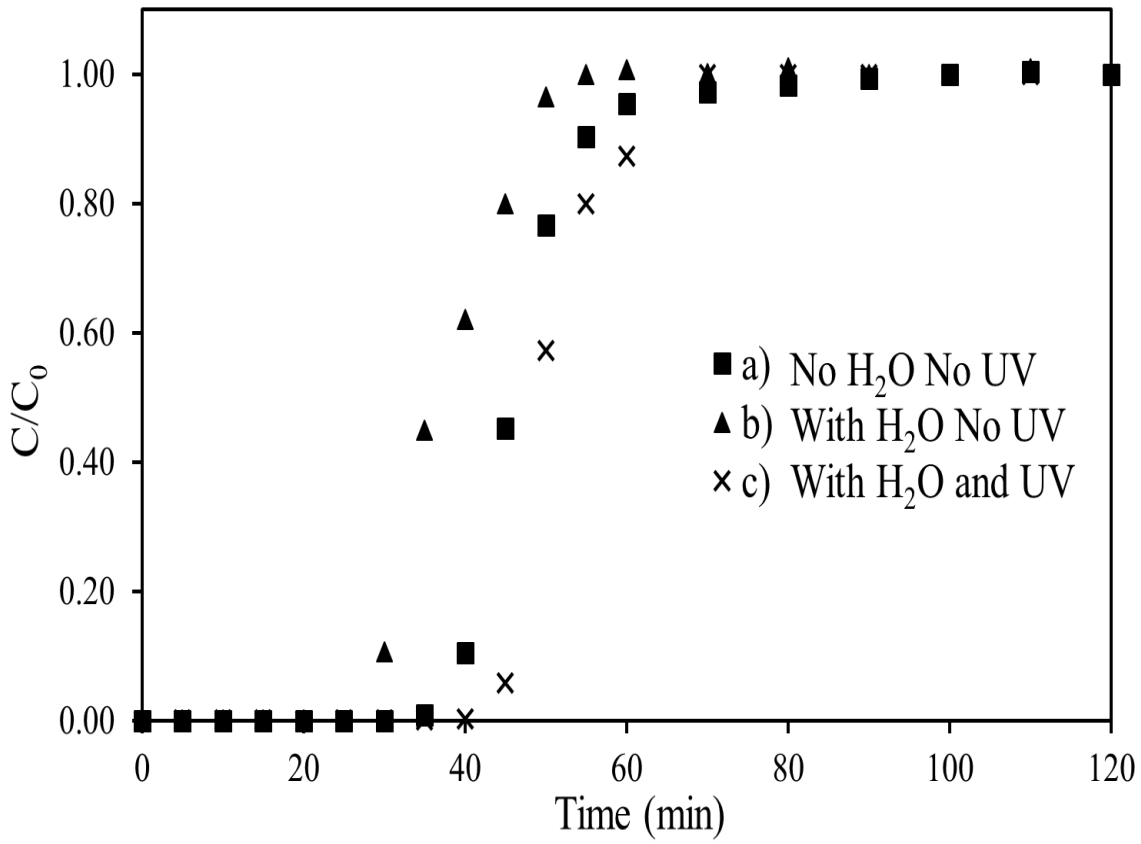

Figure IV.4. Sulfur removal capacities of 4 wt% Ag/TiO_2 from a) experiment without UV using the model fuel without H_2O; b) experiment without UV using a model fuel containing H_2O; c) study under UV using a model fuel with H_2O (bed weight: 10.0 g, LHSV: 2 h^{-1}, S concentration: 3500 ppmw S, H_2O concentration: 1000 ppmw, UV wavelength: 365 nm)

Moreover, photo-reaction of H_2O on TiO_2's surface could increase hydroxyl groups for Ag/TiO_2. Thus, the effect of $UV/H_2O/TiO_2$ on desulfurization effect was evaluated in this section. Figure IV.4 shows breakthrough curves of Ag/TiO_2 under different conditions. Desulfurization capacities of Ag/TiO_2 are listed in Table IV.2. By comparing all the results, highest sulfur capacities for Ag/TiO_2 were obtained using model fuel containing H_2O during UV-assisted desulfurization process. By combining UV and H_2O

into the system, breakthrough and saturation capacities of Ag/TiO_2 were increased to 4.91 mg S/g adsorbent and 6.35 mg S/g adsorbent, separately. Thus, $UV/H_2O/TiO_2$ system improved sulfur removal performance of Ag/TiO_2.

Finally, effects of H_2O molecules and UV irradiation on Ag/TiO_2 were tested using model fuels containing different amount of water. Four model fuels containing H_2O concentration at 100, 500, 1000 and 2000 ppmw were used for breakthrough experiments under dark and UV environment. Figure IV.5 shows the breakthrough and saturation capacities got from this set of experiments.

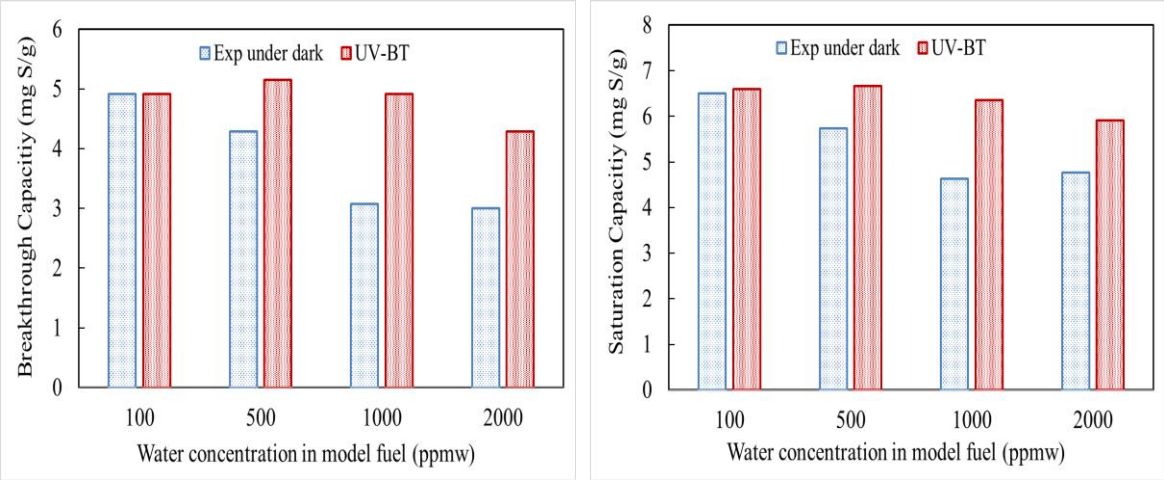

Figure IV.5. Breakthrough (left) and saturation (right) capacities of 4 wt% Ag/TiO_2 during breakthrough experiments with and without UV irradiation using model fuels containing 100, 500, 1000 and 2000 ppmw H_2O (bed weight: 10.0 g, LHSV: 2 h^{-1}, S concentration: 3500 ppmw S, UV wavelength: 365 nm)

Sulfur removal capacities of Ag/TiO_2 decreased when adding water into liquid fuels during breakthrough experiment without UV irradiation. Silver supported on TiO_2 adsorbents lost more capacities when more water presented in model fuels. However, by

comparing the results got from experiments under both dark and UV conditions, H_2O/UV system can always improve desulfurization performance for 4 wt% Ag/TiO_2 adsorbents.

IV.4. Discussion and conclusions

Ag/TiO_2 adsorbents have higher sulfur removal capacities compared to calcined TiO_2 based on our group's studies. However, UV irradiation was observed to have a different effect on Ag/TiO_2 when comparing to TiO_2. The introduction of UV irradiation had negative effects on desulfurization performance for Ag/TiO_2 adsorbent due to the photo-reduction of silver active sites on TiO_2 surface. During breakthrough process without UV, calcined TiO_2 had breakthrough and saturation capacities of 2.45 and 3.90 mg S/g adsorbent. For Ag/TiO_2, the capacities decreased to 2.45 and 3.63 mg S/g adsorbent for UV-assisted adsorptive desulfurization. Based on the results, silver based active sites on TiO_2 surface were totally eliminated by UV irradiation. The decrease in sulfur adsorptive capacities for TiO_2 was also observed on Ag/TiO_2 adsorbents when adding H_2O into the model fuel. Moisture is always considered as a problem for TiO_2 supported adsorbents or other acid based adsorbents too. In order to maintain or even improve desulfurization performance of Ag/TiO_2, photo-reduction of Ag^+ ions needs to be solved with the introduction of mild oxidants into adsorption system.

For Ag/TiO_2, best desulfurization performance was obtained during UV-irradiated adsorption process using model fuel containing H_2O. To explain this result, two facts might need to be considered. Firstly, more surface hydroxyl groups were formed on TiO_2 surface under UV in the presence of H_2O. Secondly, less silver metal particles were

formed when H_2O was acting as a mild oxidant. The summary of sulfur removal capacities of TiO_2 and Ag/TiO_2 under different operation conditions using different types of model fuels is listed in Table IV.3 and Table IV.4.

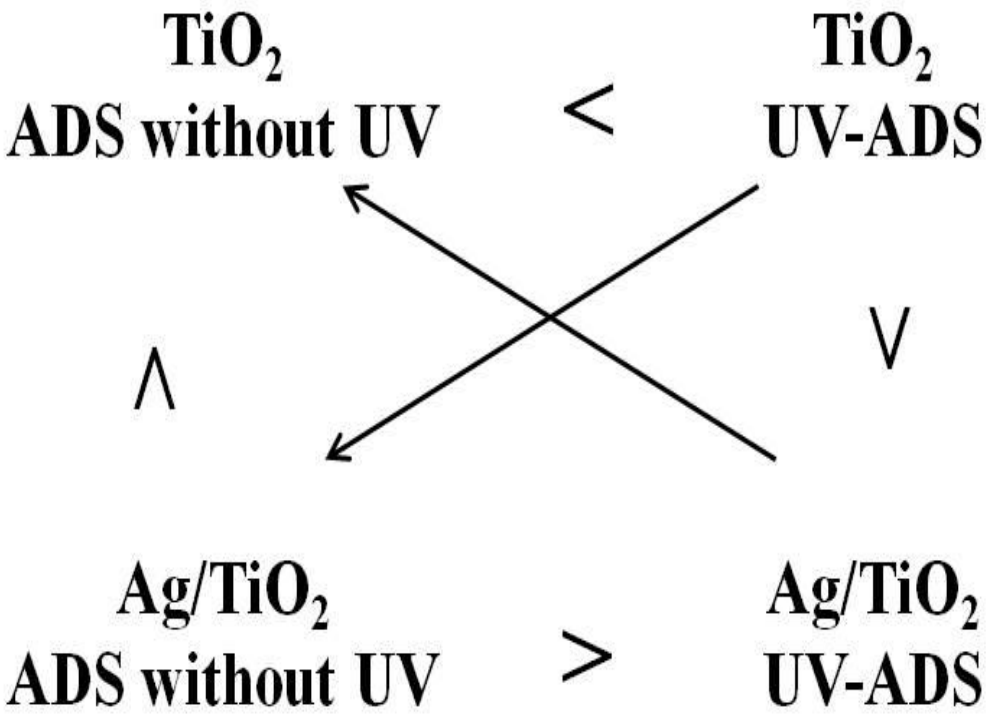

Figure IV.6. Desulfurization performances of TiO_2 and 4 wt% Ag/TiO_2 during adsorptive desulfurization using model fuels containing no H_2O

Table IV.3. Effects of UV and H_2O on sulfur removal capacities of TiO_2 using model fuels containing 3500 ppmw sulfur as benzothiophene in n-octane

Conditions	No H_2O		With 1000 ppmw H_2O	
	No UV	With UV	No UV	With UV
Breakthrough Capacity (mg S/g adsorbent)	2.45	4.05	1.59	4.91
Saturation Capacity (mg S/g adsorbent)	3.90	5.63	3.27	6.20

The sulfur removal capacities of TiO_2 during UV-assisted ADS were similar as the capacities of Ag/TiO_2 obtained from breakthrough experiments without UV when using the model fuel in the absence of H_2O. And UV irradiation can remove almost all the active Ag sites on Ag/TiO_2. Because Ag/TiO_2 during UV-assisted ADS showed the same sulfur removal capacities as calcined TiO_2 did during desulfurization without UV irradiation. The relationship between TiO_2 and Ag/TiO_2 using model fuels containing no H_2O is shown in Figure IV.6.

The relationship between TiO_2 and Ag/TiO_2 is different when using model fuels containing H_2O as shown in Figure IV.7. Ag/TiO_2 was able to maintain the desulfurization performance during UV-ADS when H_2O was added in the model fuel. Sulfur removal capacities of Ag/TiO_2 even increased by the combination of UV and H_2O. Under the UV/H_2O condition, TiO_2 and Ag/TiO_2 had similar sulfur removal capacities.

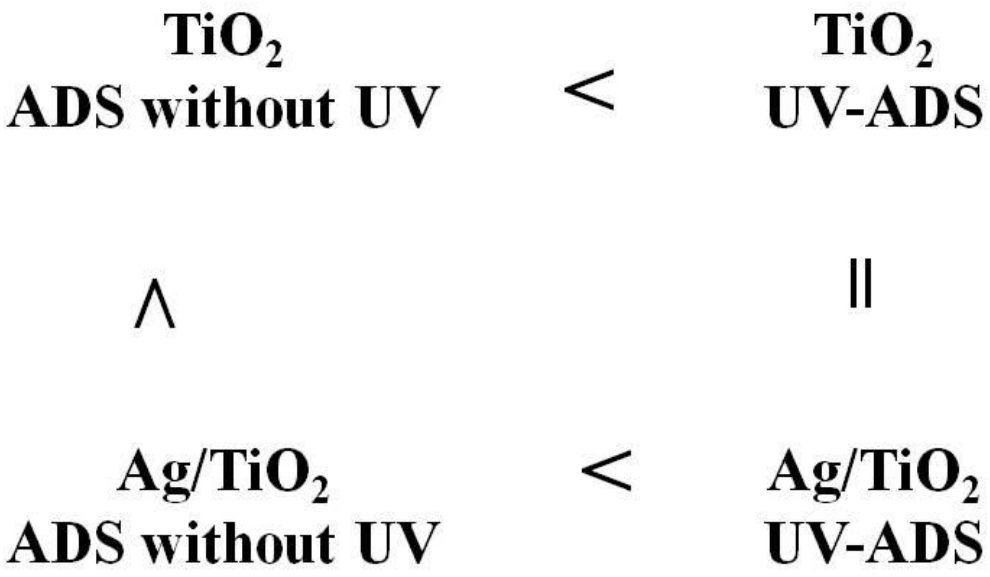

Figure IV.7. Desulfurization performances of TiO_2 and 4 wt% Ag/TiO_2 during adsorptive desulfurization using model fuels in the presence of H_2O

Based on the data obtained from desulfurization breakthrough experiments for TiO_2 and Ag/TiO_2, the role of UV irradiation on the surface active site is unique. The effect of UV irradiation on surface hydroxyl groups and other species on TiO_2 and Ag/TiO_2 surface need more investigations. Studies on TiO_2 adsorbents under UV in the presence of H_2O were also carried out by *in situ* IR and XPS. Photoreactions on TiO_2 surface and the possible mechanism will be discussed in details later.

Table IV.4. Effects of UV and H_2O on sulfur removal capacities of 4 wt% Ag/TiO_2 using model fuels containing 3500 ppmw sulfur as benzothiophene in n-octane

Conditions	No H_2O		With 1000 ppmw H_2O	
	No UV	With UV	No UV	With UV
Breakthrough Capacity (mg S/g adsorbent)	4.29	2.45	3.07	4.91
Saturation Capacity (mg S/g adsorbent)	5.84	3.63	4.63	6.35

V. Effects of UV and H_2O on Surface Hydroxyl Groups

V.1. Introduction

For adsorptive desulfurization, sulfur removal capacities mainly depend on the efficiencies of the adsorbents. The challenge of ADS technology mainly comes from the development of new adsorbents that can remove sulfur down to parts per billion (ppb) levels along with high selectivity. Among those adsorbents studied so far, silver based adsorbents have shown promising sulfur removal capacities under ambient operation conditions. Ag/TiO_2 and Ag/TiO_2-Al_2O_3 adsorbents also have good selectivity towards organosulfur compounds. And silver loaded on TiO_2 adsorbents showed consistent sulfur removal capacities after thermal regeneration.

Based on previous studies, both UV during the breakthrough process and UV treatment before an adsorptive step can enhance sulfur adsorption capacities of these TiO_2 supported adsorbents. TiO_2 and Ag/TiO_2 adsorbents both demonstrated highest capacities during UV-assisted adsorptive desulfurization using model fuels containing H_2O. Moreover, for UV initially treated TiO_2 adsorbents, sulfur capacities were able to maintain at high values after the thermal regeneration step. To optimize the application of UV irradiation into adsorptive desulfurization, efforts to understand photo-irradiated reactions on TiO_2 surface and surface active sites generated under illumination are involved. We observed a relationship between surface acidity and sulfur removal capacities for Ag/TiO_2 and Ag/TiO_2-Al_2O_3 [98, 100].

The number of surface acidic hydroxyl groups on TiO_2 are related to the sulfur adsorptive capacities of these TiO_2 supported adsorbents. Thus, acidic -OH groups have been postulated to be the main active sites on TiO_2 based adsorbents. The surface acidity was also related to the photocatalytic activity of TiO_2 [118]. Photo-activated species especially surface hydroxyl groups on TiO_2 under UV irradiation and the effect of H_2O were characterized by *in situ* IR and XPS.

The oxidants generated under UV which are surface hydroxyl radicals were studied by fluorescence spectroscopy. This technique is rapid, simple and has high sensitivity. The relative concentration of surface hydroxyl radicals for calcined TiO_2 with and without UV irradiation can be easily determined by fluorescence technique. The results got from this analysis can be further used to estimate the quantum yields for liquid-solid phase photo-reaction on TiO_2 adsorbents.

V.2. Experimental

For *in situ* IR analysis, 50 mg dry TiO_2 powders in 251-354 μm were pressed into a self-supporting pellet by Carver hydraulic press at 16000 psi. TiO_2 pellets were then calcined at 450 ℃ for 2 h in flowing dry air. Then, the calcined TiO_2 pellet was loaded into a customized IR cell equipped with ZnSe windows. The customized IR cell with ZnSe windows was first heated to 200 ℃ and kept for 1 h in flowing dry air followed by N_2 treatment for 1 h at room temperature in order to remove any impurities before the pretreatment. The IR cell was then evacuated to 100 mTorr before further treatment. After the pretreatment procedure, sample cell was treated under different conditions. UV

sources were applied directly on IR cell during treatment step in order to investigate the effect of photo-illumination on TiO_2. Different adsorbates were introduced to the sample pellet by N_2 bubbling at room temperature during the pretreating step. The IR cell was treated with water vapor with and without UV for a certain time to study the effect of H_2O molecule on TiO_2 surface active sites. Evacuation of the cell at 100 mTorr was carried out before final IR analysis. Both pretreatment and analysis steps were performed *in situ*. IR spectra for all samples and background were collected by Thermo Scientific Nicolet IR100 spectrometer in a region between 400-4000 cm^{-1}.

XPS data were collected by AXIS Ultra delay lines detector (DLD) X-ray photoelectron spectrometer (XPS) from Kratos Analytical Ltd. Calcined TiO_2 pellet was analyzed in SAC under 10^{-9} Torr. To study the effect of UV on surface hydroxyl groups, TiO_2 sample pellets were firstly exposed to UV light for 2 h through the quartz window in load lock area under 10^{-8} Torr followed by entering the analysis chamber. A monochromatic Al Kα X-ray source was used as the photon source. High resolution spectra were obtained for C 1s, O 1s and Ti 2p using a passing energy of 20 eV. The binding energy shifts due to surface charging were corrected using the C 1s level at 284.6 eV. Core level peaks of O 1s were deconvoluted by using Gaussian-Lorentzian (20%) peaks.

To measure the relative concentration of surface hydroxyl radicals, terephthalic acid (TA) was used for fluorescence spectroscopy. Terephthalic acid was dissolved in 0.2 M NaOH solution to form a mixed solution with a concentration of 0.05 M. 10.0 g calcined TiO_2 was loaded into the packed column in a continuous flow tubular system. 100 mL mixed solution flowed from bottom to top through the packed bed. The outlet liquid went

back to the mixed solution container and mixed well with the initial solution. The recirculation remained for 2 h under UV or without any irradiation followed by final analysis. For UV-treated TiO_2 samples, the bed reactor was first exposed to UV irradiation for 2 h followed by recirculation without any UV. Also, for reference, this experiment was also conducted using empty bed loaded with clear quartz beads without UV.

The relative concentration of hydroxyl radicals can be determined by resulting fluorescence spectra of generated 2-hydroxyterephthalic acid products in final mixed solution. The determination of surface hydroxyl radicals was conducted under room temperature on a Shimadzu RF-5301PC spectrophotometer which was equipped with 150 W xenon lamp as the light source. The excitation wavelength is at 315.0 nm and emission wavelength ranges from 320 to 600 nm.

V.3. Surface hydroxyl groups on TiO_2 under UV

V.3.1. *In situ* IR spectroscopy

In situ IR on calcined TiO_2 samples and background have been measured by Thermo Scientific Nicolet IR100 spectrometer in a region between 400-4000 cm^{-1}. Spectra were recorded using a resolution of 4 cm^{-1} with 32 averaged scans under ambient lab conditions. It has been demonstrated that photo-induced reactions did not occur at the ZnSe surface and UV irradiation at ZnSe window did not affect final IR spectra [119]. Thus, UV sources were applied directly on IR cell during the final vacuum treatment step to study the effect of UV on TiO_2 surface in the absence of H_2O. Two UV lamps were put

on both sides of the IR cell in order to ensure full penetration of UV irradiation onto TiO_2 samples during *in situ* IR analysis.

In situ IR spectroscopy was performed on calcined TiO_2 samples treated with and without UV irradiation to determine the effect of UV on TiO_2's surface hydroxyl groups. The resulting IR absorbance spectra of calcined TiO_2 samples treated without and with UV are shown in Figure V.1. For calcined TiO_2 adsorbents treated with and without UV irradiation, both broad and sharp peaks were observed in IR region between 3000-4000 cm^{-1}, indicating stretching vibrations of different kinds of -OH groups [120]. The broad and complex peaks located between 3500-3600 cm^{-1} region were assigned to H-bonded and bridged hydroxyl groups [121-128]. And sharp peaks located between 3600-3800 cm^{-1} region belonged to different types of isolated or terminal hydroxyl groups. Based on research results on anatase TiO_2, it has been claimed that the peak located around 3640 cm^{-1} was assigned to Ti(IV)-OH groups while the peak located at a higher vibrational frequency around 3700 cm^{-1} was assigned to Ti(III)-OH groups [129]. One noticeable peak was observed for both samples at 3650 cm^{-1} which belonged to Ti(IV)-OH groups. However, the respective intensities for the two samples were different. For TiO_2 sample treated with UV irradiation, the intensity of Ti(IV)-OH groups at 3650 cm^{-1} increased apparently compared to calcined TiO_2 sample treated without UV, as shown in Figure V.1. This result implied the formation of more Ti(IV)-OH hydroxyl groups on TiO_2 surface after UV treatment. Photo-induced holes trapping at Ti(IV)-OH centers forming OH radicals had a characteristic vibration at 3683 cm^{-1}, which was not observed in our case by *in situ* IR [129]. Small peaks were located at 3700 cm^{-1} for both samples. No obvious change was detected at 3700 cm^{-1}. Multiple peaks at 3500-3600 cm^{-1} region

disappeared for TiO_2 sample treated under UV, indicating the removal of H-bonded and bridged hydroxyl groups after exposure to UV irradiation. After treating TiO_2 samples under UV irradiation, the number of Ti(IV)-OH groups increased based on the resulting IR spectra. Possible mechanisms will be investigated next.

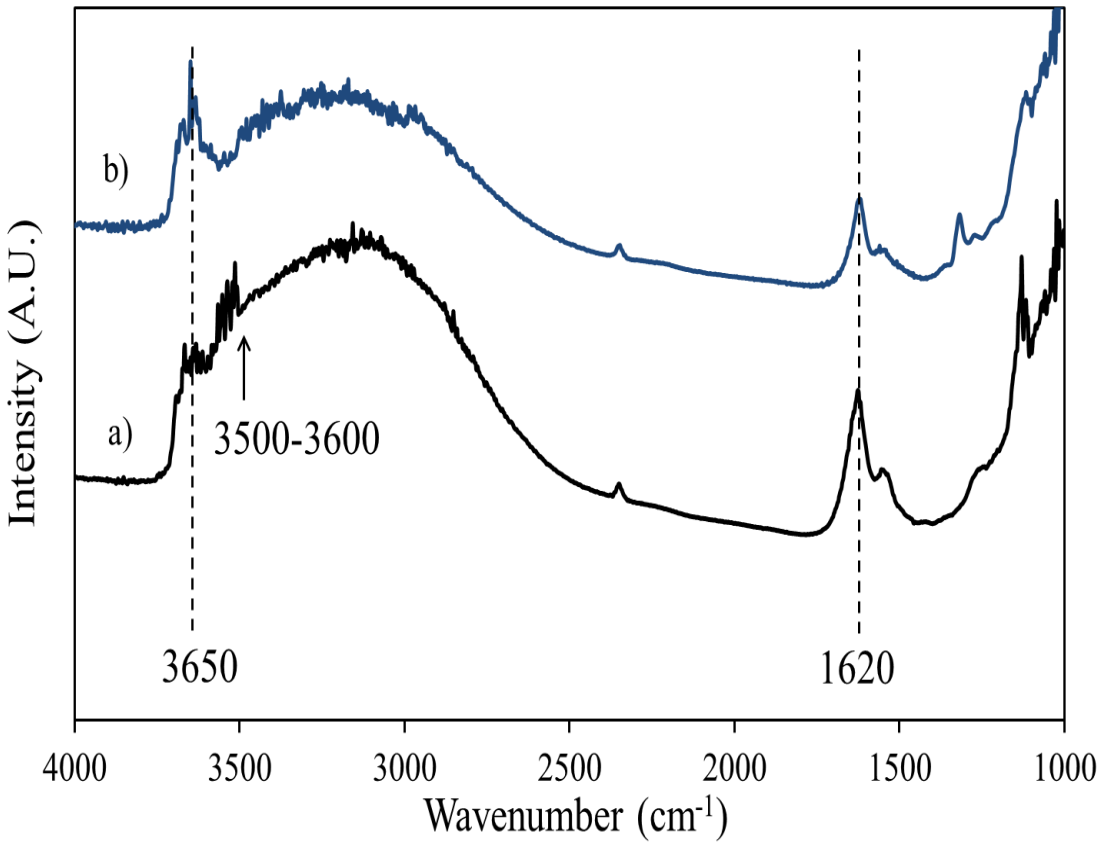

Figure V.1. *In situ* IR spectra (in absorbance mode) of calcined TiO_2 a) treated without UV; b) treated under UV irradiation (UV wavelength: 365 nm)

At 1000-2000 cm^{-1} region, calcined TiO_2 sample without UV treatment showed a strong peak centered at 1620 cm^{-1} which was assigned to δ(HOH) bending mode of the chemisorbed H_2O molecules [130, 131]. Also, a small peak located at 1140 cm^{-1} was observed for the TiO_2 sample under dark, which can be assigned to surface hydroperoxo

species TiOOH and different types of H-bonded H_2O molecules as shown in Figure V.2 [107, 119, 124, 130].

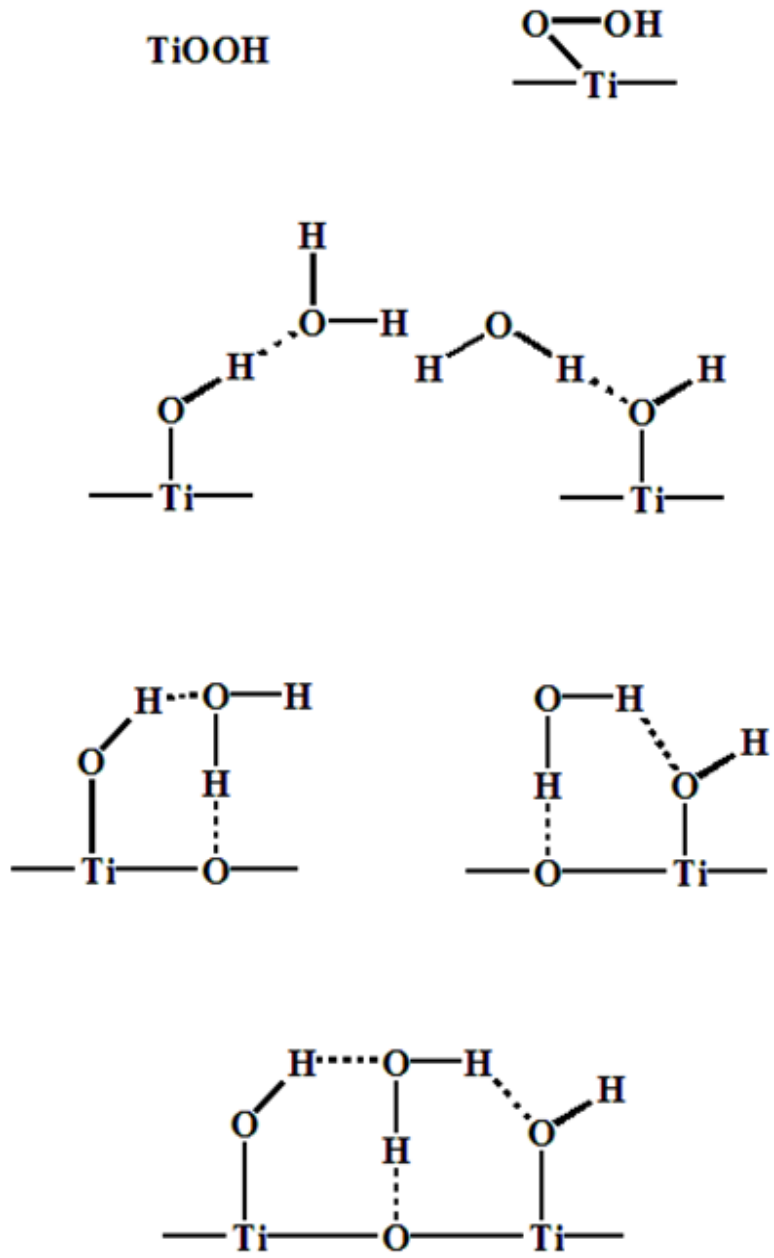

Figure V.2. Surface structures of H-bonded H_2O and TiOOH on TiO_2 samples (reproduced from Nakamura, R. et al. Journal of the American Chemical Society 2003 [119]; Berzrodna, T. et al. Journal of Molecular Structure 2004 [130])

Table V.1. IR peaks and their respected assignments for calcined TiO_2 treated with and without UV irradiation

Wavenumber (cm^{-1})	Assignments
1140	TiOOH H-bonded H_2O with -OH
1620	δ(HOH) bending mode of the chemisorbed H_2O
3500-3600	stretching vibration of H-bonded and bridged -OH groups
3640	stretching vibration of Ti(IV)-OH
3683	photo-induced holes trapping at Ti(IV)-OH centers
3700	stretching vibration of Ti(III)-OH

Chemisorbed H_2O and TiOOH were stabilized by H-bonds with neighboring Ti anion and other hydroxyl groups, which can be removed at high temperature. The intensity of the peak at 1620 cm^{-1} decreased dramatically after the UV treatment as shown in Figure V.1 b). And the peak at 1140 cm^{-1} almost disappeared for TiO_2 sample under UV irradiation. Results indicated clearly that adsorbed water molecules and bridged hydroxyl groups were removed during the UV treatment procedure while more surface hydroxyl

groups were formed on TiO_2 under UV. The IR peaks and their respected assignments for calcined TiO_2 treated with and without UV are listed in Table V.1.

Based on *in situ* IR spectra, the photo-assisted pathway to generate Ti(IV)-OH groups on TiO_2's surface were postulated. Many experimental and theoretical results indicated that adsorbed water molecules could dissociate on oxygen vacancies and react with bridged -OH groups under certain circumstance, giving rise to chemisorbed hydroxyl groups on TiO_2 surface [132, 133]. Possible pathway to generate isolated hydroxyl groups from bonded -OH sites without the involvement of H_2O molecules under UV is illustrated in Figure V.3. As a result, sulfur removal capacities were increased during UV-assisted desulfurization process using TiO_2 adsorbents due to the formation of extra isolated hydroxyl groups under UV.

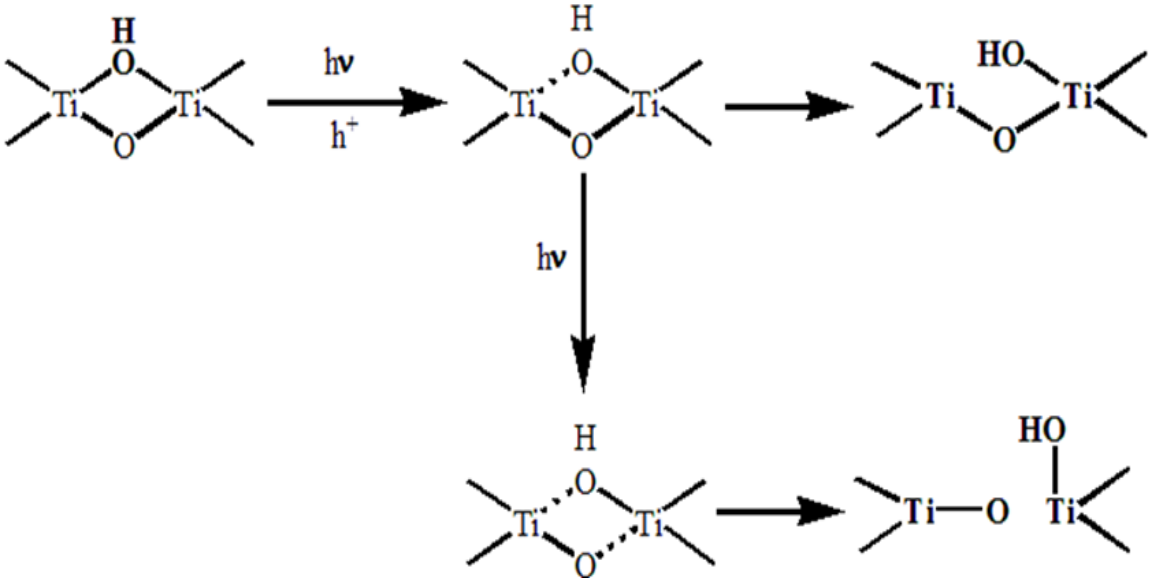

Figure V.3. Formation of isolated hydroxyl groups from bonded -OH sites on TiO_2 under UV in the absence of H_2O molecules

However, IR spectra indicated that chemisorbed H_2O was also involved in the photo-assisted formation of Ti(IV)-OH on TiO_2's surface. The effect of absorbed H_2O on surface hydroxyl groups will be studied and discussed in details later.

V.3.2. XPS study

In order to confirm the effects of UV on surface hydroxyl groups on TiO_2, XPS measurements were also performed on calcined TiO_2 samples treated with and without UV. High resolution XPS spectra of Ti 2p for TiO_2 treated with and without UV irradiation are shown in Figure V.4.

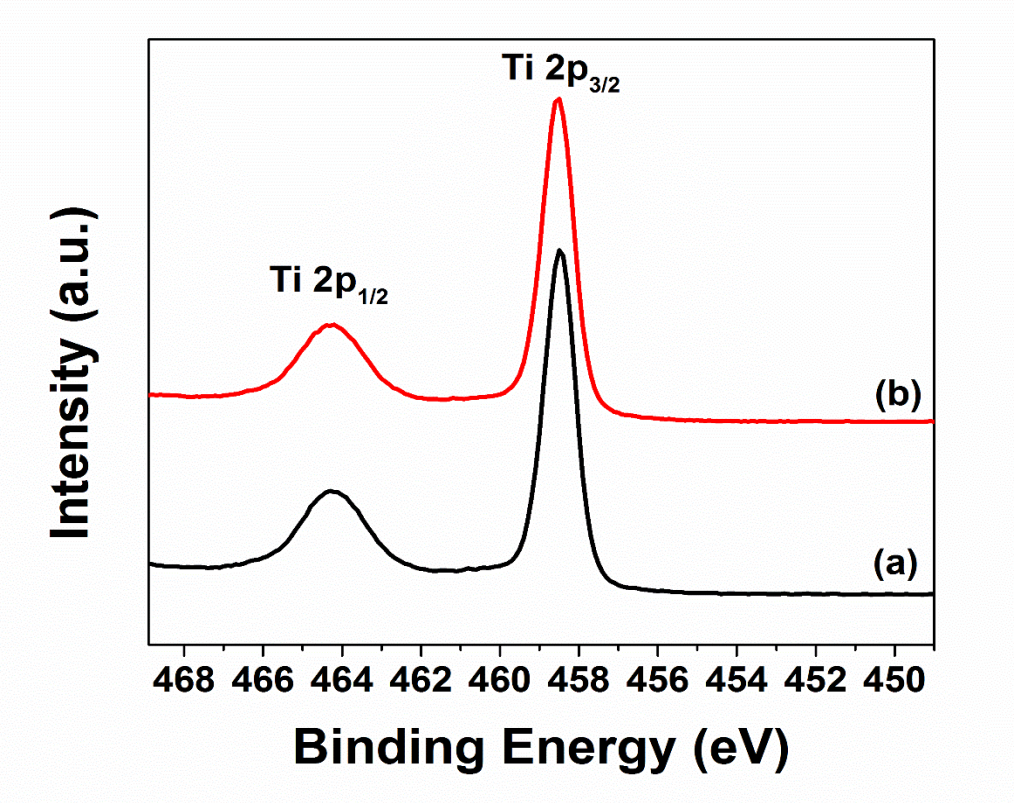

Figure V.4. High resolution XPS spectra of Ti 2p for TiO_2 samples treated a) without UV and b) with UV irradiation (UV wavelength: 365 nm)

Binding energies for Ti 2p and O 1s core levels, as well as the ratio of -OH/O^{2-} are all listed in Table V.2. The binding energy values of Ti $2p_{1/2}$ and $2p_{3/2}$ were observed at 464.3 eV and 458.5 eV for two samples which were identified as TiO_2 [134, 135]. Based on XPS analysis on Ti 2p core level, no Ti^{3+} species were detected, and the UV treatment did not affect the final chemical state of Ti^{4+}. This conclusion confirmed the results we got from *in situ* IR spectra, where Ti(III)-OH groups were not observed on TiO_2's surface treated with and without UV. Then the intensity changing in surface -OH groups after UV treatment was studied in details. The effect of UV irradiation on surface species on Ag/TiO_2 is currently under investigation.

Table V.2. Binding energy values for Ti 2p and O 1s core levels and the area ratio of hydroxyl group (-OH)/O^{2-} by XPS

TiO_2	Binding Energy (eV)				Area Ratio -OH/O^{2-}
	Ti $2p_{1/2}$	Ti $2p_{3/2}$	Bulk O^{2-}	-OH	
Without UV	464.3	458.5	529.7	531.5	0.13
Treated with UV	464.3	458.5	529.7	531.5	0.25

Figure V.5 show O 1s spectra measured under dark and UV environment separately. On the basis of various XPS studies on TiO_2, the peak at approximately 529.7 eV and the shoulder at 531.5 eV were attributed to lattice O^{2-} and hydroxyl groups (-OH), respectively [110, 116, 136, 137]. As shown in Figure V.5, the peak positions for these two components remained similar under different treating conditions.

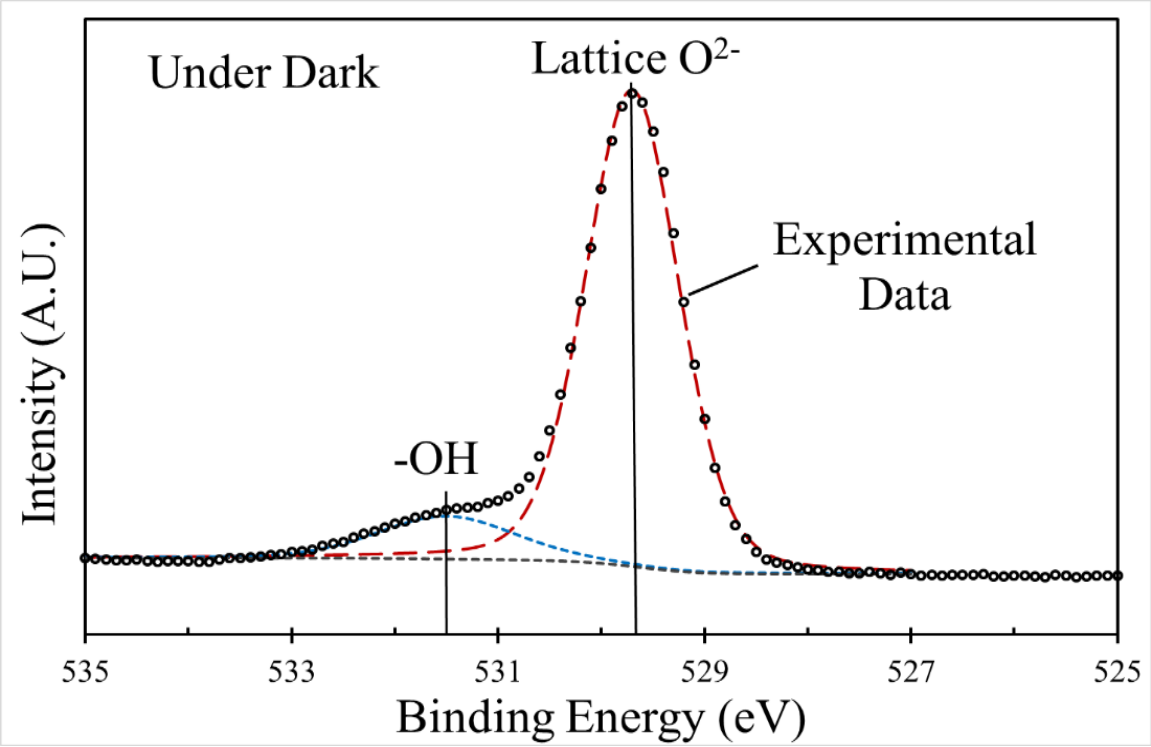

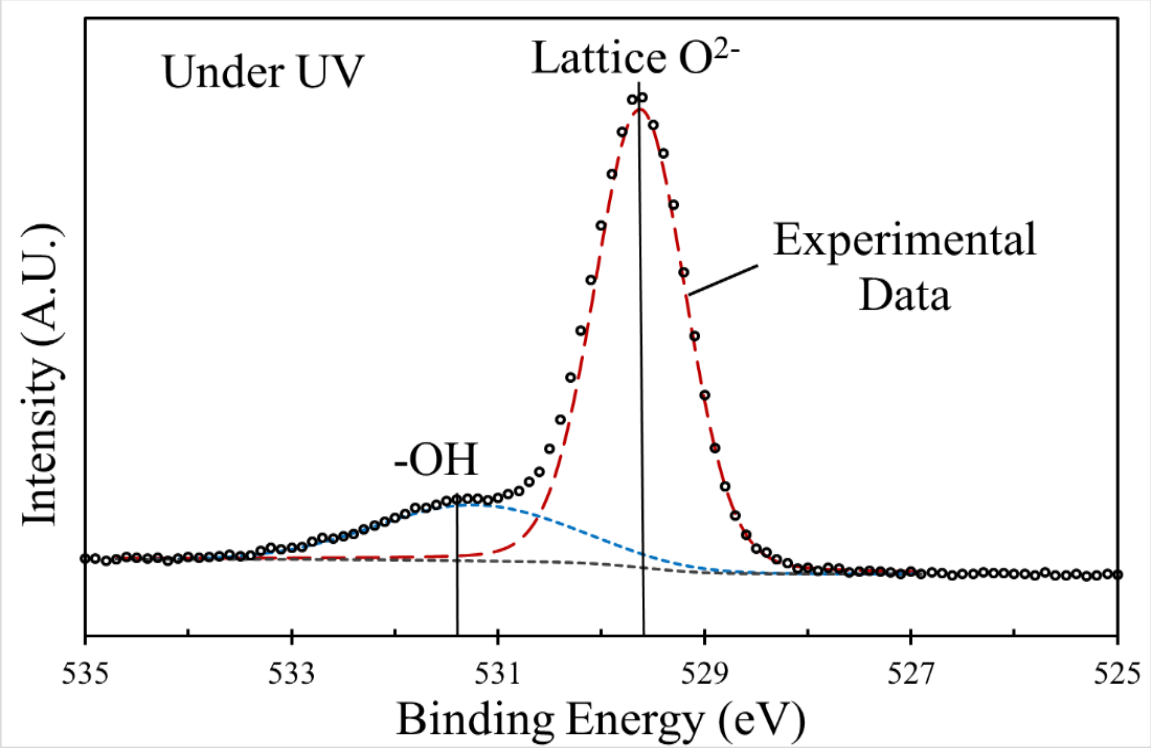

Figure V.5. O 1s XPS spectra of calcined TiO_2 treated without UV (top); and TiO_2 treated under UV irradiation (bottom) (UV wavelength: 365 nm)

However, the relative intensities of the peaks changed as listed in Table V.2. After exposure to UV irradiation for 2 h, the ratio of the area for hydroxyl group (-OH)/O^{2-} was increased from 0.13 to 0.25. The change in the intensity at 531.5 eV was mainly due to the increase in the concentration of surface hydroxyl groups on TiO_2 samples treated with UV. Resulting XPS spectra indicates more hydroxyl groups were formed on TiO_2 surface under UV along with the decrease in lattice oxygen, which is consistent with the conclusion we got from our previous *in situ* IR studies. In addition, the mechanism we postulated before on formation of isolated hydroxyl groups from bonded -OH sites on TiO_2 under UV in the absence of H_2O molecules can also be explained by this XPS result.

V.4. Effect of H_2O on TiO_2 surface

Breakthrough results showed that sulfur removal capacities of TiO_2 adsorbents decreased in the presence of water molecules without UV. However, the performance was further improved with H_2O under UV environment. The effect of H_2O molecules and the surface intermediates generated under UV in the presence of H_2O were investigated by *in situ* infrared (IR) spectroscopy under room temperature. *In situ* IR studies were carried out on TiO_2 treated without and with H_2O molecules as shown in Figure V.6.

By comparing IR spectra got in Figure V.6 a) and b), the peaks at 3500-3600 cm^{-1} region were diminished in intensity and the peaks at 3650 cm^{-1} also decreased after the hydration treatment, indicating the interaction between surface Ti(IV)-OH hydroxyl groups and water molecules. The peak intensity at 1620 cm^{-1} increased apparently after the H_2O treatment, suggesting absorption of more water molecules on TiO_2 surface. Thus,

the decrease in a number of surface acid sites (-OH groups) caused by H_2O molecules had a negative effect on desulfurization performance of TiO_2 adsorbents.

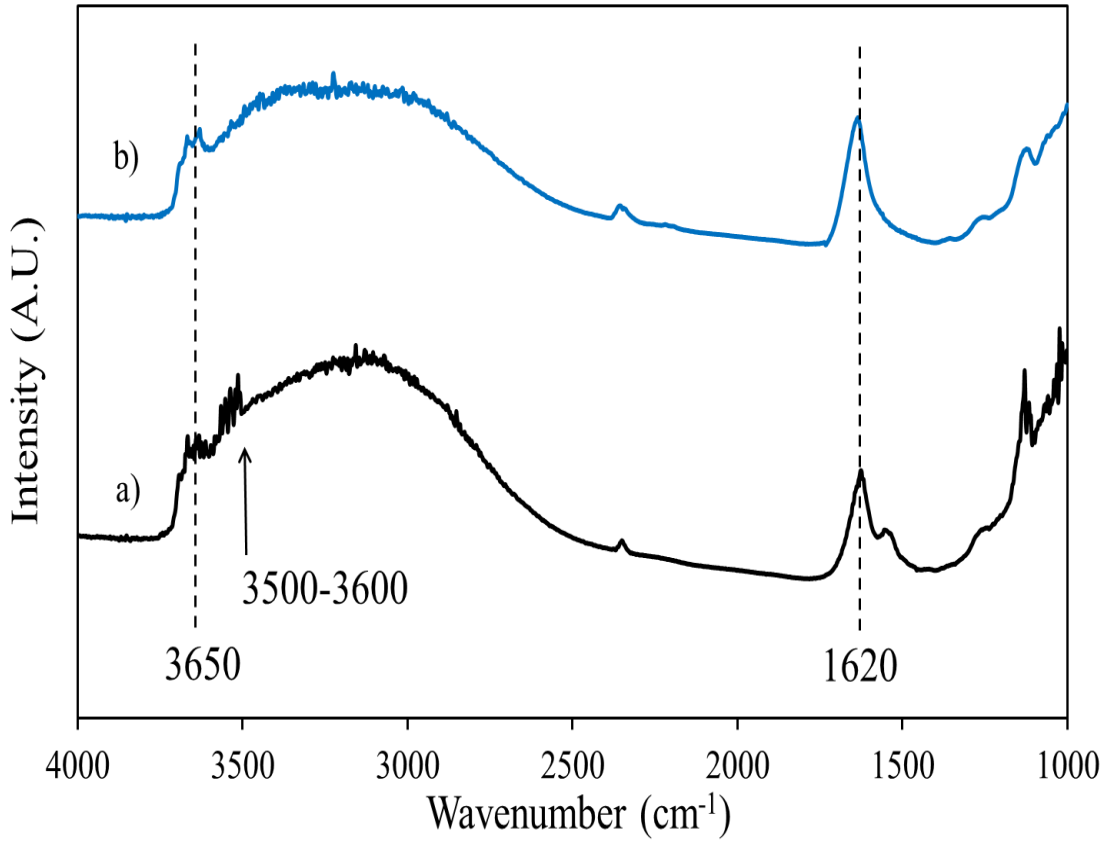

Figure V.6. *In situ* IR spectra (in absorbance mode) of calcined TiO_2 a) treated without H_2O; b) treated with H_2O

Although water as a common fuel additive had a negative effect on desulfurization performance of TiO_2 based adsorbents, sulfur removal capacities can be further increased with hydration treatment under UV environment demonstrated by breakthrough experiments under UV using model fuels containing water. Final IR results for calcined TiO_2 adsorbent and TiO_2 treated with H_2O molecules under dark and UV conditions were

all shown in Figure V.7. At 3650 cm^{-1}, sharp peak with highest intensity was observed for TiO_2 adsorbents treated with H_2O under UV as shown in Figure V.7 c). This characteristic peak represented surface Ti(IV)-OH groups as we mentioned before. And, the intensity of the characteristic band at 1620 cm^{-1} reduced apparently under UV irradiation in the presence of H_2O when comparing IR spectra got from Figure V.6 b) and c).

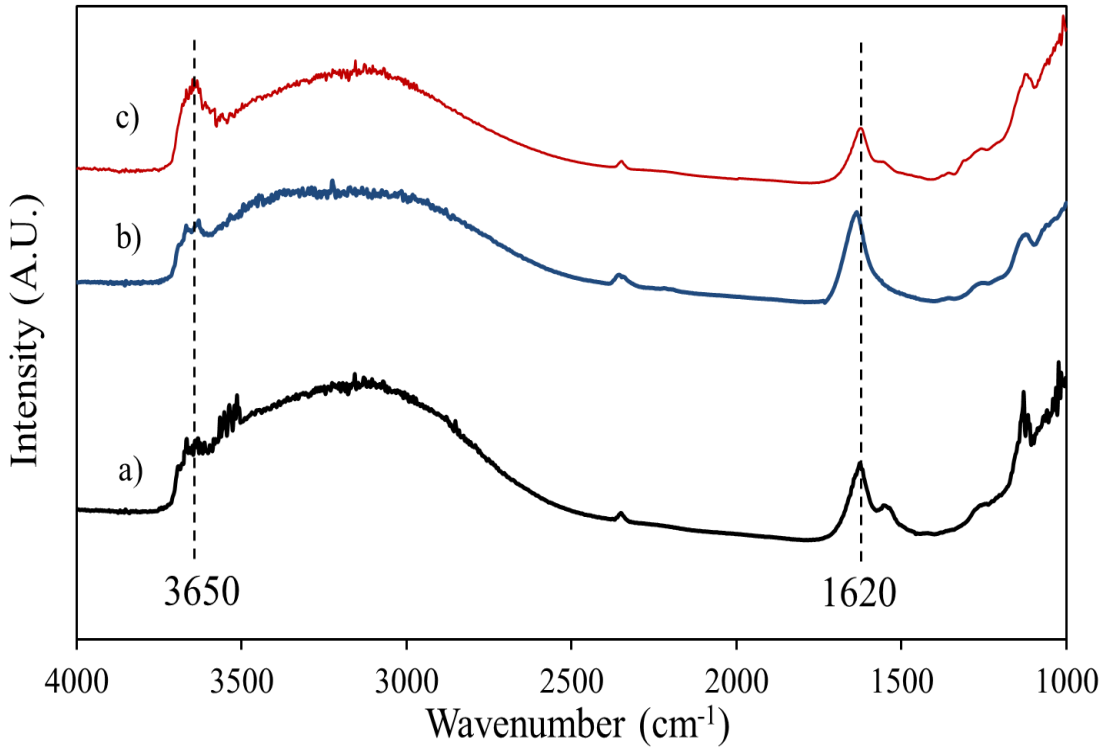

Figure V.7. *In situ* IR spectra (in absorbance mode) of calcined TiO_2 a) treated without UV without H_2O; b) treated without UV with H_2O; c) treated under UV with H_2O (UV wavelength: 365 nm)

These results indicated that less H_2O molecules adsorbed on TiO_2 surface while more Ti(IV)-OH groups formed by the introduction of UV illumination. Possible pathways of forming surface hydroxyl groups from bridged -OH and bridged O sites in the presence of H_2O were illustrated in Figure V.8 [107, 109]. Thus, for TiO_2 based adsorbents, UV treatment along with water can further increase the total number of Bronsted acid sites (-OH groups) which had a positive effect on desulfurization performance of TiO_2.

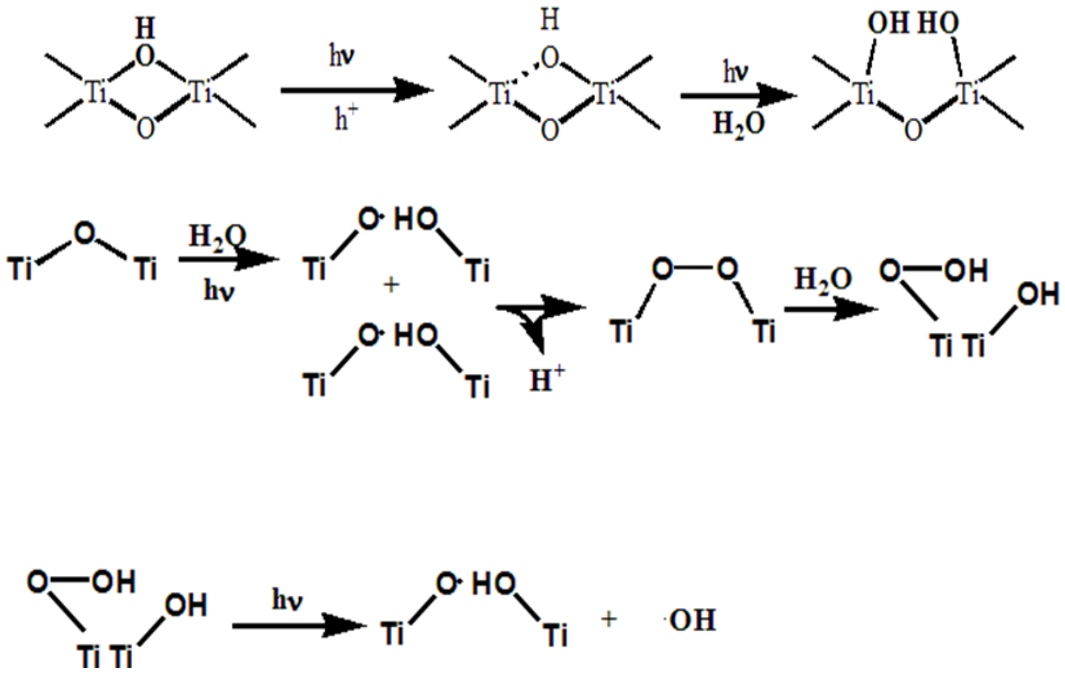

Figure V.8. Possible mechanisms to generate isolated hydroxyl groups from bonded -OH and bridged O sites in presence of H_2O molecules under UV irradiation on TiO_2

V.5. Study on surface hydroxyl radicals

One of the main active species produced on TiO_2 photocatalysts was surface hydroxyl radical [138]. These hydroxyl radicals were not observed by *in situ* IR or XPS so far in our study. Here, the fluorescence spectroscopy was applied to investigate surface

hydroxyl radicals. This technique is rapid, simple and has high sensitivity. What's more, fluorescence is mainly affected by hydroxyl radicals while other water radicals such as $H\cdot$ and $HO_2\cdot$ generated under UV do not significantly influence the fluorescence spectra [102]. Based on these results, a fluorescent compound which is 2-hydroxyterephthalic acid produced by UV illumination on TiO_2 which is stable could be ascribed to the reaction between hydroxyl radicals and terephthalic acid.

Four experiments were carried out here. For calcined TiO_2 sample, the recirculation of TA mixture remained 2 h without UV. For UV continuous irradiation experiment calcined TiO_2 adsorbents were loaded into packed bed reactor. And the recirculation of TA mixed liquid was carried out under UV for 2 h. For UV-treated TiO_2 samples, the TiO_2 bed was firstly exposed to UV for 2 h followed by recirculation without any irradiation. Finally, for reference, the experiment was also conducted without UV using empty bed full of clear quartz beads. The determination of surface hydroxyl radicals was conducted under room temperature on a Shimadzu RF-5301PC spectrophotometer. The excitation wavelength is at 315.0 nm and emission wavelength ranges from 320 to 600 nm.

And the relative concentration of surface hydroxyl radicals can be easily determined by such technique. The resulting fluorescence spectra got under different conditions are shown in Figure V.9. The relative concentration of hydroxyl radicals can be estimated by the intensity of fluorescence spectra. The higher the intensity, the greater the concentration of OH radicals the sample had. As a result, UV-treated TiO_2 had the highest fluorescence intensity meaning the highest amount of OH radicals were generated on the surface as shown in Figure V.9 d). Also, a certain amount of hydroxyl radicals was

formed during continuous flow experiment with UV irradiation on as shown in Figure V.9 c). For calcined TiO_2 and empty bed, no hydroxyl radical were observed based on the spectral results as shown in Figure V.9 a) and b). The lifetime and the effect of surface hydroxyl radicals on desulfurization performance of TiO_2 adsorbents still need further investigation.

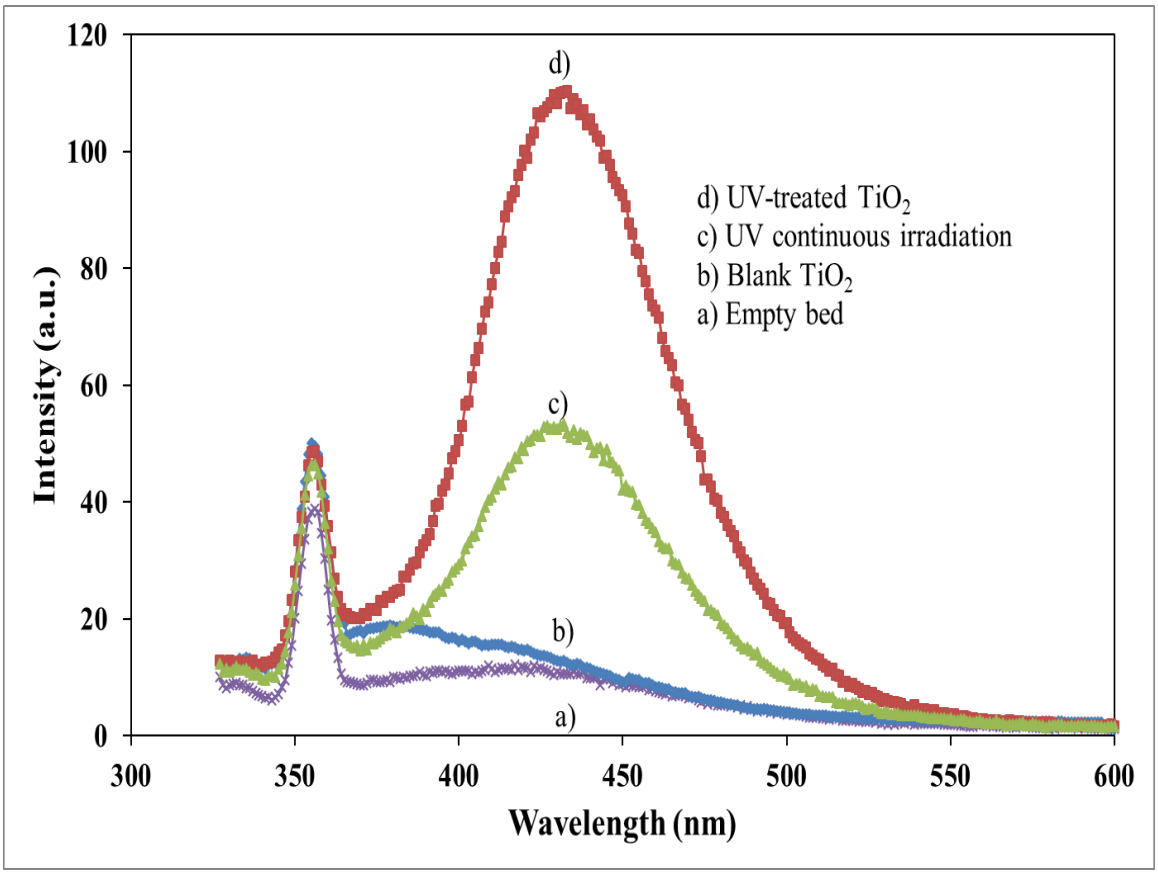

Figure V.9. Fluorescence spectra of various samples: a) empty bed without UV; b) calcined TiO_2 without UV; c) process with UV; d) process without UV using UV-treated TiO_2 (excitation wavelength: 315.0 nm; emission wavelength: 320-600 nm; UV wavelength: 365 nm)

V.6. Conclusions

Effects of UV and H_2O molecules on surface hydroxyl groups on TiO_2 adsorbents had been investigated by *in situ* IR and XPS. Based on *in situ* IR spectra, the number of surface hydroxyl groups Ti(IV)-OH increased apparently after UV treatment in the absence of H_2O molecules, while bridged and H-bonded hydroxyl groups were removed after exposure to UV irradiation. Same results were got from XPS spectra. At the same time, a certain amount of surface chemisorbed H_2O molecules were also removed under UV condition. As a result, sulfur removal capacities of TiO_2 adsorbents were increased with UV treatment.

For TiO_2 samples treated with H_2O molecules, IR results indicated the interaction between surface hydroxyl groups and water molecules. Such interaction caused the decrease in surface acid site. This result also confirmed the negative effect of H_2O on desulfurization performance of TiO_2 adsorbents. However, more surface hydroxyl groups were formed on TiO_2 surface confirmed by IR analysis on TiO_2 sample treated with H_2O under UV. The problem caused by H_2O molecules can be also solved by the introduction of UV system. Thus, for TiO_2 based adsorbents, UV treatment along with water can further increase the number of surface active sites (-OH groups) which had a positive effect on desulfurization performance. Possible pathways of forming surface hydroxyl groups from bridged -OH and bridged O sites were discussed in this chapter.

Finally, the fluorescence spectroscopy was applied to investigate surface hydroxyl radicals, which are main active species produced on TiO_2 photocatalysts under UV. UV-treated TiO_2 had the highest fluorescence intensity meaning the largest amount of OH radicals were generated on the surface of this sample. And a certain amount of hydroxyl

radicals was formed during continuous flow experiment with UV irradiation. For calcined TiO_2 and empty bed, no hydroxyl radicals were observed based on the spectral results. The lifetime and the role of surface hydroxyl radicals during adsorptive desulfurization using TiO_2 adsorbents still need further investigation.

VI. Sulfur Removal Pathways under UV Irradiation

VI.1. Introduction

During the last decades, photocatalysis has gained considerable research interests on desulfurization from liquid fuels. TiO_2/UV system has already been introduced into sulfur removal process based on its high oxidative efficiency. Photo-oxidation of organic sulfur compounds in liquid oil had been studied since the 1990s [64].

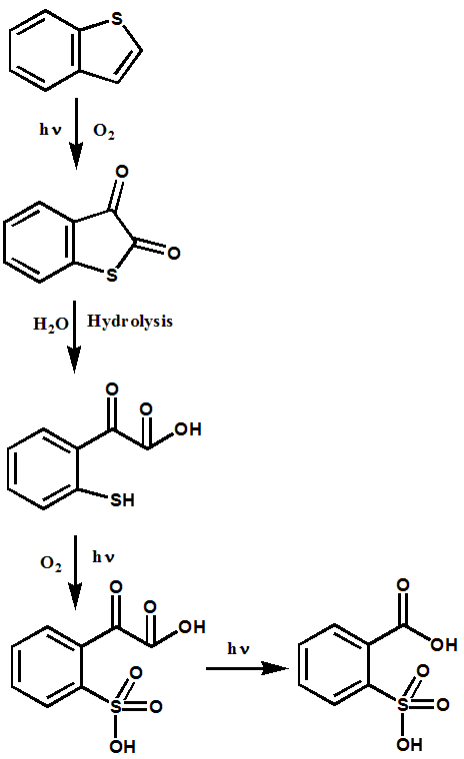

Figure VI.1. Photo-reaction pathway for benzothiophene under photo-irradiation (reproduced from Shiraishi, Y. et al. Industrial Engineering Chemistry Research 1999 [65])

UV source and solar irradiation were first used for photo-oxidation of benzothiophene and dibenzothiophene. Benzothiophene and dibenzothiophene were photo-decomposed under UV lights and the resulting oxidized compounds were removed by novel two-phase liquid-liquid extraction step [48, 53, 65]. The oxidative products and photoreaction pathways for benzothiophene had already been identified as shown in Figure VI.1.

Based on sulfur photo-oxidation mechanisms, TiO_2, and TiO_2 based photocatalysts have been introduced into oxidative desulfurization process called photocatalytic oxidative desulfurization (PODS). PODS has been proven to be an effective organosulfur removal method [139]. Photocatalytic oxidative desulfurization has been studied for TiO_2 under both laboratory and pilot-plant scale using UV light, simulated and natural solar lights [69]. Recently, technology for ultra-deep removal of thiophene compounds over catalyst assisted by ultraviolet irradiation (URTCU) was developed successfully in 2013 using TiO_2 loaded zeolite [70]. Based on experimental results, about 99% of the thiophene compounds can be oxidized under UV irradiation and removed from model fuels. Moreover, ultra-deep desulfurization by PODS was now able to be carried out under the low molar ratio of H_2O_2 and sulfur [63]. The reported conversion of dibenzothiophene in model fuels using TiO_2 catalysts in the ionic liquid can achieve 96%. Thus, desulfurization by photocatalysts is a potential method to remove sulfur aromatic compounds from liquid fuels. However, PODS is based on photocatalytic oxidative mechanisms of organosulfur species and it usually takes a long time for organosulfur compounds to reach complete photo-decomposition.

For our research on adsorptive desulfurization process under UV irradiation using TiO_2 based adsorbents, no strong oxidative agent was needed to be applied during the

procedure. The photo-assisted adsorptive desulfurization is different from photocatalytic oxidative desulfurization process. Although the water was added to the model fuel as a mild oxidative agent, the total desulfurization time is too short compared to PODS. Photocatalytic reactions of organosulfur compounds on TiO_2 surface in the presence of H_2O was hard to occur in such a short time period. However, the surface hydroxyl radicals and lattice oxygen could react as strong oxidants which can react with sulfur compounds under UV environment. Photo-oxidative reactions may occur on TiO_2 surface. In order to determine possible photo-decomposed products in the liquid phase during UV-assisted breakthrough tests and the photo-assisted desulfurization mechanism on TiO_2 surface, the sulfur removal pathway on TiO_2 adsorbent during UV-assisted adsorptive desulfurization (ADS) need further investigation.

VI.2. Experimental

To determine possible photo-decomposed products of benzothiophene in the liquid phase under UV irradiation, liquid fuel samples were first analyzed with GC-PFPD and GC-FID. GC-PFPD analysis was first conducted in Varian CP 3800 GC with PFPD using Restek RXI-5 column of 30 m length and 0.25 mm ID. The column temperature was at 200 ℃ initially and then was raised to 300 ℃ at 10 ℃/min. Then the temperature was kept at 300 ℃ for 2 min. Liquid sample injection volume was 10 μL with the splitting ratio between 0 to 20. GC-FID analysis was conducted in Hewlett-Packard 5890 Series II equipped with Resteck Rt-Q-BOND of 30 m length and 0.53 mm ID. Sample injection volume was 1 μL with the splitless mode. The column temperature was 70 ℃ at the beginning. Then the temperature was increased to 270 ℃ at 40 ℃/min and kept there for

7 min. Injection temperature was at 175 ℃. Fuel samples were collected at the end of breakthrough experiments with and without UV irradiation using only calcined TiO_2. For GC-PFPD analysis, liquid samples were all diluted from 3500 ppmw to 35 ppmw using pure n-octane. For GC-FID, original liquid samples were analyzed without any dilution. Reference samples were obtained from a breakthrough test using empty bed without UV.

FTIR analysis with different treating molecules was recorded in order to study the possible sulfur removal pathways under UV on TiO_2 surface. Dried TiO_2 powder was pressed into self-supporting pellet followed by calcination in dry air at 450 ℃ for 2 h. The calcined TiO_2 disk was then loaded into customized IR cell with ZnSe windows and pretreated in dry air at 200 ℃ for 1 h followed by cooling down in dry N_2. After those pretreatment steps, TiO_2 adsorbent sample inside the IR cell was treated with different organic molecules with and without UV irradiation at room temperature. The treating molecules were bubbled into IR cell by N_2. Two UV lamps were put on both sides of the IR cell in order to ensure full penetration of UV irradiation onto TiO_2 samples during *in situ* IR analysis. Finally, the cell was evacuated to 100 mTorr before final IR analysis. FTIR spectra for TiO_2 have been measured by Thermo Scientific Nicolet IR100 spectrometer in a region between 400-4000 cm^{-1}. Spectra were recorded using a resolution of 4 cm^{-1} with 32 averaged scans under ambient lab conditions.

VI.3. Photo-decomposed products under UV

For adsorptive desulfurization under UV irradiation, lattice oxygen, surface hydroxyl groups, and radicals on TiO_2 surface can all act as oxidative agents. Under that condition,

photo-oxidative reactions might occur in the liquid phase. Also, when water was added to the model fuel, photo-decomposition and oxidation of organosulfur compounds are possible to be observed. As a result, photo-oxidative products of organic sulfur compounds can form in liquid model fuels. To determine sulfur species and possible photo-oxidative products in the liquid phase, liquid fuel samples after breakthrough experiments with and without UV conditions were analyzed by GC-PFPD and GC-FID.

GC-PFPD chromatogram of the liquid reference sample containing 35 ppmw sulfur as benzothiophene in n-octane is shown in Figure VI.2 a). This reference sample was obtained from the breakthrough study without UV using empty bed loading with clear quartz beads. Figure VI.2 b) and c) show the gas chromatogram of diluted liquid samples from breakthrough experiments using TiO_2 under dark and UV irradiation separately. Only one strong peak appeared at 2.5 min as shown in GC-PFPD chromatograms. By comparing GC results, this strong peak at 2.5 min on gas chromatogram belonged to benzothiophene. And no new peaks appeared for the UV-assisted experimental sample, indicating no photo-oxidative products in the liquid phase.

The photo-decomposition of the hydrocarbon model fuel can be also detected by GC-FID. Also, possible photo-oxidative products of n-octane could also be determined based on GC-FID results. Comparing the GC-FID results got from Figure VI. 3 a) and b), no photo-decomposition of n-octane was observed. Furthermore, GC-FID results shown in Figure VI.3 were consistent with GC-PFPD results as shown in Figure VI.2. No traceable amount of photo-oxidative products of organic sulfur or n-octane was detected by GC-FID. Based on GC-PFPD and GC-FID results, no photo-oxidative products of organic sulfur compounds were observed in liquid fuels.

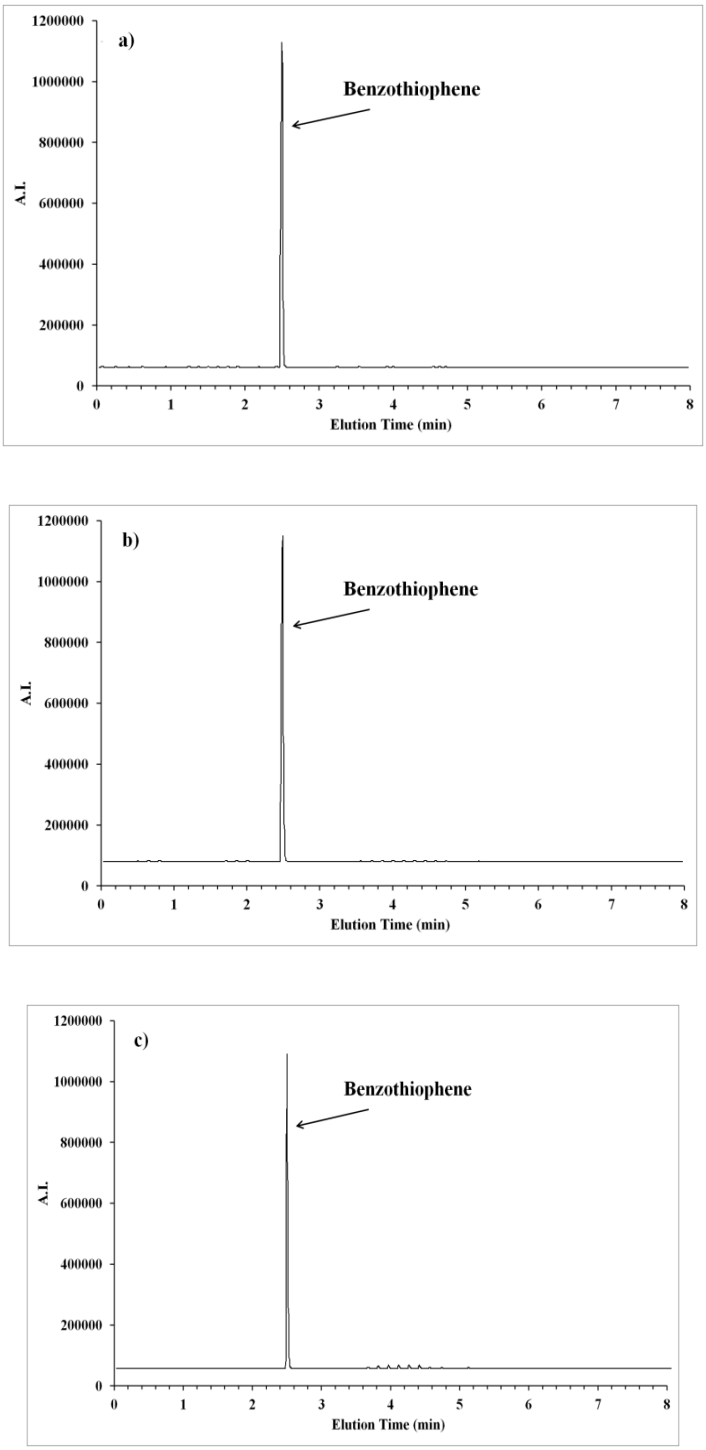

Figure VI.2. GC-PFPD chromatograms for a) liquid reference sample; b) liquid fuel sample after 2-h breakthrough experiment using TiO_2 without UV; c) liquid fuel sample after 2-h UV-assisted breakthrough experiment using TiO_2

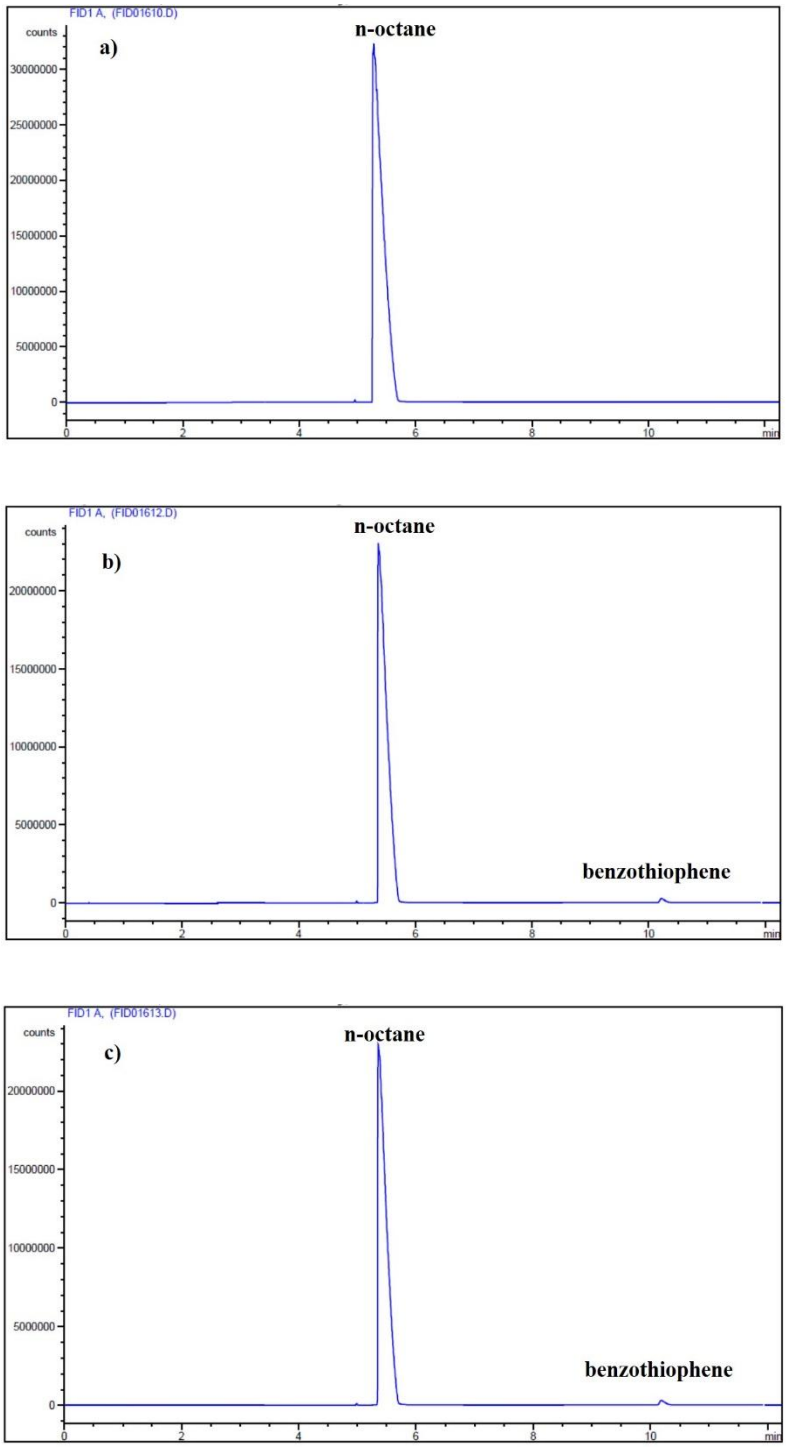

Figure VI.3. GC-FID chromatograms for a) n-octane; b) benzothiophene in n-octane; c) model fuel sample after 2-h breakthrough experiment under UV irradiation using TiO_2 adsorbents

For dynamic desulfurization process, we can conclude from GC results that on photo-oxidative reaction occurred in the liquid phase during photo-assisted adsorptive desulfurization process. However, photoreaction and sulfur removal pathway on TiO_2 surface cannot be determined by GC analysis. Thus, sulfur adsorption pathways onto solid phase with and without UV irradiation were then investigated by *in situ* IR.

VI.4. Sulfur adsorption pathways onto TiO_2 under UV

In situ IR spectroscopy was performed on calcined TiO_2 samples treated with n-octane and the model fuel with and without UV irradiation in order to investigate sulfur removal pathways on the surface. As all samples were subjected to the vacuum before final IR analysis, it was assumed that adsorbent surface contained mostly chemisorbed species. Figure VI.4 show the resulting IR spectra of calcined TiO_2 treated with n-octane and 3500 ppmw sulfur as benzothiophene in n-octane without UV. Figure VI.4 a) shows the spectrum of calcined TiO_2 treated with n-octane alone for reference.

The calcined TiO_2 sample spectra treated with n-octane showed bands in the 3600-3700 cm^{-1} wavenumber region, which have been assigned to stretching vibrations of isolated hydroxyl groups [120, 125, 129, 131]. Model fuel containing benzothiophene was then used to treat calcined TiO_2 without UV, and the resulting spectrum is shown in Figure VI.4 b). The bands at 3600-3700 cm^{-1} were diminished in intensity, indicating that the hydroxyl groups were interacting with organic sulfur species. Figure VI.5 shows the spectra of calcined TiO_2 treated with n-octane and the model fuel without UV in the 1000-2000 cm^{-1} wavenumber region.

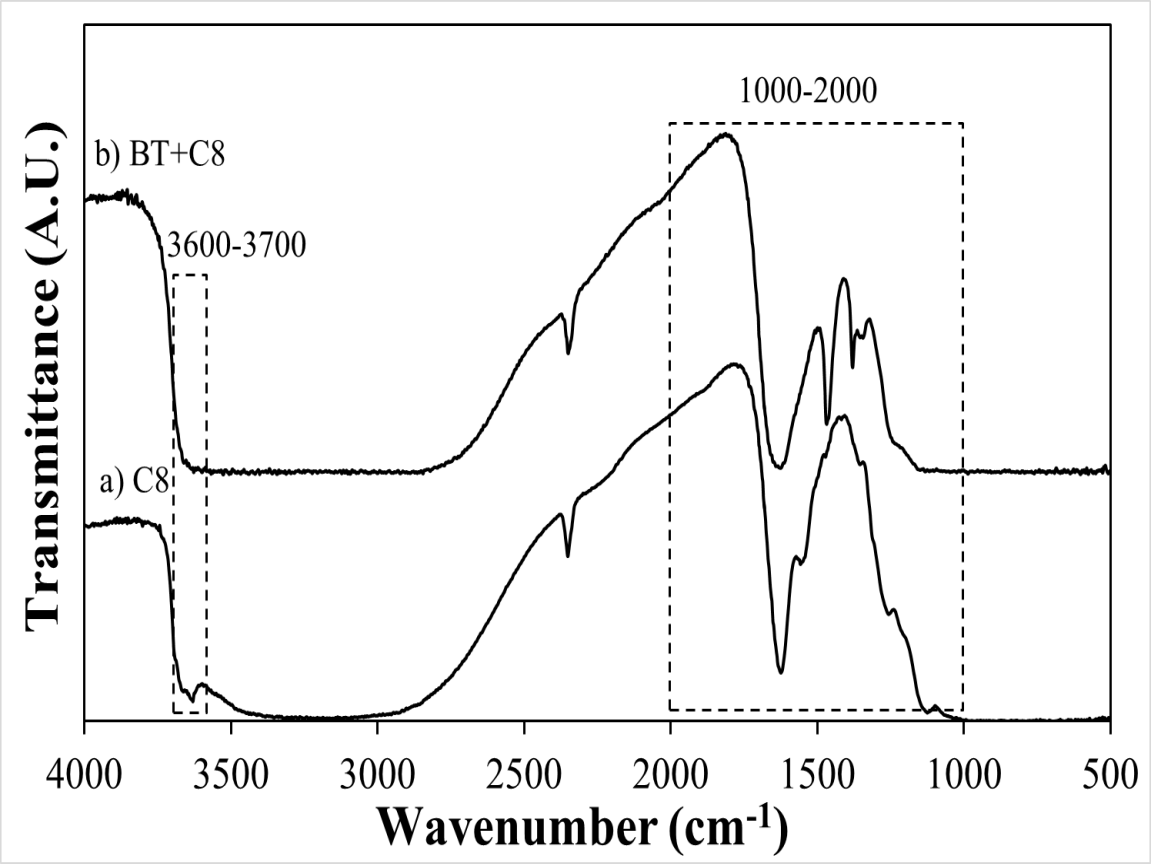

Figure VI.4. *In situ* IR spectra (in transmission mode; wavenumber: 500-4000 cm^{-1}) of calcined TiO_2 treated without UV with a) n-octane; b) 3500 ppmw sulfur as benzothiophene in n-octane (UV wavelength: 365 nm)

Two noticeable bands were observed at 1360 cm^{-1} and 1640 cm^{-1} in two treated adsorbent samples. The strong band at 1640 cm^{-1} might be assigned to chemisorbed H_2O on TiO_2 surface [129, 140]. And the 1360 cm^{-1} band can be ascribed to the $\delta(CH_3)_s$ bending vibrations of adsorbed octane [141]. These results indicated that some of the octane molecules were adsorbed on adsorbent surfaces, but most of the surface hydroxyl groups were not interact with octane molecules. Figure VI.5 b) shows the IR spectrum of TiO_2 treated with model fuel (BT + C8) without UV. In the 1200-1600 cm^{-1} wavenumber region, two new bands were observed at 1390 and 1460 cm^{-1}. The band at 1390 cm^{-1}

represented $\delta(C=C)_s$ stretching vibrations of thiophene ring adsorbed on surface hydroxyl groups as shown in Figure VI.6 a) [142-144]. The other band at 1460 cm^{-1} represented vibrations of the aromatic ring, and the another possible interaction between the hydroxyl group and benzothiophene is shown in Figure VI.5 b) [100, 145]. Also, the band at 1460 cm^{-1} might represent $–CH_2$ bending and antisymmetric $–CH_3$ deformation of aliphatic compounds, indicating ring opening reactions [141]. IR bands and their respected assignments for calcined TiO_2 treated with different molecules without UV are listed in Table VI.1.

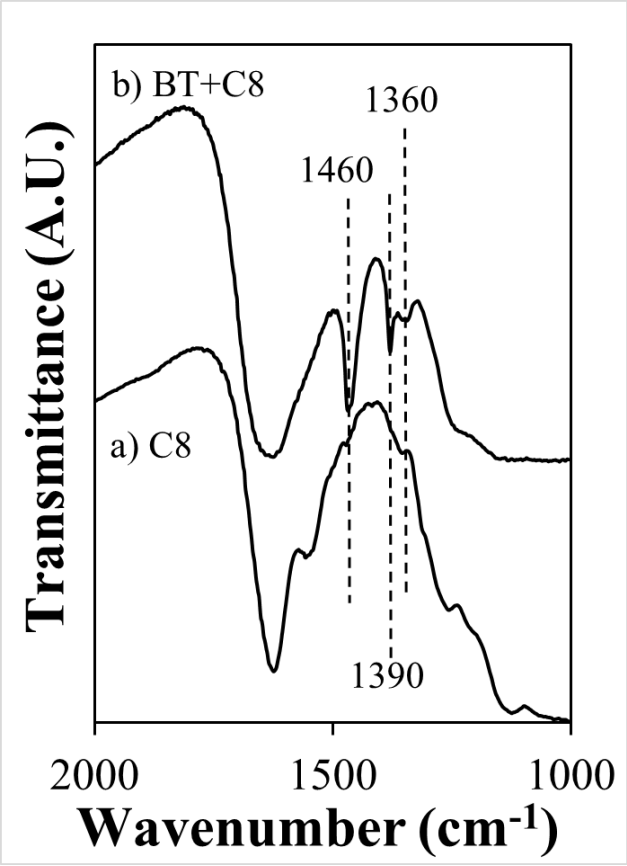

Figure VI.5. *In situ* IR spectra (in transmission mode; wavenumber: 1000-2000 cm^{-1}) of calcined TiO_2 treated without UV with a) n-octane; b) 3500 ppmw sulfur as benzothiophene in n-octane

Benzothiophene were chemisorbed on TiO_2 surface through the interactions between surface -OH and thiophene and aromatic rings based on *in situ* IR results. The possible interactions are illustrated in Figure VI.6. As we mentioned before, the IR band at 1460 cm^{-1} might represent $–CH_2$ bending and antisymmetric $–CH_3$ deformation of aliphatic compounds, which could indicate ring opening reactions. As a result, more studies should be carried out to determine whether there is ring opening reaction of benzothiophene on TiO_2's surface.

Table VI.1. IR bands and their respected assignments for calcined TiO_2 treated with different molecules without UV

Wavenumber (cm^{-1})	Assignments
1360	$\delta(CH_3)$ bending vibration of adsorbed C8
1390	δ(C=C)s stretching vibration of thiophene ring adsorbed on surface -OH groups
1460	vibration of aromatic ring or interaction between -OH and benzothiophene
1640	δ(HOH) bending vibration of H_2O
3600-3700	stretching vibrations of hydroxyl groups

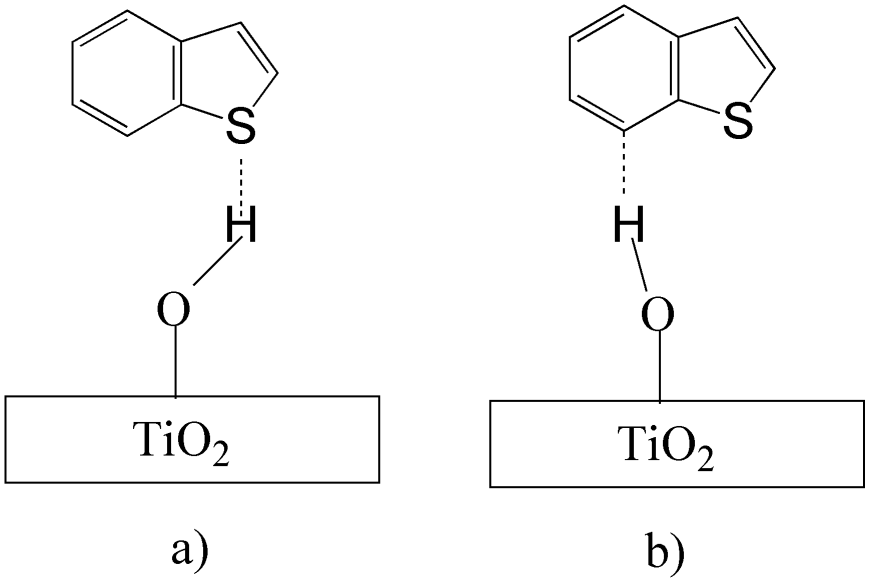

Figure VI.6. Interactions between surface hydroxyl groups and a) thiophene ring; b) aromatic ring

Many new active species could generate on TiO_2 surface under UV irradiation. Strong oxidative agents which are hydroxyl radicals were proven to be generated on TiO_2 surface under photo-irradiation. Photo-oxidative reactions of benzothiophene could occur on TiO_2 surface during photo-assisted adsorptive desulfurization process under such circumstance. Thus, photo-assisted sulfur removal process from liquid hydrocarbon over TiO_2 is a very complicated process. Thus, the fundamental investigation is essential to understand the surface reaction and possible mechanism. *In situ* IR was applied to help understand sulfur removal pathway onto TiO_2 under UV irradiation. Figure VI.7 show the resulting IR spectra for TiO_2 treated with 3500 ppmw sulfur as benzothiophene in n-octane with and without UV irradiation. As shown in Figure VI.7 a) and b), the bands at 3600-3700 cm^{-1} were diminished in intensity in both cases, indicating that the hydroxyl groups were interacting with benzothiophene. And in the 1000-2000 cm^{-1} wavenumber region, four bands were observed at 1360, 1390, 1460 and 1640 cm^{-1} and these bands

were present in two cases. The 1360 cm^{-1} has been ascribed to $\delta(CH3)_s$ bending vibrations of adsorbed octane. The strong band at 1640 cm^{-1} might be assigned to chemisorbed H_2O. The bands at 1390 and 1460 cm^{-1} were assigned to vibrations of thiophene ring and benzene ring separately. Those bands at 1360, 1390, 1460 and 1640 cm^{-1} shown in Figure VI.8 were also observed on calcined TiO_2 treated with benzothiophene in n-octane without any UV irradiation. So some benzothiophene were adsorbed onto TiO_2 via interactions between hydroxyl groups and thiophene ring during UV-assisted ADS.

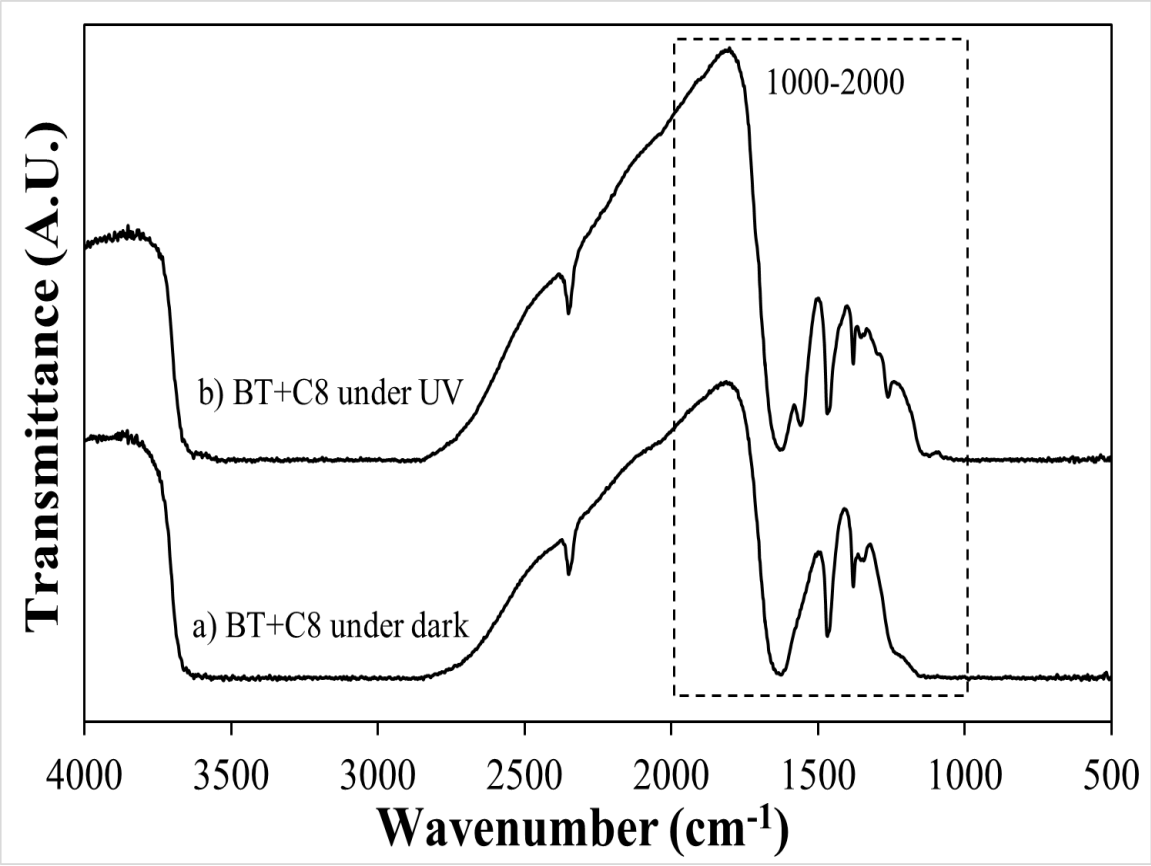

Figure VI.7. *In situ* IR spectra (in transmission mode; wavenumber: 500-4000 cm^{-1}) of calcined TiO_2 treated with 3500 ppmw sulfur as benzothiophene in n-octane a) without UV; b) under UV irradiation (UV wavelength: 365 nm)

New bands were then observed for calcined TiO_2 treated with organosulfur molecules under UV condition. In the 1000-2000 cm^{-1} wavenumber region, two new noticeable bands were observed at 1260 and 1550 cm^{-1} as shown in Figure VI.8. The band at 1260 cm^{-1} represented the $\delta(-CH_2-)$ wagging vibration of methylene groups attached to sulfur atoms ($-CH_2-S-$) [141]. This band might indicate thiophene ring opening as shown in Figure VI.9. The other new band at 1550 cm^{-1} can be associated with the vibrations of surface carboxylates, indicating possible photo-oxidative reactions of benzothiophene on TiO_2 surface [146].

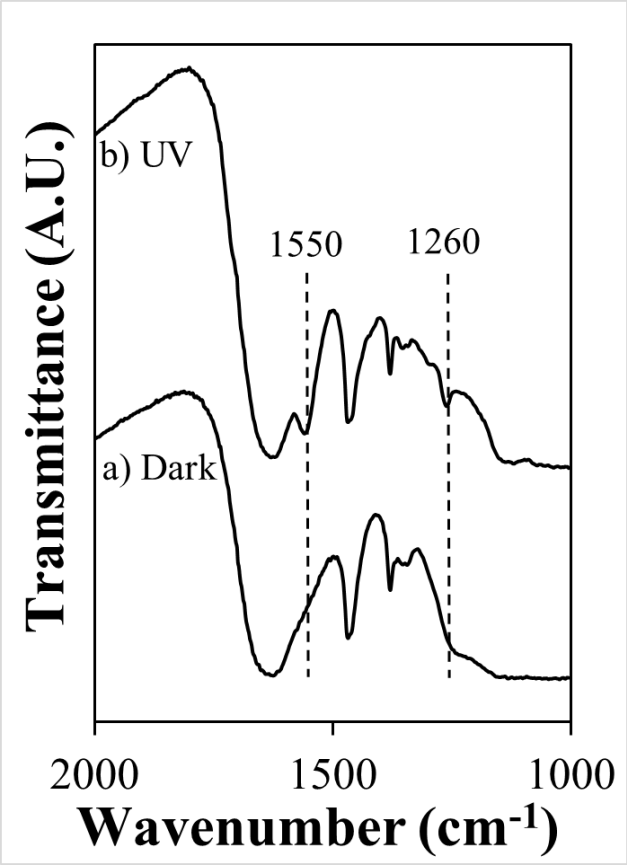

Figure VI.8. *In situ* IR spectra (in transmission mode; wavenumber: 1000-2000 cm^{-1}) of calcined TiO_2 treated with 3500 ppmw sulfur as benzothiophene in n-octane a) without UV; b) under UV irradiation

The photo-oxidative reaction pathway and oxidative products of benzothiophene under UV had been studied in details and already identified as shown in Figure VI.1. The summary of IR band and their respected assignments for calcined TiO_2 treated with different molecules with and without UV are listed in Table VI.2.

Table VI.2. IR bands and their respected assignments for calcined TiO_2 treated with different molecules with and without UV

Wavenumber (cm^{-1})	Assignments
1260	$\delta(-CH_2-)$ wagging vibration of methylene groups attached to sulfur atoms ($-CH_2-S-$)
1360	$\delta(CH_3)$ bending vibration of adsorbed C8
1390	$\delta(C=C)$s stretching vibration of thiophene ring adsorbed on surface -OH groups
1460	vibration of aromatic ring or interaction between -OH and benzothiophene
1550	vibrations of surface carboxylates
1640	$\delta(HOH)$ bending vibration of H_2O
3600-3700	stretching vibrations of hydroxyl groups

Thus, during photo-assisted adsorptive desulfurization process, organosulfur was mainly removed by the interaction between surface hydroxyl (-OH) groups and thiophene or benzene rings. Also, photo-oxidation reaction and thiophene ring opening reaction occurring on TiO_2 surface under UV irradiation could be another possible sulfur removal pathway. Possible sulfur removal pathways onto TiO_2 surface under UV irradiation were illustrated in Figure VI.6 and Figure VI.8.

VI.5. Conclusions

TiO_2 based adsorbents demonstrated enhanced sulfur removal capacities during and after UV treatment step. The adsorbent had 165% higher breakthrough capacity during UV-assisted sulfur removal process than desulfurization without UV irradiation. Isolated -OH groups contributed in the removal of sulfur aromatic molecules, as observed by *in situ* IR. Sulfur adsorption mechanisms for thiophenic compounds onto TiO_2 adsorbents under dark and UV conditions were investigated in this chapter. Thiophenic compounds were considered to be removed via π-interactions (1390 and 1460 cm^{-1}) between surface hydroxyl groups with thiophene ring and aromatic ring under both dark and UV conditions. Photo-oxidation and ring opening reactions were occurring on TiO_2 surface under UV irradiation. The resulting oxidative products were also adsorbed via π-interactions onto the TiO_2 surface. No photo-oxidative products were detected in the liquid phase as confirmed by GC-PFPD and GC-FID results. This work can provide insights into sulfur adsorption mechanisms under UV environment. Further investigations will be focused on surface active sites and species generated on TiO_2 surface under UV irradiation.

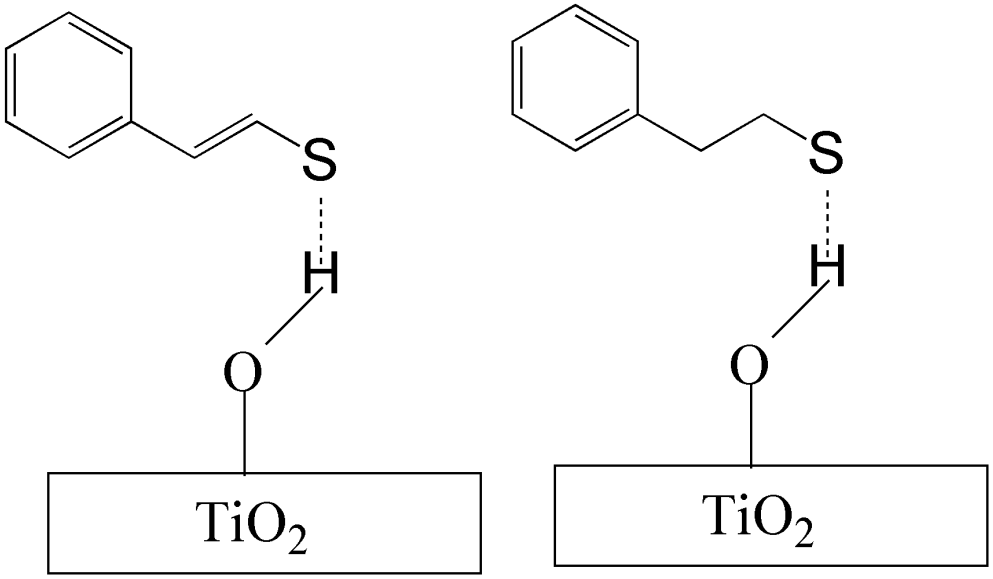

Figure VI.9. Adsorption of benzothiophene under UV with thiophene ring opening.

VII. Conclusions and Recommendations for Future Work

VII.1. Conclusions

Conclusions regarding various studies on photo-assisted sulfur removal process from hydrocarbon fuels over TiO_2 and Ag/TiO_2 adsorbents have been discussed at the end of each chapter. The summary of all research work will be presented here.

1. A unique photo-assisted adsorptive desulfurization process was developed to modify traditional sulfur removal process.
2. The desulfurization performance of TiO_2 adsorbents had been improved significantly by 50% during the UV-assisted sulfur removal process.
3. H_2O molecules can reduce TiO_2 surface acid sites which will decrease its sulfur removal capacity. But photo-assisted desulfurization process can solve the problem caused by H_2O. And highest sulfur removal capacities for TiO_2 and Ag/TiO_2 adsorbents were achieved during UV-assisted breakthrough experiments when adding H_2O molecules into model fuels.
4. UV-irradiated TiO_2 adsorbents also demonstrated much higher sulfur adsorption capacities than calcined TiO_2 adsorbents with no UV treatment.
5. For TiO_2 adsorbents which were initially treated with UV irradiation, sulfur adsorption performance was consistent after multiple adsorption-regeneration cycles. UV-treated TiO_2 adsorbents maintained high sulfur adsorption capacities after thermal regeneration step.

6. A variety of characterization techniques such as GC-PFPD, GC-FID, IR spectroscopy, XPS, and fluorescence spectroscopy were employed to evaluate the effect of UV on TiO_2 surface and adsorption mechanism under irradiation.
7. The effects of UV irradiation and H_2O molecules on TiO_2 surface active sites were investigated by *in situ* IR and XPS. The number of isolated hydroxyl groups formed on TiO_2 surface increased under UV environment which can be confirmed by IR and XPS results.
8. The relative concentrations of hydroxyl radicals generated under UV on TiO_2 were determined by fluorescence technique using terephthalic acid.
9. The sulfur adsorption mechanisms on TiO_2 surface under both dark and UV were both investigated by *in situ* IR. Photo-oxidation and ring opening reactions were found to be occurring on TiO_2 surface under UV based on *in situ* IR investigation.
10. No photo-oxidative products of organosulfur species were detected by GC-PFPD and GC-FID in the liquid phase.

UV-irradiated desulfurization technology developed in current research work can significantly improve sulfur removal performance comparing to traditional ADS technique for TiO_2 supported adsorbents. The UV-assisted dynamic sulfur removal process was demonstrated to effectively desulfurize hydrocarbon fuels down to ultra-low level. Moreover, the negative effects caused by H_2O molecules can be solved by this UV-irradiated desulfurization process. Highest sulfur adsorption capacities for calcined TiO_2 and Ag/TiO_2 were achieved during UV-assisted breakthrough studies using model fuels in the presence of H_2O. The effect of UV irradiation on surface active sites which are hydroxyl groups was the significant finding of this work. Those sulfur removal active

sites generated under UV illumination on TiO_2 surface were persistent and very stable after thermal regeneration cycle under high temperature.

Several characterization techniques were applied to study surface active sites and sulfur removal mechanisms on TiO_2 surface under UV environment. The increase in isolated hydroxyl groups on TiO_2 surface under UV was confirmed by IR and XPS spectra. The possible desulfurization pathway for sulfur aromatic compounds under UV was also studied and discussed in this research. The overall study is important not only for ultra-deep desulfurization technique and fuel cell application but also for surface characterization for TiO_2 related material.

VII.2. Recommendations for future work

VII.2.1. Selectivity towards different sulfur compounds

Although sulfur removal capacities of TiO_2 based adsorbents increased during UV-assisted adsorptive desulfurization using model fuels, the improvement was not that obvious during photo-irradiated ADS using jet fuel. It is known that hydrocarbon fuels are a mixture of various organic compounds including different types of organosulfur species, aromatics, and other additives. UV-assisted sulfur removal from hydrocarbon fuels is a complicated process thus the detailed investigation is essential for understanding the mechanisms involved. Sulfur selectivity is a vital criterion for an effective adsorbent. The adsorption affinities towards different aromatic-sulfur species, non-aromatic sulfur compounds, and other common fuel additives need to be included in future work. Equilibrium saturation experiments on TiO_2, Ag/TiO_2 and Ag/TiO_2-Al_2O_3

using model fuels containing different types of organosulfur compounds will give a general idea of the selectivity of TiO_2 adsorbents towards aromatic sulfur species.

Equilibrium saturation experiments were carried out for calculating saturation capacities. For equilibrium saturation experiments, adsorbents were treated with model fuels containing different sulfur (T, BT, DBT, 4, 6-DMDBT) compounds in n-octane. The sulfur compounds were dissolved into n-octane individually where the total sulfur concentration was kept at 1000 ppmw S in each case. In every saturation test, the fuel was mixed to the adsorbent, and the fuel to adsorbent ratio was 20 mL/g sorbent. Then the mixture was agitated mechanically for 48 h at ambient conditions. The equilibrated fuel was analyzed to measure the sulfur concentration in liquid phase after saturation. Finally, the equilibrium saturation capacity was calculated from the following formula:

$$Q_{Sat} = \frac{(1 - C_{Sat}/C_0)\rho V C_0}{1000}$$

Where,

$Q_{Sat} =$ equilibrium saturation capacity (mg S/g adsorbent)

$C_{Sat} =$ sulfur concentration of fuel after saturation (ppmw)

$C_0 =$ initial sulfur concentration of fuel (ppmw)

$\rho =$ density of fuel (g/mL)

$V =$ volume of fuel/adsorbent weight (mL/g adsorbent)

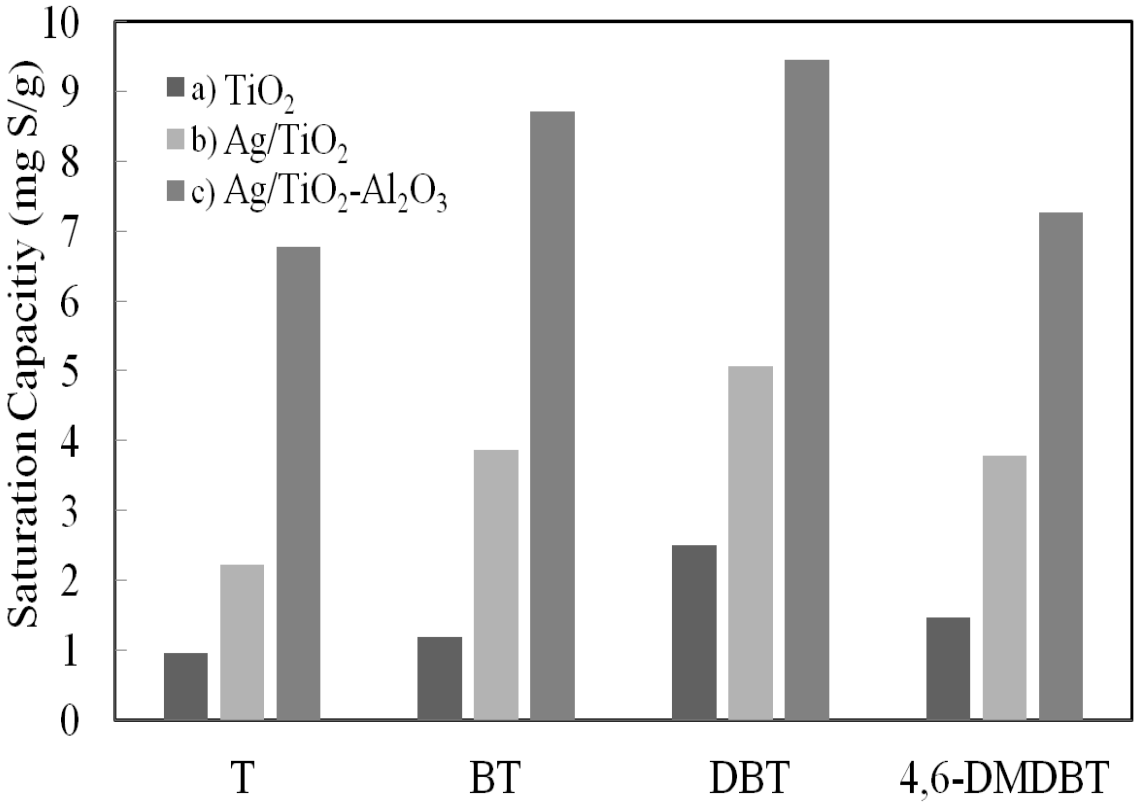

Figure VII.1. Equilibrium saturation capacities from saturation experiments for a) TiO_2, b) 4 wt% Ag/TiO_2 and c) 10 wt% Ag/TiO_2-Al_2O_3 (duration: 48 h, fuel to adsorbent ratio: 20 mL/g, sulfur concentration in model fuel: 1000 ppmw S)

Figure VII.1 shows the saturation capacities of TiO_2, Ag/TiO_2 and Ag/TiO_2-Al_2O_3 for model fuels with T, BT, DBT and 4, 6-DMDBT. In terms of saturation capacity, the order from high to low was DBT>4, 6-DMDBT>BT>T. The results indicated that the addition of benzene rings resulted in higher adsorption capacity. However, the adsorption capacity for 4, 6-DMDBT was lower than DBT due to the steric hindrance by methyl groups. The effects of aromatic rings and methyl groups on desulfurization performance during UV-assisted adsorptive desulfurization also need to be investigated in details.

VII.2.2. Photo-assisted ADS in lab and pilot scales under different light sources

Based on the results got from photo-assisted adsorptive desulfurization (ADS), UV irradiation on bed reactor during dynamic sulfur removal process can significantly improve desulfurization performance of calcined TiO_2 adsorbents. It was found that more desulfurization active sites were generated on TiO_2 surface under UV irradiation which increased sulfur removal capacities. Our studies here were only carried out using UV lights at 365 nm. For anatase TiO_2, the band gap was around 3.4 eV. And for TiO_2-Al_2O_3 and silver loaded on TiO_2 adsorbents, band gaps were much lower than calcined TiO_2. In that case, charges' excitation and transfer would be more easily achieved under UV lights at short wavelength. UV sources at 254 nm were also widely used in many photocatalytic application areas. Thus, more active species may be formed on TiO_2 surface under UV lights at 254 nm during photo-assisted ADS. Moreover, sunlight is another source of ultraviolet radiation. As a result, natural sunlight might be considered to have the same effect on TiO_2 during adsorptive desulfurization and to replace UV lights. Also, sulfur removal experiments under pilot scales will be more easily to be carried out using the natural sunlight.

In current research work, UV light cannot penetrate deeply into the reactor because of the large TiO_2 particles and the size of the reactor bed. In order to further increase the number of surface hydroxyl groups on TiO_2, smaller particles, and multi-tube reactor were suggested to be used in photo-assisted ADS. The reactor containing multiple quartz tubes loaded with TiO_2 based adsorbents in small sizes was shown in Figure VII.2. UV-assisted ADS can also be studied under large scale using this configuration.

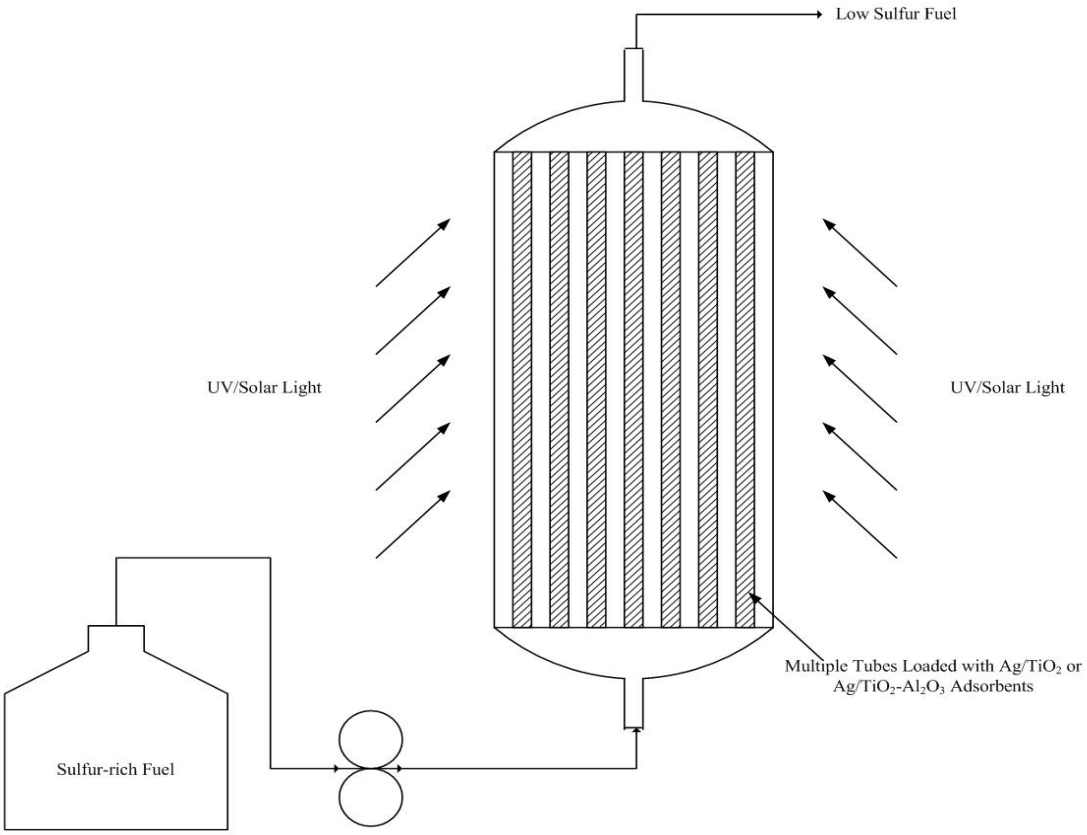

Figure VII.2. Multi-tube reactor for photo-assisted adsorptive desulfurization

VII.2.3. UV-irradiated ADS using Ag/TiO_2 and Ag/TiO_2-Al_2O_3

Ag/TiO_2 and Ag/TiO_2-Al_2O_3 adsorbents have shown promising sulfur removal capacities for liquid hydrocarbon fuels. Ag ions can act as electron acceptors which will inhibit the recombination of electron-hole pairs on TiO_2 bulk during photo-assisted ADS. Surface hydroxyl groups can be generated more easily and stable by impregnation Ag on TiO_2 adsorbents. As a result, photocatalytic desulfurization activities of Ag/TiO_2 and Ag/TiO_2-Al_2O_3 should also be studied in details. But sulfur removal capacities for Ag/TiO_2 adsorbents were decreased under UV irradiation because active silver ions were

reduced to Ag metals under illumination. However, adding H_2O as a mild oxidant can maintain silver phase and further improve its desulfurization performance. Ag/TiO_2 showed highest adsorption capacities using model fuel containing water additive during UV-assisted ADS. In order to maintain active silver phase and increase sulfur capacities, H_2O, O_2 or other oxidant agents might be needed during adsorptive desulfurization under UV using Ag loaded TiO_2 adsorbents.

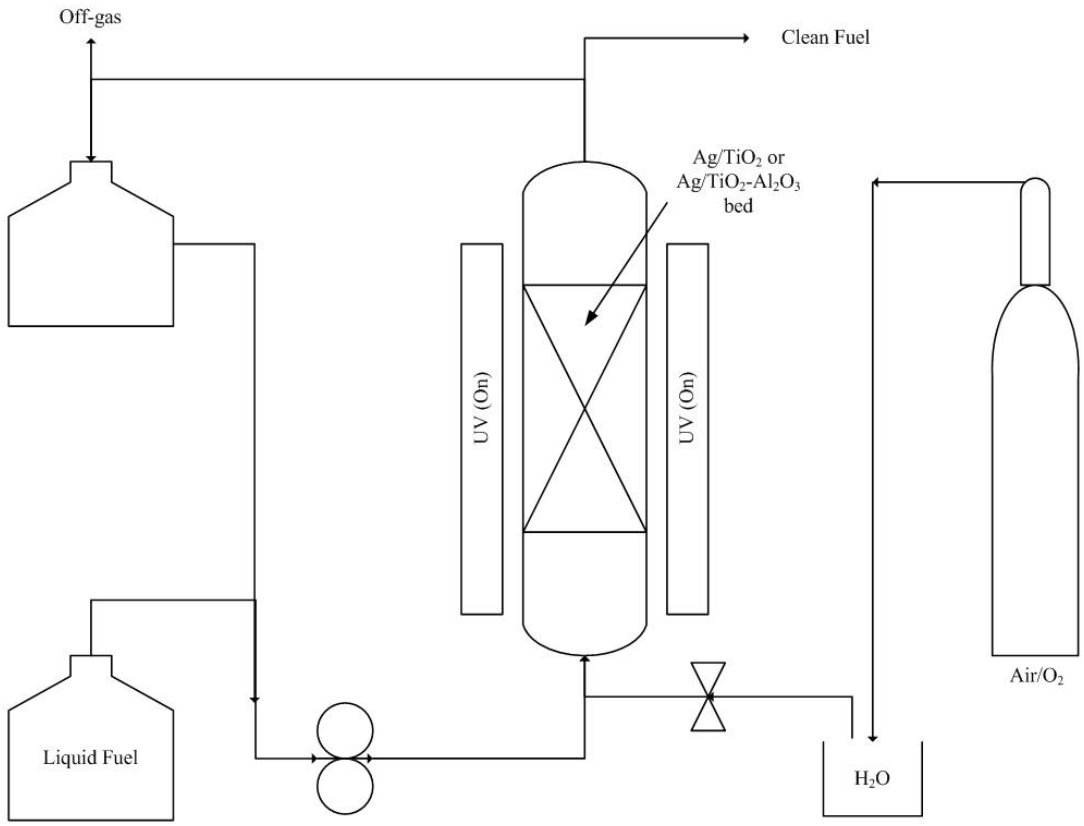

Figure VII.3. Experimental setup for UV-assisted bed reactor under different RH using Ag/TiO_2 and Ag/TiO_2-Al_2O_3 adsorbents

To investigate the photo-assisted adsorptive desulfurization performance of Ag/TiO_2 and Ag/TiO_2-Al_2O_3 adsorbents, breakthrough experiments should be carried out under

UV in the presence of moisture treatment along with air or oxygen. All studies should be performed at room temperature and atmospheric pressure under different relative humidity (RH) in order to reach maximum sulfur removal capacities. When introducing oxidants into the system, photo-oxidative reactions of organosulfur compounds might occur on adsorbents' surface under UV. Therefore, final products in liquid phase must be analyzed to ensure sulfur is removed by adsorption process. Experimental setup for UV-irradiated desulfurization test is shown in Figure VII.3.

In order to fully understand the photo-assisted adsorptive desulfurization activities of TiO_2 based adsorbents, fundamental studies such as band gap values should be carried out on TiO_2, TiO_2-Al_2O_3, Ag/TiO_2 and Ag/TiO_2-Al_2O_3. To determine the band gap values of TiO_2, TiO_2–Al_2O_3 supports, Ag/TiO_2 and Ag/TiO_2–Al_2O_3 adsorbents, UV-vis DRS needs to be employed. The band gap values of silver loaded TiO_2 based adsorbents can be calculated from the absorbance data. The spectra of those adsorbents are shown in Figure VII.4 and values of band gap for Ag loaded TiO_2 adsorbents under room temperature are listed in Table VII.1.

Table VII.1. Band gap values for TiO_2, TiO_2–Al_2O_3, Ag/TiO_2 and Ag/TiO_2–Al_2O_3

Adsorbents	TiO_2	TiO_2–Al_2O_3	Ag/TiO_2	Ag/TiO_2–Al_2O_3
E(eV)	3.50	3.43	3.34	3.20

Calcined TiO_2 has the highest band gap value while dispersed TiO_2 loaded on Al_2O_3 support has lower band gap than that of anatase TiO_2. What's more, silver impregnation

on TiO_2 and TiO_2–Al_2O_3 supports further lowered the band gap. Lower bandgap enabled the charges' excitation and transfer more easily under low UV energy input. Thus, the bonding between active sites and sulfur aromatic compounds can be formed more easily. Furthermore, Ag^+ ions can act as electron acceptors which will inhibit the recombination of the electron-hole pair on TiO_2 bulk during photo-adsorptive desulfurization process.

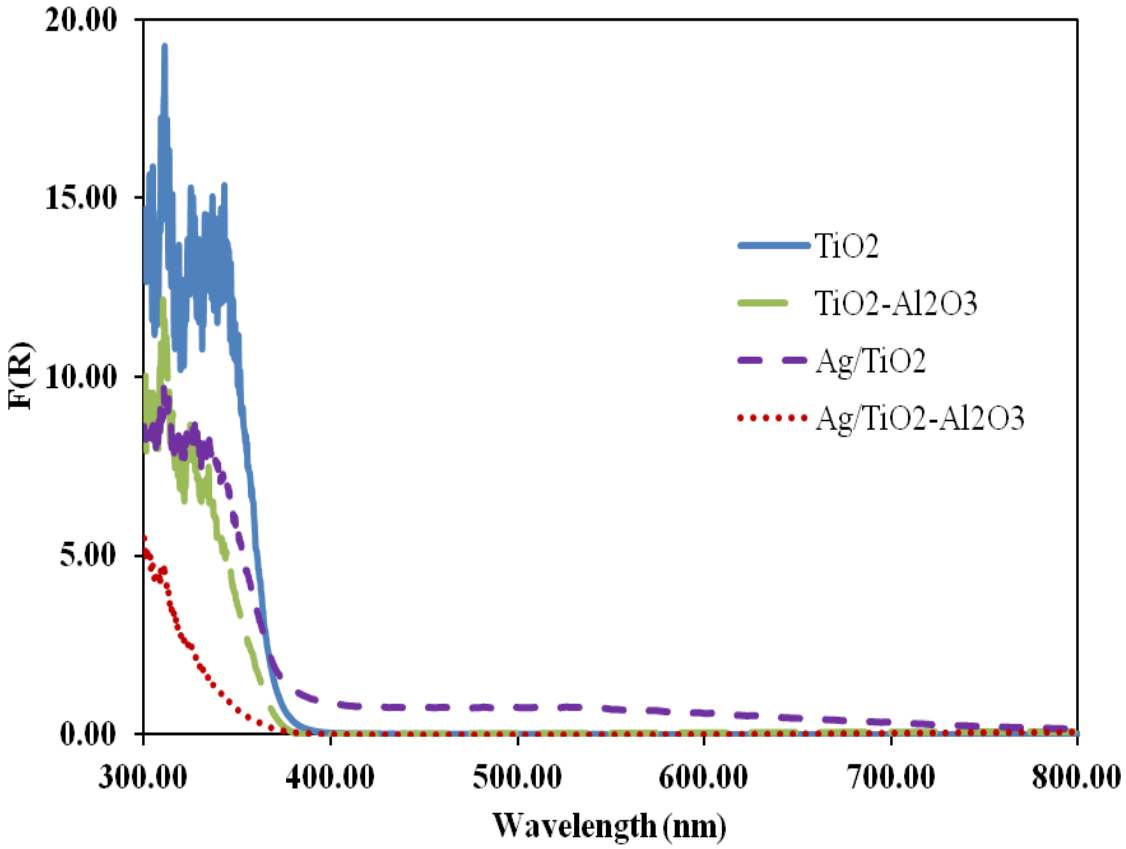

Figure VII.4. UV-vis DRS spectra for TiO_2, TiO_2-Al_2O_3, Ag/TiO_2 and Ag/TiO_2-Al_2O_3 adsorbents

Apparently, band gap value can affect the desulfurization performance of TiO_2 based adsorbents during UV-assisted adsorptive desulfurization (ADS) process. However, the relationship between band gap and photo-assisted sulfur removal capacity of TiO_2

adsorbent is still unclear. As a result, photocatalytic activities of TiO_2–Al_2O_3 and Ag/TiO_2–Al_2O_3 should also be studied in the future.

VII.2.4. Roles of Ti^{4+}, Ti^{3+} and lattice O on adsorption of organosulfur species

Several techniques have been employed to analyze the structure and active sites on TiO_2 surface. Sulfur adsorption pathway under both dark and UV environments still need further investigations. To the best of our knowledge, isolated surface hydroxyl groups contributed in the adsorptive removal of thiophene and its derivatives using TiO_2. Photo-oxidative reactions of organosulfur compounds also occurred on TiO_2 surface during UV-assisted desulfurization process. For Ag/TiO_2, silver impregnation on TiO_2 supports enhances sulfur affinity via π-interactions. And multiple adsorption sites including acidic sites and Ag^+ sites consists the sulfur removal mechanism.

Recently, the role of Ti^{4+}, Ti^{3+} and lattice O in desulfurization activity of thiophene has been studied using rutile and anatase TiO_2 materials [147, 148]. It has shown that thiophene is bonded to Ti^{4+} sites with its ring parallel to the surface at small sulfur coverage. And bonding through S atom becomes more stable with increasing thiophene concentration at Ti^{4+} sites. Also, weak adsorption on surface defects Ti^{3+} sites is discovered. The bonding configurations for thiophene on TiO_2 on Ti^{4+} and Ti^{3+} sites are shown in Figure VII.5. Characterization of Ti phase and the interactions between sulfur species with Ti^{4+} and Ti^{3+} can be useful to investigate different surface treatment methods for achieving more active sites on TiO_2 surface. The interactions between sulfur atom and lattice O or O vacancies have been not clear yet, which need more experiments and

information. To study the roles of these O species, *in-situ* IR analysis can be performed on TiO_2 treated with electron scavenger such as O_2 or hole scavenger under UV. Also, the density functional theory (DFT) study can be conducted in order to develop a fundamental understanding of the sulfur adsorption mechanism of thiophene compounds on TiO_2 based adsorbents for ultra-deep desulfurization of liquid hydrocarbon fuels.

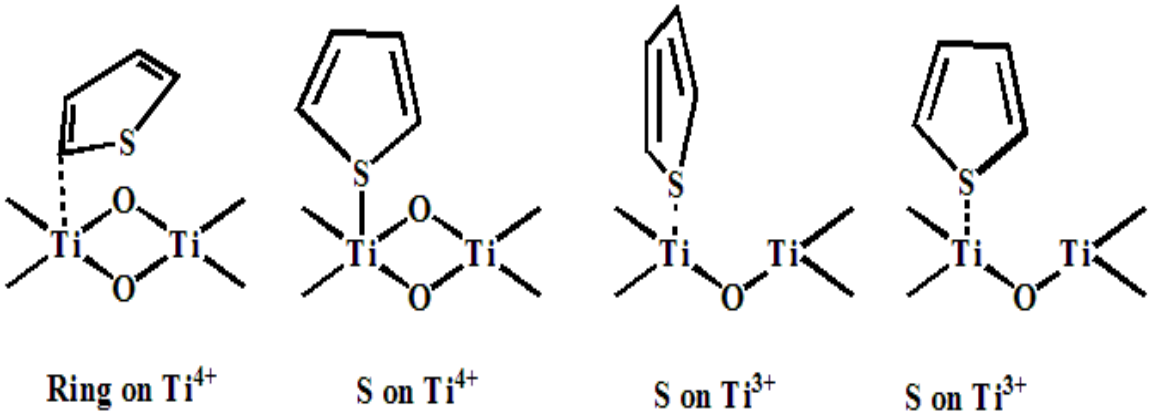

Figure VII.5. Bonding configurations for thiophene on TiO_2's Ti^{4+} and Ti^{3+} sites (reproduced from Liu, G. et al. Journal of Molecular Catalysis A: Chemical 2003 [148])

VII.2.5. TiO_2 surface active species under UV

Active sites and new species generated through UV treatment still need further investigation. Possible pathway to form those species on TiO_2 surface under UV will help us understand desulfurization mechanism better. Sulfur removal performance can be improved by surface modification on TiO_2 based on fundamental studying results. *In-situ* IR and XPS will be useful tools to get details on surface characterization such as active sites generated under UV for sulfur adsorption, the state change of Ti and Ag species as well as the relaxation time. Based on research results, sulfur adsorption capacities mainly

depend on the number of isolated hydroxyl groups on TiO_2 surface. More hydroxyl groups were formed on TiO_2 surface under UV irradiation which was confirmed by IR and XPS spectra. Also, H_2O molecules are expected to affect surface hydroxyl groups on TiO_2 differently under dark and UV based on IR analysis. Thus, more experiments should be carried out in order to understand the mechanism of the formation of hydroxyl groups under UV and the effect of H_2O on TiO_2 surface. Once we understand those details, we can gain more information towards desulfurization mechanism.

References

[1] V.C. Srivastava, RSC Advances. 2 (2012) 759-783.

[2] C.S. Song, Catalysis Today. 86 (2003) 211-263.

[3] A. Stanislaus, A. Marafi, M.S. Rana, Catalysis Today. 153 (2010) 1-68.

[4] R. Abro, A.A. Abdeltawab, S.S. Al-Deyab, G.R. Yu, A.B. Qazi, S.R. Gao, X.C. Chen, RSC Advances. 4 (2014) 35302-35317.

[5] A. Samokhvalov, B.J. Tatarchuk, Catalysis Reviews-Science and Engineering. 52 (2010) 381-410.

[6] C.S. Song, Catalysis Today. 77 (2002) 17-49.

[7] C. Song, X.L. Ma, Applied Catalysis B-Environmental. 41 (2003) 207-238.

[8] M. Breysse, G. Djega-Mariadassou, S. Pessayre, C. Geantet, M. Vrinat, G. Perot, M. Lemaire, Catalysis Today. 84 (2003) 129-138.

[9] S. Brunet, D. Mey, G. Perot, C. Bouchy, F. Diehl, Applied Catalysis a-General. 278 (2005) 143-172.

[10] T. Kabe, A. Ishihara, H. Tajima, Industrial & Engineering Chemistry Research. 31 (1992) 1577-1580.

[11] C. Pophal, F. Kameda, K. Hoshino, S. Yoshinaka, K. Segawa, Catalysis Today. 39 (1997) 21-32.

[12] X.L. Ma, K.Y. Sakanishi, I. Mochida, Industrial & Engineering Chemistry Research. 33 (1994) 218-222.

[13] S.W. Shorey, D.A. Lomas, W.H. Keesom, Hydrocarbon Processing. 78 (1999) 43-51.

[14] S. Hatanaka, M. Yamada, O. Sadakane, Industrial & Engineering Chemistry Research. 36 (1997) 1519-1523.

[15] S. Hatanaka, M. Yamada, O. Sadakane, Industrial & Engineering Chemistry Research. 37 (1998) 1748-1754.

[16] E. Furimsky, F.E. Massoth, Catalysis Today. 52 (1999) 381-495.

[17] L.S. Byskov, B. Hammer, J.K. Norskov, B.S. Clausen, H. Topsoe, Catalysis Letters. 47 (1997) 177-182.

[18] G.M. Dhar, B.N. Srinivas, M.S. Rana, M. Kumar, S.K. Maity, Catalysis Today. 86 (2003) 45-60.

[19] B. Pawelec, R. Mariscal, J.L.G. Fierro, A. Greenwood, P.T. Vasudevan, Applied Catalysis a-General. 206 (2001) 295-307.

[20] K. Segawa, K. Takahashi, S. Satoh, Catalysis Today. 63 (2000) 123-131.

[21] S.K. Bej, S.K. Maity, U.T. Turaga, Energy & Fuels. 18 (2004) 1227-1237.

[22] H. Farag, D.D. Whitehurst, I. Mochida, Industrial & Engineering Chemistry Research. 37 (1998) 3533-3539.

[23] I. Mochida, K. Sakanishi, X.L. Ma, S. Nagao, T. Isoda, Catalysis Today. 29 (1996) 185-189.

[24] R. Shafi, G.J. Hutchings, Catalysis Today. 59 (2000) 423-442.

[25] E. Lecrenay, K. Sakanishi, I. Mochida, Catalysis Today. 39 (1997) 13-20.

[26] X.L. Ma, K. Sakanishi, I. Mochida, Industrial & Engineering Chemistry Research. 35 (1996) 2487-2494.

[27] X.L. Ma, K. Sakanishi, T. Isoda, I. Mochida, Energy & Fuels. 9 (1995) 33-37.

[28] M.J. Girgis, B.C. Gates, Industrial & Engineering Chemistry Research. 30 (1991) 2021-2058.

[29] V. Vanrysselberghe, G.F. Froment, Industrial & Engineering Chemistry Research. 35 (1996) 3311-3318.

[30] I.A. Vanparijs, G.F. Froment, Industrial & Engineering Chemistry Product Research and Development. 25 (1986) 431-436.

[31] B.C. Gates, H. Topsoe, Polyhedron. 16 (1997) 3213-3217.

[32] D.D. Whitehurst, H. Farag, T. Nagamatsu, K. Sakanishi, I. Mochida, Catalysis Today. 45 (1998) 299-305.

[33] M. Egorova, R. Prins, Journal of Catalysis. 225 (2004) 417-427.

[34] H. Farag, K. Sakanishi, M. Kouzu, A. Matsumura, Y. Sugimoto, I. Saito, Industrial & Engineering Chemistry Research. 42 (2003) 306-310.

[35] S.T. Sie, Fuel Processing Technology. 61 (1999) 149-171.

[36] K.G. Knudsen, B.H. Cooper, H. Topsoe, Applied Catalysis a-General. 189 (1999) 205-215.

[37] M.K. Andari, F. AbuSeedo, A. Stanislaus, H.M. Qabazard, Fuel. 75 (1996) 1664-1670.

[38] H. Gomez-Bernal, L. Cedeno-Caero, A. Gutierrez-Alejandre, Catalysis Today. 142 (2009) 227-233.

[39] F.M. Collins, A.R. Lucy, C. Sharp, Journal of Molecular Catalysis a-Chemical. 117 (1997) 397-403.

[40] H. Mei, B.W. Mei, T.F. Yen, Fuel. 82 (2003) 405-414.

[41] S. Otsuki, T. Nonaka, N. Takashima, W.H. Qian, A. Ishihara, T. Imai, T. Kabe, Energy & Fuels. 14 (2000) 1232-1239.

[42] R. Sundararaman, C.S. Song, Industrial & Engineering Chemistry Research. 53 (2014) 1890-1899.

[43] A. Chica, A. Corma, M.E. Domine, Journal of Catalysis. 242 (2006) 299-308.

[44] F. Zannikos, E. Lois, S. Stournas, Fuel Processing Technology. 42 (1995) 35-45.

[45] J.T. Sampanthar, H. Xiao, H. Dou, T.Y. Nah, X. Rong, W.P. Kwan, Applied Catalysis B-Environmental. 63 (2006) 85-93.

[46] D.H. Wang, E.W.H. Qian, H. Amano, K. Okata, A. Ishihara, T. Kabe, Applied Catalysis a-General. 253 (2003) 91-99.

[47] K. Yazu, Y. Yamamoto, T. Furuya, K. Miki, K. Ukegawa, Energy & Fuels. 15 (2001) 1535-1536.

[48] Y. Shiraishi, K. Tachibana, T. Hirai, I. Komasawa, Industrial & Engineering Chemistry Research. 41 (2002) 4362-4375.

[49] A. Ishihara, D.H. Wang, F. Dumeignil, H. Amano, E.W.H. Qian, T. Kabe, Applied Catalysis a-General. 279 (2005) 279-287.

[50] J.M. Campos-Martin, M.C. Capel-Sanchez, P. Perez-Presas, J.L.G. Fierro, Journal of Chemical Technology and Biotechnology. 85 (2010) 879-890.

[51] P.S. Tam, J.R. Kittrell, J.W. Eldridge, Industrial & Engineering Chemistry Research. 29 (1990) 321-324.

[52] L.F. Ramirez-Verduzco, E. Torres-Garcia, R. Gomez-Quintana, V. Gonzalez-Pena, F. Murrieta-Guevara, Catalysis Today. 98 (2004) 289-294.

[53] S. Matsuzawa, J. Tanaka, S. Sato, T. Ibusuki, Journal of Photochemistry and Photobiology a-Chemistry. 149 (2002) 183-189.

[54] M.H. Habibi, H. Vosooghian, Journal of Photochemistry and Photobiology a-Chemistry. 174 (2005) 45-52.

[55] J. Robertson, T.J. Bandosz, Journal of Colloid and Interface Science. 299 (2006) 125-135.

[56] J.A. Byrne, B.R. Eggins, N.M.D. Brown, B. McKinney, M. Rouse, Applied Catalysis B-Environmental. 17 (1998) 25-36.

[57] P. Pichat, J. Disdier, C. Hoang-Van, D. Mas, G. Goutailler, C. Gaysse, Catalysis Today. 63 (2000) 363-369.

[58] S.U.M. Khan, M. Al-Shahry, W.B. Ingler, Science. 297 (2002) 2243-2245.

[59] S. Sakthivel, B. Neppolian, M.V. Shankar, B. Arabindoo, M. Palanichamy, V. Murugesan, Solar Energy Materials and Solar Cells. 77 (2003) 65-82.

[60] T. Tachikawa, M. Fujitsuka, T. Majima, Journal of Physical Chemistry C. 111 (2007) 5259-5275.

[61] M. Ni, M.K.H. Leung, D.Y.C. Leung, K. Sumathy, Renewable & Sustainable Energy Reviews. 11 (2007) 401-425.

[62] K. Nakata, A. Fujishima, Journal of Photochemistry and Photobiology C-Photochemistry Reviews. 13 (2012) 169-189.

[63] M. Zarrabi, M.H. Entezari, E.K. Goharshadi, Rsc Advances. 5 (2015) 34652-34662.

[64] T. Hirai, K. Ogawa, I. Komasawa, Industrial & Engineering Chemistry Research. 35 (1996) 586-589.

[65] Y. Shiraishi, T. Hirai, I. Komasawa, Industrial & Engineering Chemistry Research. 38 (1999) 3300-3309.

[66] R. Vargas, O. Nunez, Journal of Molecular Catalysis a-Chemical. 294 (2008) 74-81.

[67] A. Samokhvalov, Chemphyschem. 12 (2011) 2870-2885.

[68] J. Zhang, D.S. Zhao, J.L. Wang, L.Y. Yang, Journal of Materials Science. 44 (2009) 3112-3117.

[69] R. Vargas, O. Nunez, Solar Energy. 84 (2010) 345-351.

[70] L. Wang, H.J. Cai, S.Z. Li, N. Mominou, Fuel. 105 (2013) 752-756.

[71] W.S. Zhu, Y.H. Xu, H.M. Li, B.L. Dai, H. Xu, C. Wang, Y.H. Chao, H. Liu, Korean Journal of Chemical Engineering. 31 (2014) 211-217.

[72] A.A. Nuhu, Reviews in Environmental Science and Bio-Technology. 12 (2013) 9-23.

[73] M. Soleimani, A. Bassi, A. Margaritis, Biotechnology Advances. 25 (2007) 570-596.

[74] M.A. Kertesz, Fems Microbiology Reviews. 24 (2000) 135-175.

[75] N. Gupta, P.K. Roychoudhury, J.K. Deb, Applied Microbiology and Biotechnology. 66 (2005) 356-366.

[76] D. Boniek, D. Figueiredo, A.F.B. dos Santos, M.A.D. Stoianoff, Clean Technologies and Environmental Policy. 17 (2015) 29-37.

[77] K.A. Gray, G.T. Mrachko, C.H. Squires, Current Opinion in Microbiology. 6 (2003) 229-235.

[78] A.J. Hernandez-Maldonado, R.T. Yang, Catalysis Reviews-Science and Engineering. 46 (2004) 111-150.

[79] X.L. Ma, L. Sun, C.S. Song, Catalysis Today. 77 (2002) 107-116.

[80] S. Velu, C.S. Song, M.H. Engelhard, Y.H. Chin, Industrial & Engineering Chemistry Research. 44 (2005) 5740-5749.

[81] J. Xiao, X.X. Wang, Y.S. Chen, M. Fujii, C.S. Song, Industrial & Engineering Chemistry Research. 52 (2013) 15746-15755.

[82] S. Velu, X.L. Ma, C.S. Song, Industrial & Engineering Chemistry Research. 42 (2003) 5293-5304.

[83] R.T. Yang, A.J. Hernandez-Maldonado, F.H. Yang, Science. 301 (2003) 79-81.

[84] Wardenck.W, Staszews.R, Journal of Chromatography. 91 (1974) 715-722.

[85] P. Jeevanandam, K.J. Klabunde, S.H. Tetzler, Microporous and Mesoporous Materials. 79 (2005) 101-110.

[86] A.J. Hernandez-Maldonado, F.H. Yang, G. Qi, R.T. Yang, Applied Catalysis B-Environmental. 56 (2005) 111-126.

[87] A.J. Hernandez-Maldonado, G.S. Qi, R.T. Yang, Applied Catalysis B-Environmental. 61 (2005) 212-218.

[88] Y.H. Wang, F.H. Yang, R.T. Yang, J.M. Heinzel, A.D. Nickens, Industrial & Engineering Chemistry Research. 45 (2006) 7649-7655.

[89] J.H. Kim, X.L. Ma, A.N. Zhou, C.S. Song, Catalysis Today. 111 (2006) 74-83.

[90] R.T. Yang, A. Takahashi, F.H. Yang, Industrial & Engineering Chemistry Research. 40 (2001) 6236-6239.

[91] S. Nair, B.J. Tatarchuk, Fuel. 89 (2010) 3218-3225.

[92] A. Hussain, B.J. Tatarchuk, Fuel. 107 (2013) 465-473.

[93] A. Hussain, H.Y. Yang, B.J. Tatarchuk, Abstracts of Papers of the American Chemical Society. 244 (2012) 1.

[94] A. Samokhvalov, S. Nair, E.C. Duin, B.J. Tatarchuk, Applied Surface Science. 256 (2010) 3647-3652.

[95] A. Samokhvalov, E.C. Duin, S. Nair, B.J. Tatarchuk, Surface and Interface Analysis. 42 (2010) 1476-1482.

[96] A. Samokhvalov, E.C. Duin, S. Nair, M. Bowman, Z. Davis, B.J. Tatarchuk, Journal of Physical Chemistry C. 114 (2010) 4075-4085.

[97] A. Samokhvalov, E.C. Duin, S. Nair, B.J. Tatarchuk, Applied Surface Science. 257 (2011) 3226-3232.

[98] S. Nair, A. Hussain, B.J. Tatarchuk, Fuel. 105 (2013) 695-704.

[99] S. Nair, B.J. Tatarchuk, Adsorption-Journal of the International Adsorption Society. 17 (2011) 663-673.

[100] A. Hussain, H.Y. Yang, B.J. Tatarchuk, Energy & Fuels. 27 (2013) 4353-4362.

[101] B. Serrano, H. deLasa, Industrial & Engineering Chemistry Research. 36 (1997) 4705-4711.

[102] K. Ishibashi, A. Fujishima, T. Watanabe, K. Hashimoto, Electrochemistry Communications. 2 (2000) 207-210.

[103] A. Vittadini, A. Selloni, F.P. Rotzinger, M. Gratzel, Physical Review Letters. 81 (1998) 2954-2957.

[104] R.L. Richardson, S.W. Benson, Journal of Physical Chemistry. 61 (1957) 405-411.

[105] A.P. Kulkarni, D.S. Muggli, Applied Catalysis a-General. 302 (2006) 274-282.

[106] H. Perron, J. Vandenborre, C. Domain, R. Drot, J. Roques, E. Simoni, J.J. Ehrhardt, H. Catalette, Surface Science. 601 (2007) 518-527.

[107] M. Takeuchi, G. Martra, S. Coluccia, M. Anpo, Journal of Physical Chemistry C. 111 (2007) 9811-9817.

[108] Y. Murakami, E. Kenji, A.Y. Nosaka, Y. Nosaka, Journal of Physical Chemistry B. 110 (2006) 16808-16811.

[109] R. Nakamura, Y. Nakato, Journal of the American Chemical Society. 126 (2004) 1290-1298.

[110] B.F. Xin, L.Q. Jing, Z.Y. Ren, B.Q. Wang, H.G. Fu, Journal of Physical Chemistry B. 109 (2005) 2805-2809.

[111] E. Kowalska, Z. Wei, B. Karabiyik, A. Herissan, M. Janczarek, M. Endo, A. Markowska-Szczupak, H. Remita, B. Ohtani, Catalysis Today. 252 (2015) 136-142.

[112] S.S. Liu, N. Wang, Y.C. Zhang, Y.R. Li, Z. Han, P. Na, Journal of Hazardous Materials. 284 (2015) 171-181.

[113] Y.L. Kuo, H.W. Chen, Y. Ku, Thin Solid Films. 515 (2007) 3461-3468.

[114] H.M. Sung-Suh, J.R. Choi, H.J. Hah, S.M. Koo, Y.C. Bae, Journal of Photochemistry and Photobiology a-Chemistry. 163 (2004) 37-44.

[115] B.H. Mao, R. Chang, L. Shi, Q.Q. Zhuo, S. Rani, X.S. Liu, E.C. Tyo, S. Vajda, S.D. Wang, Z. Liu, Physical Chemistry Chemical Physics. 16 (2014) 26645-26652.

[116] M. Lampimaki, S. Schreiber, V. Zelenay, A. Krepelova, M. Birrer, S. Axnanda, B.H. Mao, Z. Liu, H. Bluhm, M. Ammann, Journal of Physical Chemistry C. 119 (2015) 7076-7085.

[117] K. Luo, T.P. St Clair, X. Lai, D.W. Goodman, Journal of Physical Chemistry B. 104 (2000) 3050-3057.

[118] K. Kobayakawa, Y. Nakazawa, M. Ikeda, Y. Sato, A. Fujishima, Berichte Der Bunsen-Gesellschaft-Physical Chemistry Chemical Physics. 94 (1990) 1439-1443.

[119] R. Nakamura, A. Imanishi, K. Murakoshi, Y. Nakato, Journal of the American Chemical Society. 125 (2003) 7443-7450.

[120] K.I. Hadjiivanov, D.G. Klissurski, Chemical Society Reviews. 25 (1996) 61-69.

[121] A. Fujishima, X.T. Zhang, D.A. Tryk, Surface Science Reports. 63 (2008) 515-582.

[122] A.S. Vuk, R. Jese, M. Gaberscek, B. Orel, G. Drazic, Solar Energy Materials and Solar Cells. 90 (2006) 452-468.

[123] R.J. Lobo-Lapidus, B.C. Gates, Chemistry-a European Journal. 16 (2010) 11386-11398.

[124] D.A. Panayotov, J.T. Yates, Chemical Physics Letters. 410 (2005) 11-17.

[125] M. Primet, P. Pichat, M.V. Mathieu, Journal of Physical Chemistry. 75 (1971) 1216-1220.

[126] K. Suriye, R.J. Lobo-Lapldus, G.J. Yeagle, P. Fraserthdam, R.D. Britt, B.C. Gates, Chemistry-a European Journal. 14 (2008) 1402-1414.

[127] P.M. Kumar, S. Badrinarayanan, M. Sastry, Thin Solid Films. 358 (2000) 122-130.

[128] B. Erdem, R.A. Hunsicker, G.W. Simmons, E.D. Sudol, V.L. Dimonie, M.S. El-Aasser, Langmuir. 17 (2001) 2664-2669.

[129] S.H. Szczepankiewicz, A.J. Colussi, M.R. Hoffmann, Journal of Physical Chemistry B. 104 (2000) 9842-9850.

[130] T. Bezrodna, G. Puchkovska, V. Shymanovska, J. Baran, H. Ratajczak, Journal of Molecular Structure. 700 (2004) 175-181.

[131] C. Deiana, E. Fois, S. Coluccia, G. Martra, Journal of Physical Chemistry C. 114 (2010) 21531-21538.

[132] L.M. Liu, P. Crawford, P. Hu, Progress in Surface Science. 84 (2009) 155-176.

[133] N. Sakai, A. Fujishima, T. Watanabe, K. Hashimoto, Journal of Physical Chemistry B. 107 (2003) 1028-1035.

[134] J.G. Yu, X.J. Zhao, Q.N. Zhao, Materials Chemistry and Physics. 69 (2001) 25-29.

[135] G.N. Raikar, J.C. Gregory, J.L. Ong, L.C. Lucas, J.E. Lemons, D. Kawahara, M. Nakamura, Journal of Vacuum Science & Technology a-Vacuum Surfaces and Films. 13 (1995) 2633-2637.

[136] G.W. Simmons, B.C. Beard, Journal of Physical Chemistry. 91 (1987) 1143-1148.

[137] N. Ohtsu, N. Masahashi, Y. Mizukoshi, K. Wagatsuma, Langmuir. 25 (2009) 11586-11591.

[138] X.J. Wang, F.T. Li, J.X. Liu, C.G. Kou, Y. Zhao, Y.J. Hao, D.S. Zhao, Energy & Fuels. 26 (2012) 6777-6782.

[139] A. Samokhvalov, Catalysis Reviews-Science and Engineering. 54 (2012) 281-343.

[140] R. Wang, K. Hashimoto, A. Fujishima, M. Chikuni, E. Kojima, A. Kitamura, M. Shimohigoshi, T. Watanabe, Advanced Materials. 10 (1998) 135-138.

[141] T.L. Thompson, D.A. Panayotov, J.T. Yates, Journal of Physical Chemistry B. 108 (2004) 16825-16833.

[142] F. Tian, W. Wu, Z. Jiang, C. Liang, Y. Yang, P. Ying, X. Sun, T. Cai, C. Li, Journal of Colloid and Interface Science. 301 (2006) 395-401.

[143] H. Wang, L. Song, H. Jiang, J. Xu, L. Jin, X. Zhang, Z. Sun, Fuel Processing Technology. 90 (2009) 835-838.

[144] W.C. Wu, Z.L. Wu, Z.C. Feng, P.L. Ying, C. Li, Physical Chemistry Chemical Physics. 6 (2004) 5596-5602.

[145] A. Hussain, B.J. Tatarchuk, Fuel Processing Technology. 126 (2014) 233-242.

[146] D.V. Kozlov, A.V. Vorontsov, P.G. Smirniotis, E.N. Savinov, Applied Catalysis B-Environmental. 42 (2003) 77-87.

[147] J.H. Guo, S. Watanabe, M.J. Janik, X.L. Ma, C.S. Song, Catalysis Today. 149 (2010) 218-223.

[148] G. Liu, J.A. Rodriguez, J. Hrbek, B.T. Long, D.A. Chen, Journal of Molecular Catalysis a-Chemical. 202 (2003) 215-227.